Journal of Engineering and Technology

of The Open University of Sri Lanka

Volume 08 No. 02 September 2020 ISSN 2279-2627

JET – OUSL | Faculty of Engineering Technology

JET- OUSL

The Journal of Engineering and Technology of the Open University of Sri Lanka is a peer-reviewed journal, published biannually by the Faculty of Engineering Technology of the Open University of Sri Lanka.

Scope
The journal accepts only original research articles based on theoretical and applied research in all aspects of Engineering and Technology specializations.

Research Articles
Articles are full length papers presenting complete description of original research or technological achievements. Statements and opinions expressed in all the articles of this Journal are those of the individual contributors and the Editorial Boards of the Faculty of Engineering Technology of the Open University of Sri Lanka do not hold the responsibility of such statements and opinions.

Peer Review Policy
The practice of peer review is to ensure that only good knowledge is published. It is an unbiased process at the good scholarly publishing and is carried out by all reputable scientific journals. Our referees play a vital role in maintaining the high standards and all manuscripts are peer reviewed following the procedure outlined below.

Initial manuscript evaluation
The Editor first evaluates all manuscripts. Manuscripts rejected at this stage are not sufficiently original or are outside the aims and scope of the journal. Those that meet the minimum criteria are normally passed on to at least 2 experts for review.

Type of Peer Review
JET-OUSL employs double blind reviewing, where both the referee and author remain anonymous throughout the process. Referees are matched to the paper according to their expertise preferably from outside of the Open University of Sri Lanka.

Referee Reports
Referees are asked to evaluate whether the manuscript is original, methodologically sound, ethically sound, clearly presented results followed by discussion and conclusions with correct references of preceding relevant work. Referees are provided with a structured form along with the manuscript for constructive comments. Language correction is not part of the peer review process, but referees may suggest corrections to the manuscript.

Printer at The Open University Press
ISSN 2279-2627
Published in September 2020

Journal of Engineering and Technology

of the Open University of Sri Lanka

Volume 08 No. 02 September 2020 ISSN 2279-2627

Editorial / Correspondences

All correspondences including manuscripts for submissions should be addressed to:

Editor in Chief – Journal of Engineering and Technology
Faculty of Engineering Technology
The Open University of Sri Lanka
Nawala, Nugegoda
Sri Lanka
Email: bcliy@ou.ac.lk, Telephone: +94112881111

Contents

Volume 08 No. 02 September 2020 ISSN 2279-2627

Journal of Engineering and Technology
of The Open University of Sri Lanka (JET-OUSL), Vol. 08, No.2, pp 1-10

Automated Floral Foam Cutting Machine for Industry

H.L.P. Samarasinghe[1], R.J. Wimalasiri[2*], S. Thrikawala[1]

[1]Department of Agricultural and Plantation Engineering, The Open University of Sri Lanka, Nawala, Nugegoda, Sri Lanka.
[2]Department of Mechanical Engineering, The Open University of Sri Lanka, Nawala, Nugegoda, Sri Lanka.

*Corresponding Author: email: rjwim@ou.ac.lk, Tele: +94772751939

Abstract - *The floriculture industry has been growing up in the past thirty years and today Sri Lanka is one of the largest floriculture producing countries in the world. With earnings of around US$ 16 million worth of foreign exchange annually, the floriculture industry has a tremendous potential for generating employment for rural populations. The floral foam is an excellent solid rooting media that use to plant rooted cuttings for export market. Standard size blocks of floral foams are imported and then cut into cubes of four distinct sizes to accommodate different plants. Currently the cutting is being done manually by skilled workers. Even the leading exporters have found it difficult to maintain the quality of floral foams cubes being cut by existing manual cutting method. Requiring skilled labour, generating unproductive time, wastage of material due to irregular cutting, breakages and dust formation are the drawbacks of this manual method. Therefore, this study is focused on designing and developing an automated floral foam cutting machine and validating the same for improved efficiency and product accuracy.*

An automated floral foam cutting machine was designed and developed. It is powered by grid electricity, where all pneumatic and mechanical operations are handled by a micro-controller to a pre-programmed sequence. Specially designed cutters enable size floral foam blocks in both horizontal and vertical directions to specific dimensions with minimum deformation. Cutting time, productivity, product accuracy and wastage were compared with existing manual method. The cost of manufacturing was calculated, and payback period of the capital cost was analyzed.

The results revealed that the automated floral foam cutting machine has improved the productivity by 71%-81%. The geometrical variance is only 0.67. With the new machine dust formation drops by 69%, which is not only significant, but reduce environmental pollution compared to manual method. The machine saves the labour cost by 80%, and the capital cost can be recovered within 8 months.

Key Words: *Floral foam, Cutting machine, Automation, Micro controller, Pneumatics.*

Nomenclature

L - Length in *mm*
W - Width in *mm*
H - Height in *mm*

Subscripts
P - Plants
SD - Standard deviation
CV - Coefficient of variance
AFFCM - Automated floral foam cutting machine
FF - Floral foam

1 INTRODUCTION

The floriculture industry in Sri Lanka has been growing in the past thirty years and since 1980s it has been evolving as an export-oriented industry which provided direct employment to many people from semi-urban to rural areas (De Silva, 2014). Today, Sri Lanka is recognized as one with largest floriculture production centres in the world. Europe is the main market for Sri Lankan floriculture products having 60% of exports, while Japan, Middle East, USA and South Korea make up the other key markets (EDB, 2019). In 2017, Sri Lanka was able to earn US$ 16 million worth of foreign exchange by exporting floriculture to Netherlands, Japan, Saudi Arabia, and UAE (EDB, 2019).

The vast botanical diversity and a wide range of floricultural species (Floriculture sector in Sri Lanka, e-brochure) have made Sri Lanka a favourable location to excel different floriculture markets in the world (Dhanasekara, 1998). Export Development Board (EDB) is the apex state body dealing with export of floriculture products, while the Department of National Botanical Gardens (DNBG) is providing technical expertise to the floriculture industry (Rathnayake and Rathnayake, 2019). Currently around 55 local floriculture exporters are exploring the possibility of expanding their business into emerging markets in Swaziland, Uruguay, and Iraq (Rathnayake and Rathnayake, 2019). Besides resulting in higher income generation, the floriculture sector has also shown tremendous potential for generating employment opportunities for rural populations, particularly for women (Daily News, 2017). In fact, according to the National Planning Framework (2010) Sri Lanka is planning to establish 1500 horticultural villages and 30,000 employment opportunities particularly for sub-urban and rural areas. De Silva (2014) in his article on Daily FT pointed out that Sri Lanka could be the regional leader in horticulture industry soon.

Floriculture planting media 'floral foam (FF)' is imported. Among many other materials FF has been widely used as the rooting materials for stem cuttings as they weigh less, retain water, are packable and can be produced to export standards (EDB, 2019). FF blocks with standard dimension (L230xW110xH80 *mm*) are imported and cut to the required sizes. Four distinct sizes of FF cubes required to accommodate different types of plants. Even though automated cutting machines are available (alibaba.com, D&T Industry Co. Ltd), they are expensive and not affordable by any of the local industries. Depending on the capacity, features and the level of automation the prices of machines available for online purchasing are in the range of US$ 3,000 to 15,000 (Hebei Huiya Floral Foam Special Equipment Co., Ltd., Everen Industry Co. Ltd.).

Mike Flora International (PVT) Ltd is one of the pioneering floriculture-based product exporters in Sri Lanka which exports around 17 million plants of 64 varieties annually to 20 countries around the world. It has a work force of around 300 people (Personnel communication, Mr. WMHD Weerakoon, Supervisor, Nursery Management, Mike Flora Pvt Ltd). They still use labour intensive methods to cut the FF block into cubes in four different sizes. This manual cutting is being done by using cutters made from 0.4 *mm* gauged steel wires fixed to a wooden frame (Fig.1). Since the FF cubes (Fig.2) are different in length, width and height, different sets of cutters with accurately spaced steel wires are required. The cutting should also be performed in two steps as the FF block need to be cut both horizontally and vertically. The manual cutting process which needs skilled labour is not only unproductive but also generates wastages due to odd shaped or deformed or unevenly sized cubes. The dust formation in the cutting process cause health hazards among workers. Further, the steel wires tend to erode and break frequently resulting high downtime. Having seen the mentioned deficits, an automated floral foam cutting machine

was designed and developed. The machine could be used by the others in this industry, which contributes to the GDP in Sri Lanka.

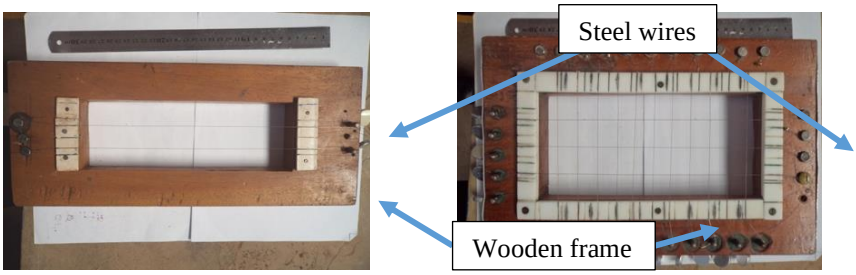

a. Vertical cutter b. Horizontal cutter

Fig.1. Horizontal and vertical cutters.

2 METHODOLOGY

This study was conducted at the premises of Mike Flora International (PVT) Ltd, located at Kalagedihena in the Gampaha district. Seeing deficiencies in the existing cutting process, an automated floral form cutting machine was developed to minimize the handling while cutting the floral foam, with more time efficiency, enhanced accuracy, and less wastage. The designing of machine was done considering the following aspects.

- System of operation.
- Structural integrity.
- Strength and durability of cutters.
- Time efficiency in handling and cutting.
- Accuracy in terms of shape and size.
- Wastage in cutting.
- Health hazards to workers.
- Capability of cutting different sizes of blocks (Fig.2) as per the requirement.

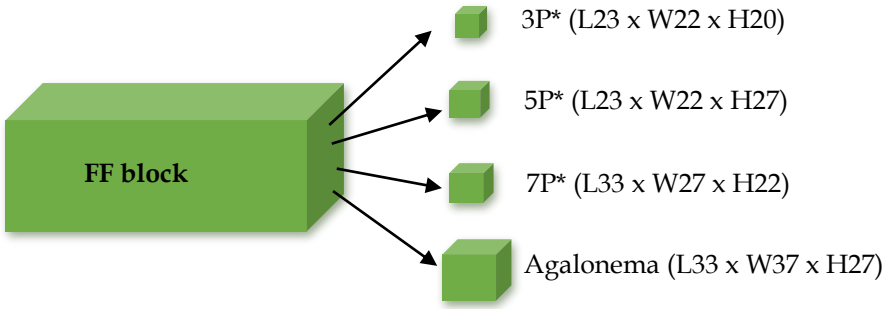

Fig.2. Different sizes (mm) of FF cubes required by the industry for plant types (P)

The aim is to develop the machine with low cost while incorporating necessary mechanical and electronic devices for automation. The four different sizes of FF cubes can be produced by just changing the cutters. The performance of the machine was compared with the existing manual process by considering the relevant aspects, using statistical techniques.

3 RESULTS AND DISCUSSION

3.1. Development of the Automated Floral Form Cutting Machine (AFFCM)

The AFFCM was designed and developed with the following main features.

Horizontal Cutters and Cutting Angles: Three different cutters, shown in Fig.3-a, b, c, (yellow, red, and blue colours) are made to accommodate different sizes of FF cubes as mentioned. Cutters were designed to attach and remove easily to the actuator mechanism. Fig.7 shows a cutter fixed to the machine.

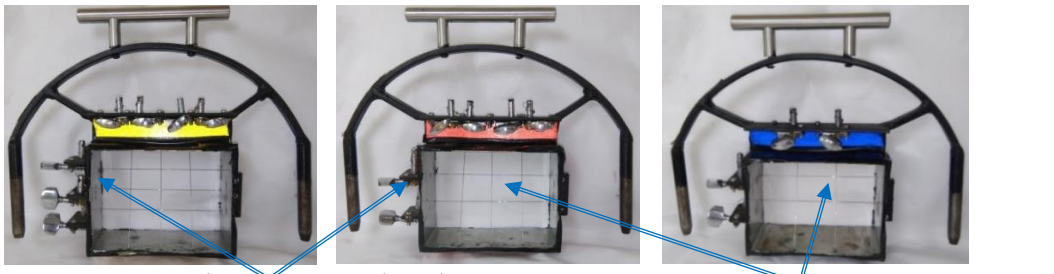

a. 3P cutter (yellow) **b. 5P/7P cutter (red)** **c. Agalonema cutter (blue)**

Fig.3. Three different types of horizontal cutters

The FF block is pushed through the cutting wires (of the horizontal cutter) to cut horizontally. Inclined angle of the wires β (Fig.4) is optimized to have a perfect cut with minimum deformation. The cutting force is also varying with β and the Table 1 gives the results of the trials. The best angle with minimum cutting force is 45°. However, considering many factors 55° angle is selected. The cutting quality is excellent at 55° and the selected piston can exert beyond 40 *N* force.

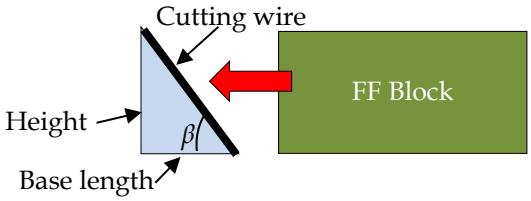

Fig.4. Horizontal cutting with cutting angle β

Table 1 Experimental results on horizontal cutting angle and force

Angle	Base length (*mm*)	Height (*mm*)	Force (*N*)
90^0	0	80	80
70^0	25	80	60
55^0	50	80	40
45^0	90	80	20

Vertical Cutters: The two vertical cutters are fabricated with appropriate spacing of SS wires. Similar to the horizontal cutters, guitar string adjusters are used to maintain the appropriate tension and differently coloured to easy identification (Fig.5). The wires are placed in such a way to coincide with the gaps of the vertical cutter box (Fig.7) which will cut the cubes to accurate sizes.

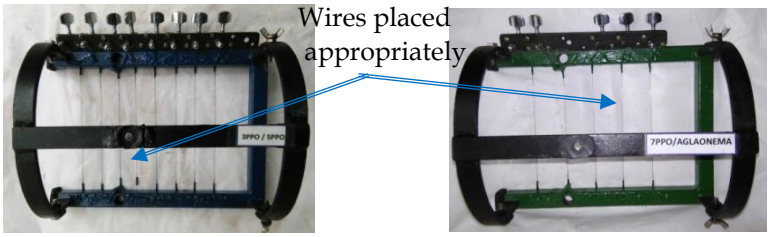

a. 3P/5P cutter b. 7P/Agalonema cutter

Fig.5. Fixed horizontals cutters

The movement of the vertical cutter is achieved by a pneumatically driven actuator attachment (Fig.7 and Fig.9). The most important aspect in the development of AFFAM was to carefully design the attachment to achieve the appropriate stroke of the actuator, and the static and dynamic balance in operation.

Actuator to Push FF block: Actuator and attachment as a unit, is made to push the FF block into the horizontal cutter imparting correct force and jerk. The actuator unit is made of 20 stainless steel pipes of gauge 16, as shown in Fig.6. Two steel shafting bars each 1*m* long, are used to obtain the movement to push the FF block.

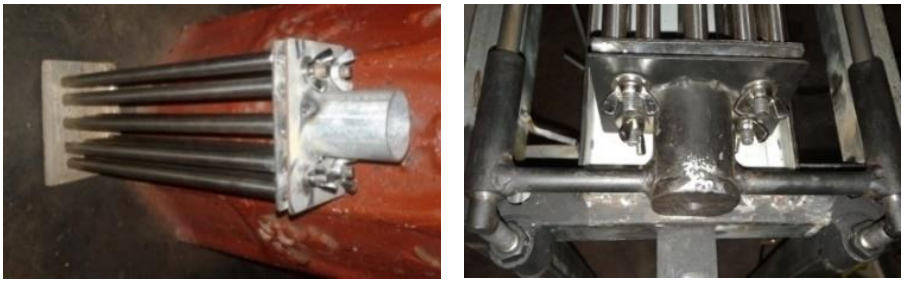

a. Actuator **b. Actuator fixed to the machine**

Fig. 6. Actuator and fixation

Control Panel: Control panel (Fig.9) consists of micro controller board, modular relays, circuit boards, etc., used for the purpose of programming the operations and power supply unit, and trip switch and fuses are used to transfer electric energy for entire operation, while the pneumatic system controls the operations. All the printed circuit boards (PCBs) are designed and manufactured inhouse.

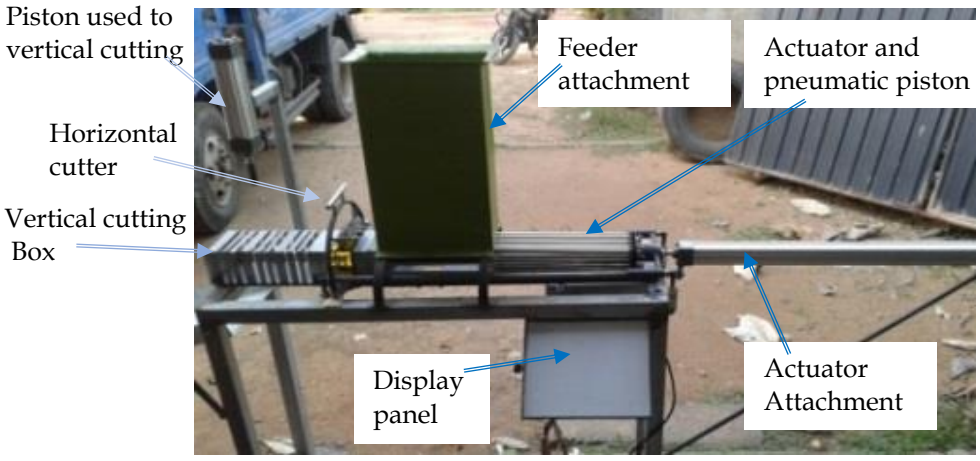

Fig.7. Actuator attachment and rest of the components at development stage

Arduino Uno has been used as the microcontroller, and 8 modular relays, LDR Sensor, circuit board, and other devices/accessories were used in automation. Exhaust fans were placed to minimize the dust deposition inside the control panel compartment.

Display Panel: The expanded view of the display panel is shown in Fig.8, which consists of pressure indicator, voltage indicator, error bulb, ON/OFF switch, start and reset switches and real time operation indicators.

Fig.8. Display panel of the machine

3.2. Developed Prototype of AFFCM

A structure is made by Zinc coded steel box bars (38 x 38 mm^2) and L shaped cross-sectioned bars (25 *mm*) after considering the structural integrity of the machine. A steel plate was sized and machine-bended to make the feeder compartment (Fig.9) which directs the loaded foam to cutting section in anticipated orientations.

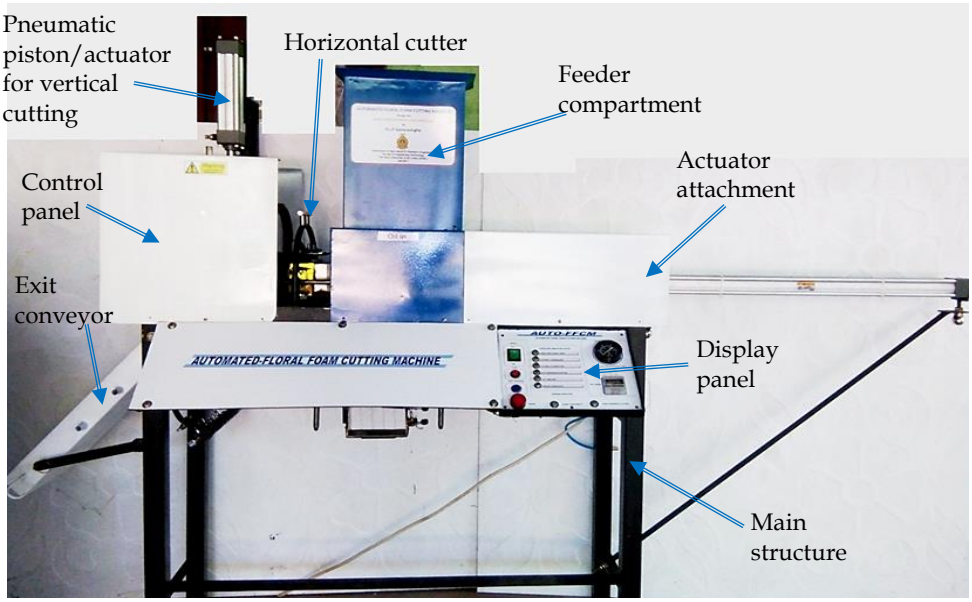

Fig.9. The final outlook of the AFFCM

Operation Sequence of the AFFCM

Five FF blocks could be accommodated in the feeder. The machine is activated when it is switched on (by ON/ OFF switch). The activation of the machine could be detected by the voltage meter on display panel. The compressor starts and triggers the pneumatic pistons/circuit. The air pressure could be checked by the pressure indicator/gauge which the optimum level is 8 bars. A pneumatic regulator is used to maintain the optimum pressure in each pneumatic piston. After attaining the correct air pressure, the Start button (on display panel) pushed on, which supplies power and activates the microcontroller and the LDR sensor sense and checked the availability of foam in the feeder. If available, the process continues, if not, it indicates the non-availability. If there are FF blocks in the feeder, the servo motors will activate and runs for around 3 *seconds* which opens the path, and the FF blocks move or rather fell into the specifically designed platform. The availability of foam in the platform is indicated by the 'floral foam feeder open' bulb in the display panel. Then a solenoid valve triggers, and a pneumatic piston activates. The relevant obstacle mechanism to restrict the motion of the FF block is also activated. The FF block is pushed through horizontal cutter to cut horizontally and then pushed into the vertical cutting box. The completion of horizontal cutting is indicated by blinking 'cutting 1 completed' blub on the display panel.

Then for vertical cutting, a signal is sent to the solenoid valve from micro control board and the movement of the vertical cutters are executed by activating the relevant pneumatic piston. The completion of vertical cutting indicates by blinking 'cutting 2 completed' blub on the display panel. This process completes in 1.5 seconds. Exhaust fans are switched on, and the dust is removed as the 'dust removing system on' bulb blinks. The exit door opens while the 'cut cube exit' bulb glows. Then the FF cubes are pushed to the basket kept outside through the exit conveyor. The pneumatic piston returns to the initial position completing one operational cycle by blinking the 'process complete' bulb along with an alarm.

The operator must reset the system/machine to start a new cycle. If the cutters are not properly located the machine will not work and it signals an 'error' and 'check horizontal cutter' starts blinking. The operator ascertains that the cutters are accurately located before starting a fresh cycle. Also, the status of presence of floral foam cubes in the feeder is indicated by the 'floral foam empty' bulb.

3.3. Comparison of the Performance of the AFFCM with the Existing Process

3.3.1. Cutting Efficiency

The cutting duration (average of five cycles) for four different sizes of FF cubes by existing method and by the AFFCM are given in Table 2.

Table 2 Cutting durations of existing method and new method average

Size	Existing Method (*s*)	AFFCM (*s*)	Time efficiency of AFFCM (%)
3P	16.4	3	81.71
5P	14.4	3	79.17
7P	12.5	3	76.00
Agalonema	10.4	3	71.15

As expected, there are no variations of cutting durations in AFFCM since it operates conforming to a programmed operational cycle. It is evident that smaller the cube size higher the average time taken to produce manually, whereas for the AFFCM the size does not matter. Hence higher efficiency could be obtained for smaller sizes by the AFFCM. The time efficiency varies from 71% of largest cube to 81% smallest as indicted.

3.3.2. Dust Formation and Cutting Accuracy

During the process of cutting, one of the major problems with existing method is the formation of dust. Dust collected after cutting of 10 FF blocks are given in Table 3. The results revealed that on average 69% of the dust formation or wastage can be reduced by using the AFFCM.

Table 3 Dust formation in two methods of FF cutting

Method	Quantity of Dust (*g*)
Existing method	0.166
AFFCM	0.051

Table 4 depicts the average differences (percentages) of the dimensions of FF cubes with required standard values. The differences vary from 1.5 to 19.62 with an average of 9.28 percent in the manual method. In contrast, AFFCM has 0.67 percent change resulting higher accuracy. These results are further justified by much lower SD values pertaining to AFFCM method compared to manual method.

Table 4 Cutting accuracy of two methods of FF cutting
(*Values in the parenthesis are the SD)*

		Expected Dimension (*mm*)	Percentage change from expected- Manual method	Percentage change from expected- AFFCM
3P	L	**23**	6.35 (1.05)	0.82 (0.57)
	W*	**22**	10.91 (1.12)	4.10 (0.63)
	H	**20**	1.50 (1.23)	0.69 (0.45)
5P	L	**23**	5.57 (0.70)	0.16 (0.44)
	W	**22**	10.64 (0.75)	0.41 (0.41)
	H	**27**	6.44 (0.75)	0.48 (0.43)
7P	L	**33**	10.24 (0.94)	0.34 (0.50)
	W	**22**	13.00 (0.83)	0.48 (0.52)
	H	**27**	7.48 (0.93)	0.08 (0.42)
Agalonema	L	**33**	10.24 (0.72)	0.00 (0.40)
	W	**37**	19.62 (0.66)	0.07 (0.42)
	H	**27**	9.33 (0.64)	0.41 (0.47)
Average			**9.28**	**0.67**

3.3.3. Cost of Manufacturing and Effectiveness of AFFCM

Cost of Manufacturing

The cost to manufacture per machine locally, which covers purchasing of components such as, microcontroller, programming, pneumatics system, etc., workmanship and materials with 10% contingency as estimated, is approximately SLR 140,000.00 compared to the lowest internationally tagged price of SLR 600,000.00 (approximately, USD 3000).

Operation and Maintenance Cost

The Mike Flora International (PVT) Ltd is producing FF cubes from around 58,000 FF blocks per month as given in Table 5 (from an interview with Mr. WMHD Weerakoon, Supervisor, Nursery Management, Mike Flora (Pvt) Ltd). The requirement of man days and the incurred costs are also given in Table 5, which calculated as if the daily wage rate is SLR 1,000.00 per person and an individual person works 8 hours per day. For AFFCM the time required for cutting blocks does not vary with the size of the cubes and total labor cost per month was calculated as SLR 60,41.67. In contrast to the existing manual method the labor cost incurred in AFFCM was SLR 28,965.28 saving SLR 22,923.61 per month. Even with an assumed overhead (mainly for electricity and, wear and tear) of SLR 5,000.00 per month, it is worthwhile to use mechanization over the manual method, by which the capital cost can be recovered within eight months (payback period is 7.67 months). The payback period would be further reduced if the cost saved by reduction of wastages is considered for the calculation.

Table 5 Operation and maintenance cost

Cutting method	**Cutting time required (*s/block*)**	**Micro Flora Requirement (*blocks/month*)**	**Labour hour requirement**	**Labour cost at SLR 125/*hr.* (*SLR/month*)**
Existing method	16.4	25,000	113.89	14,236.11
	14.4	15,000	60.00	7,500.00
	12.5	10,000	34.72	4,340.28
	10.4	8,000	23.11	2,888.89
	Total	**58,000**		**28,965.28**
AFFCM	3	58,000	48.33	6,041.67

4 CONCLUSIONS

The AFFCM was designed and developed after a detailed investigation to improve the productivity and product accuracy of the FF cubes which are comparable with FF blocks. The designed and developed AFFCM can be manufactured at a cost of SLR 137,453.00, which is relatively inexpensive when compared with those available in the international market, which a machine with minimum features would cost around US$ 3,000 (more than SLR 600,000). It is worthwhile to note that the as far as the features, productivity, product accuracy, etc., are concerned of the proposed AFFCM is superior and it can comfortably compete in the market. The AFFCM saves 71% to 80% (depending on block size) time than the existing method and could produce four sizes of FF cubes with higher accuracy, less wastage and minimum dust formation. This machine could reduce the labour cost by

almost 80% and therefore the capital cost of the machine can be recovered within eight months of operation. The manufactured AFFCM can be commercialized with the assistance of an investor.

5 ACKNOWLEDGEMENTS

The authors acknowledge the Mike Flora (Pvt) Ltd for providing the place and the technical assistant to carry out the study.

REFERENCES

De Silva, P.D. (2014). Sri Lanka could be a regional leader in floriculture exports: Daily FT e-paper.http://www.ft.lk/agriculture/srilanka-could-be-a-regional-leader-infloriculture-exports-prof-ranjithsenarathne/31-265076

Dhanasekera, D.M.U.B. (1998). Cut flower production in Sri Lanka. Food and Agriculture Organization of the United Nations Publication.

Export Development Board (EDB). (2019). Future Potential of Floriculture Industry in Sri Lanka. http://www.srilankabusiness.com/ blog/floriculture-in-sri-lanka.html

Profitability of floriculture. Daily News e-paper. (2017). http://www.dailynews.lk/2017/04/07/business/112712/profitability-floriculture.

Rathnayake, S. and Rathnayake, S.J. (2019). An Overview of Upcountry Cut Flower Industry, Sri Lanka. Asian Journal of Agricultural Extension, Economics & Sociology 33(1): 1. DOI: 10.9734/ajaees/2019/v33i130167

https://www.alibaba.com/showroom/floral-foam-cutting-machine.html

https://en.dtfirm.com/product/69.html

https://www.made-in-china.com/showroom/huiyalichee/product-detailTSbxAaVUutpv/China-Wet-Floral-Foam-Cutting-Machine.html

https://everen.en.alibaba.com/search/product?SearchText=cutting%20machine

Journal of Engineering and Technology
of The Open University of Sri Lanka (JET-OUSL), Vol. 08, No.2, pp 11-21

Comparison of the spread angle of a swirling jet with a non- swirling jet

T. K. S. Pushpakumara, I. U. Atthanayake*

Department of Mechanical Engineering, The Open University of Sri Lanka, Nawala, Nugegoda, Sri Lanka.

*Corresponding Author: email: iuatt@ou.ac.lk, Tele: +94112881318

Abstract – *Swirling jets are prevalent in nature and technology. Tornados and dust devils are example from nature where as propulsion systems in turbomachinery are example from technology. Therefor understanding the behaviour of swirling jets and their prominent features is very important to either predict the behaviour or enhance the performance of swirling jets, depending on the application In this paper an experimental results done on spread angle of a 'Swirling jet', released to an ambient environment of fluid are presented. Moreover the swirling jet spread angle is compared with the non swirling jet issued from the same nozzle. The experimental set up was built in house with all the necessary features including a rotating source, to perform the experiments. It was revealed that the spread angle of the swirling jet is greater than the that of the non swirling jet. Also the time dependency of the value of the spread angle of the swirling jet is higher than that of the non swirling jet. It can be recommended that by using swirling flows in industrial applications better spread of materials can be achieved from the beginning of the flow.*

Keywords*: Swirling jet, Spread angle*

1 INTRODUCTION

A flow is said to be "Swirling" when its mean direction of flow is aligned with its rotation axis, implying helical particle trajectories. There are atmospheric conditions that can give rise to swirling flows such as tornados, dust devils and water-spouts. On the other hand swirling flows are also observed in many engineering applications, such as combustion chambers of jet engines, turbo machinery and mixing tanks. In combustion applications, swirling jet's ability to create reverse flow regions near the jet nozzle has been exploited for the purpose of swirl-stabilizing the flame. The efficiency of chemical reactors and mixing devices is enhanced by making use of the faster spreading and more rapid mixing of the jet fluid with its surrounding by swirling compared with non- swirling jets. Therefore understanding the spread angle characteristics of a swirling jet is highly important. The present study focuses on quantify the variation of the spread angle of a swirling jet and compare the same with the non swirling jet issued by the same nozzle. The spread angle of a jet can be defined as the angle between two edges across the diameter of the jet when it is issued from a circular nozzle as shown in figure 1.

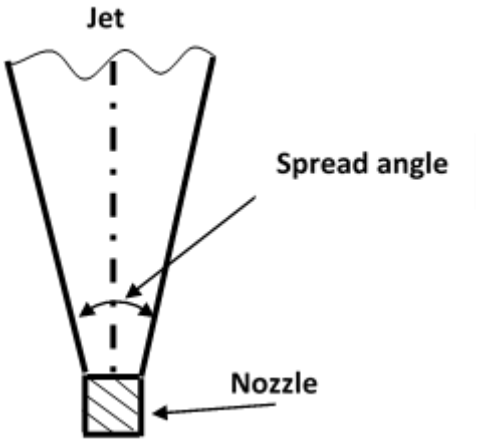

Fig. 1: Schematic diagram of a jet

2 LITERATURE REVIEW

The studies on swirling jets were motivated to analyse the flow characteristics in variety of propulsion systems involving turbo machinery, such as jet engines and turbo-pumps. In gas turbine engines, diesel engines, industrial burners, and boilers, swirling flows were originally used to control the mixing rate between fuel and oxidant streams in order to achieve flame geometries and heat release rates appropriate to the particular process application (Weber et al., 1986). Swithenbank & Chigier (1986) concluded that for a sufficient degree of swirl an internal recirculation zone is generated. This zone allows a high rate of heat release as products of combustion are recirculated and ignite the incoming fuel/oxidant streams where a stable and compact flame is generated. Syred & Beer (1974) also confirmed that this enhances the performance of difficult carbonaceous materials and poor quality gases. Therefore swirling jets have been the subject of numerous studies in the past (Kopecky & Torrance, 1973; Lessen et al., 1974; Leibovich & Stewartson, 1983; Khorrami, 1991; Mayer & Powell, 1992; Billant et al., 1998; Gallaire et al., 2004; Liang & Maxworthy, 2005; Facciolo et al., 2007; Liang & Maxworthy, 2008; Oberleithner et al., 2011; Leclaire & Jacquin, 2011). The common feature that was found is that these jets break down due to a vortex break down. It is also concluded that this breakdown is characterized by a transition of a jet-like axial velocity profile to a wake-like prole with a local minimum on the axis which leads to a stagnation point to be followed by a highly turbulent region of reverse flow farther downstream (Oberleithner et al., 2011). Therefore most recent experimental studies on swirling jets have focused on understanding the fundamental features of vortex breakdown that occurs in the flow (Liang & Maxworthy, 2005, 2008; Martinelli et al., 2007; Oberleithner et al., 2011; Meliga et al., 2012).

Moreover, most of the relevant numerical work available in literature has also been focused on this common vortex break down feature in swirling jets (Melville, 1996; Mùller & Kleiser, 2008a; Qadri et al., 2013; Luginsland, 2015; Luginsland & Kleiser, 2015; Luginsland et al., 2016). In all these studies, it has more or less been revealed that the vortex breakdown mode is consistent with helical mode break down either with single helix or double helix. But the spread angle of a swirling jet before vortex breakdown has not been investigated so far and it has not been compared with the non swirling jet issued by the same nozzle.

3 METHODOLOGY

3.1 Design and fabrication of the experimental facility

The experimental facility was built inhouse and it consists of a transparent wall tank, nozzle arrangement for generating the swirling jet, flow meter, reservoir tank and a control panel to vary the rotating speed of the nozzle.

The schematic diagram of the experimental setup is shown in figure 2. The tank has the cross sectional area of 1m × 1m and height of 1.5m and for the walls of the tank Perspex boards were used. The tank was mounted on a frame fabricated from iron as shown in figure 3. Perspex is transparent material and has required strength to withstand the pressure when the tank is filled with water. The nozzle arrangement was fixed to the centre of the bottom plate as shown in figure 4. The nozzle assembly was made such away that it rotates while issuing the flow or the jet to the ambient environment, i.e. water inside the tank. The required potential head for generating the jet flow was achieved by an overhead tank built separately. A control panel was used to vary the rotation rate of the nozzle. A flow meter fixed in between the flow from the overhead tank to the nozzle arrangement, was used to measure the flow rate.

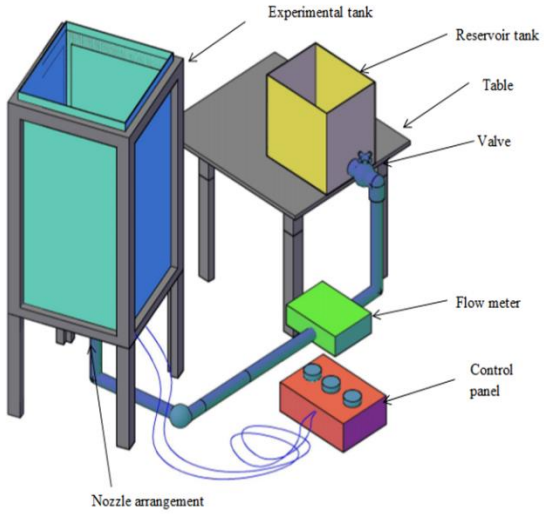

Fig. 2. Schematic diagram of the experimental facility

The nozzle was given the required rotation rate by a motor attached to a pulley and belt system of which the schematic diagram is shown in figure 5. The most important and challenging part of the design of the experimental facility is the designing of the rotating nozzle. The releasing of the flow through the nozzle should be done while rotating and there should be a proper mechanism to accommodate this without leaking the water in the tank, as the nozzle is fixed at the bottom of the tank as shown in figure 3.

Fig. 3. The tank with transparent Perspex walls

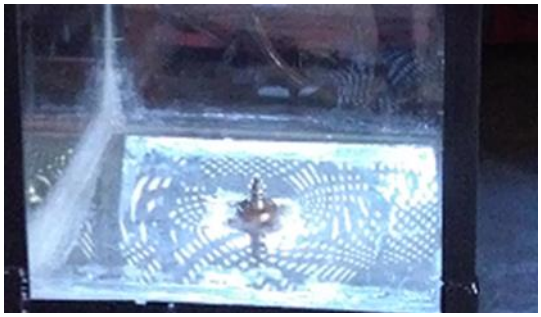

Fig. 4. A closer look of the nozzle assembly fixed to the bottom of the tank

The schematic diagram of the nozzle driving mechanism is shown in figure 4 whereas the fabricated nozzle arrangement is shown in figure 5. The nozzle arrangement was fabricated using steel and to prevent the water leaking while the nozzle is rotating, some water seals were used.

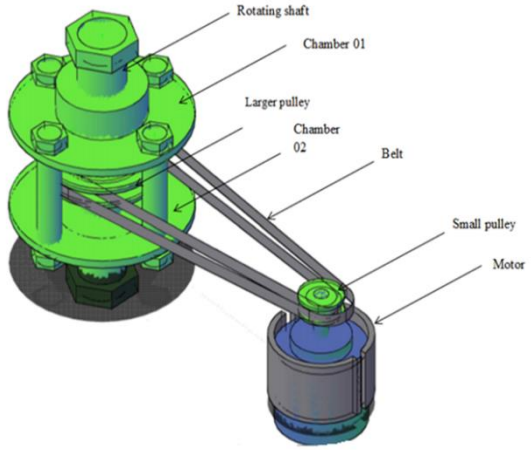

Fig. 5. Schematic diagram of the pulley and belt arrangement fixed to the nozzle assembly

Fig. 6. Fabricated nozzle and pully arrangement

3.2 Flow visualization and data analysis

The flow visualisation technique used in the present study is the use of dye for the swirling jet so that it can be clearly visualised when it flows through the tank of clear water. Blue colour dye was used. The dye was added to the reservoir tank from which the water flow through the swirling jet nozzle. Figure 6 shows a snapshot of the jet flows through the clear water tank. The data gathering was done by means of recording videos of the jet flow and analysing frames of the videos. At first the camera was set using a tripod and the flow area

was focused. Then the jet flow was started and at the same time recording of the video was also started. The images were extracted from the videos and then the same were imported to MATLAB software. All the analysis was done using MATLAB software. At first the experiment was done without rotating the nozzle to quantify the spread angle of a non swirling jet. A line was first drawn through the centre of the nozzle of the image selected for analysis from the video recording. Then the radial distance (R) from the centreline to the edge of the horizontal spread was measured and g. also the hypotenuse distance (L) was also measured. The spread angles were calculated by taking the inverse value of sin of the ratio L/H. The distance measurement arrangement for an image on MATLAB user interface is shown in figure 7.

Fig. 7. Snapshot of the jet after 3 s of starting the jet flow.

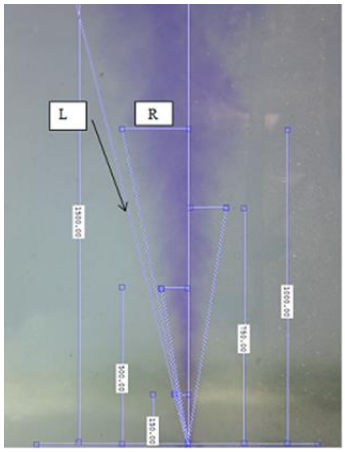

Fig. 8. Snapshot analysis in MATLAB interface

After completing the experiment with non-swirling jet, the whole experiment tank was emptied as the water inside the tank had turned into colour of the ink as shown in figure 9, where the jet is not very clear from the background. Then the tank was filled with clear water and the experiments on swirling jet was performed similar manner as in the case of non swirling jet and the videos were started to record as the jet flow starts. The angular velocity of the rotating nozzle was $4.189\ \mathrm{rad/s}$ and the flow rate was $6.68 \times 10^{-5}\ m^3/s$.

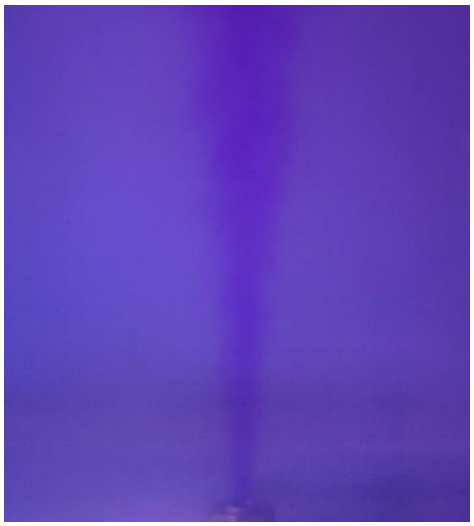

Fig. 9. The colour of the water in the tank after releasing the jet for 180s

4 RESULTS

4.1 Spread angle of the non-swirling jet

The half spread angle was calculated for selected heights from the jet issuing nozzle and at different transient conditions as well. The jet half spread angle was measured right hand side of the centre line and left hand side. Figure 11 shows the snapshot of an image extracted from the video recorded of the jet in MATLAB interface after 60s of starting the jet. The average half spread angle was calculated by averaging values calculated from the right hand side and left hand side and the time i.e. average values from the snapshots during the video, the present frame rate of the camera is 30 frames per minute. The values measured by pixels in the MATLAB interface were converted to millimeters by using the reference as the nozzle diameter. When the image was enlarged and the nozzle diameter to pixel ratio can easily be measured.

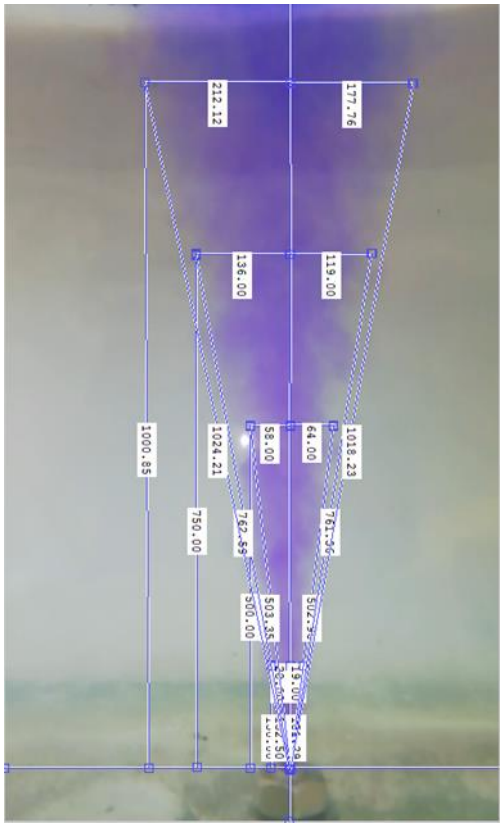

Fig. 10. Snapshot analysis of the jet at 60s after starting the jet

The average of the half spread spatial angle (i.e. average value of the spread angle right to the centreline and left to the same) plotted against the jet height is shown in figure 11. It can be seen from the graph that the half spread angle varies from 7^0 to 10^0 when it is measured independently along the height. By assuming the symmetry the full spread angle of the jet can be calculated by multiplying the half spread angle by two. The jet is observed to be highly time dependent as the spread angle of one location at selected height was measured with time. The variation of the spread angle is shown in figure 12, where the observation height is 132mm from the nozzle.

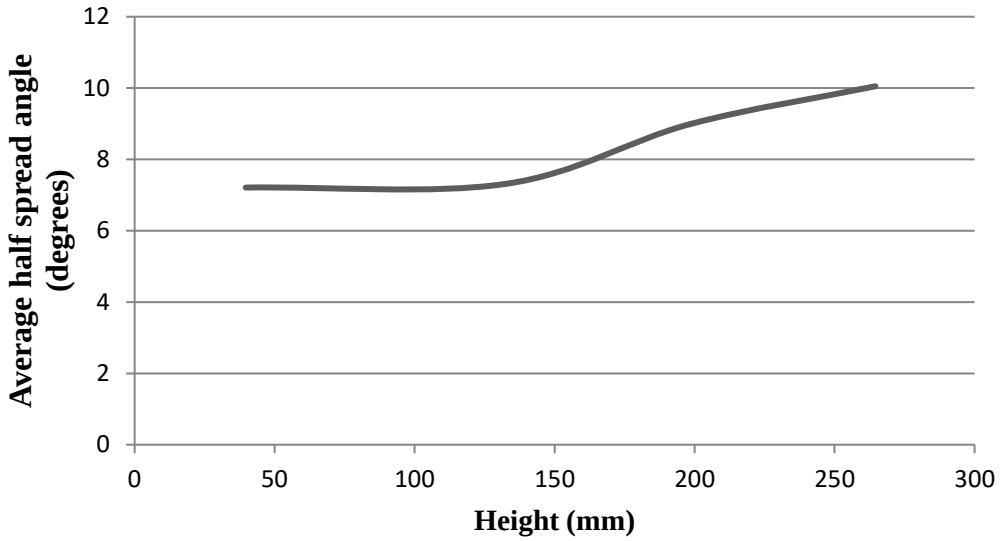

Fig. 11. Variation of the average of half spread angle with the jet height at 60s after starting the jet.

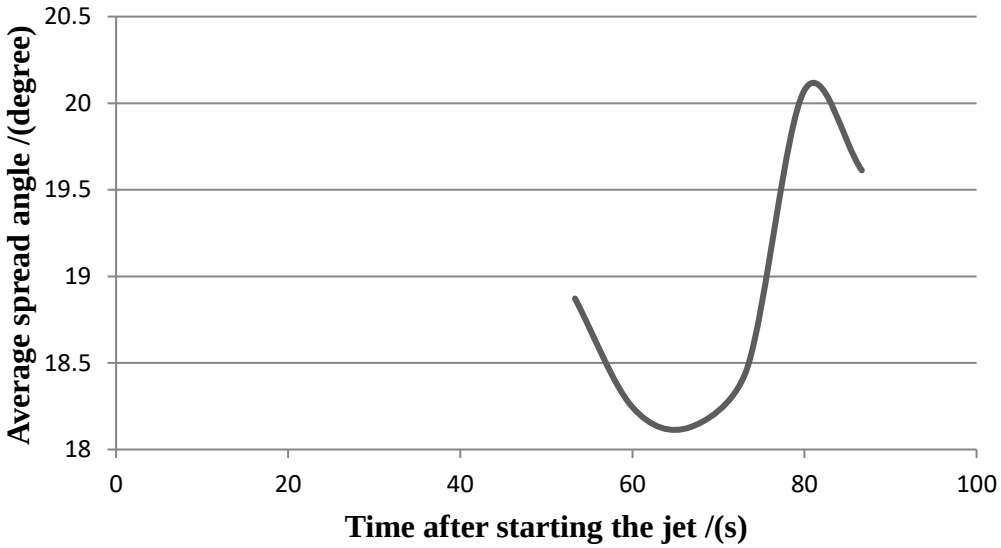

Fig. 12. Variation of the spread angle with time after starting the jet (jet height is 132mm)

4.2 Spread angle of the swirling jet

The variation of the average of the half spread angle of the swirling jet with the height from the nozzle, after 60 s of starting the jet, is shown in figure 12. It can be seen from figure 11, that average of the half spread angle varies between 18^0 to 25^0, which indicated that the full spread angle of the swirling jet is in the range of 36^0 to 50^0. Figure 12 shows the variation of the average half spread angle with the time. It can be seen from the figure that the value of the average half spread angle varies rapidly with time compared to the figure 10, which shows the same for the non swirling jet.

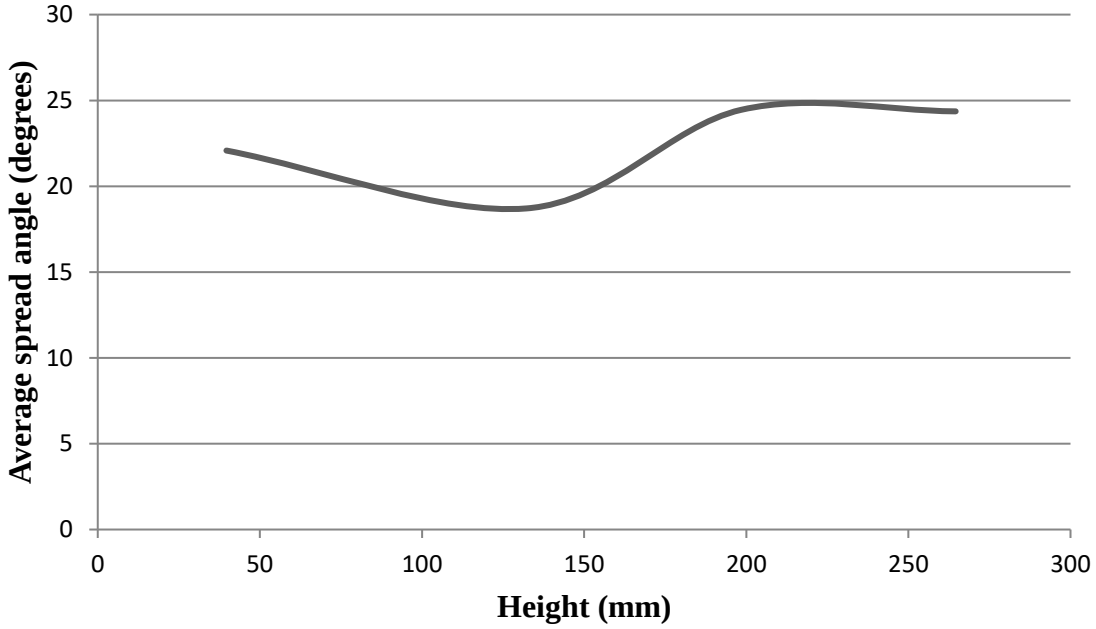

Fig. 13. Variation of average spread angle with the jet height at 60s after starting the jet.

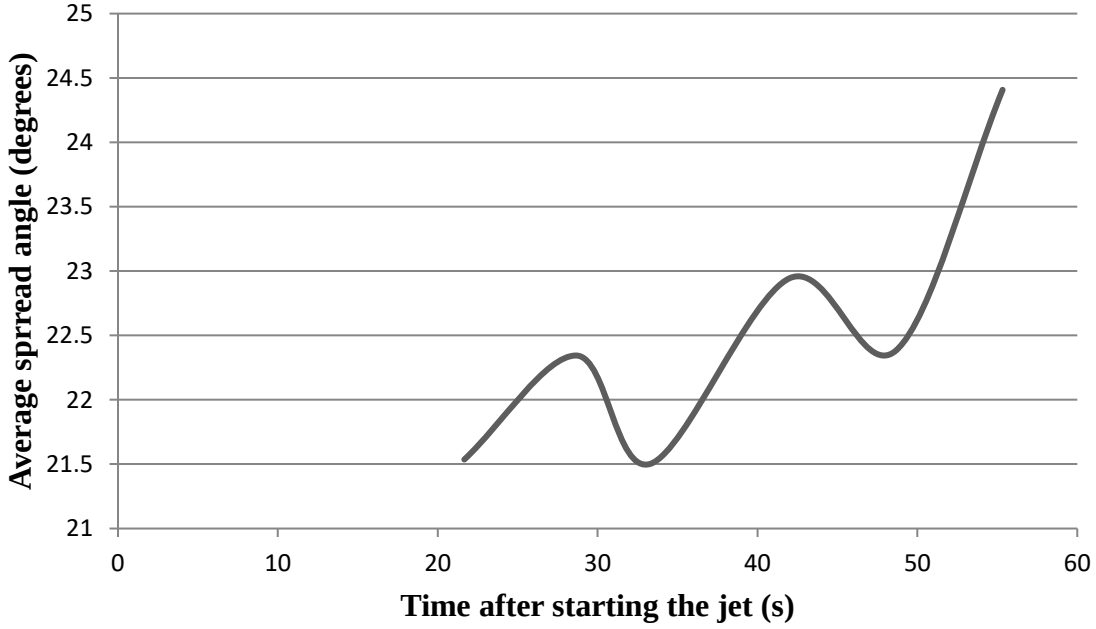

Fig. 14. Variation of the spread angle with time after starting the jet (jet height is 132mm)

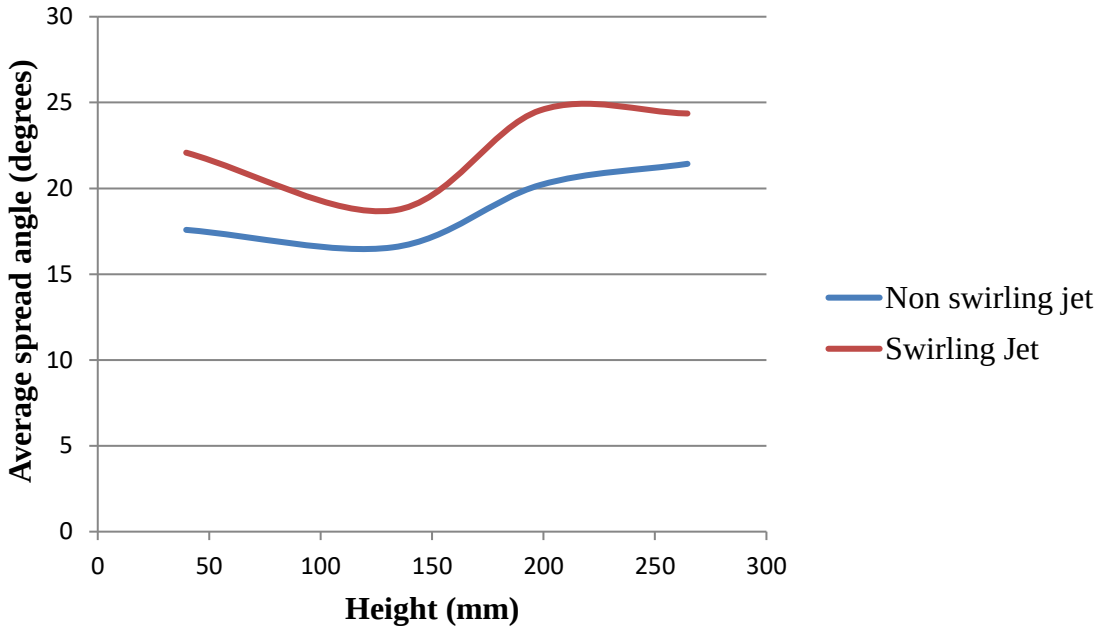

Fig. 15. Variation of the spread angle with height for the non swirling jet and the swirling jet.

5 CONCLUSION

The comparison of the spread angle of a swirling and non swirling jets has not been performed directly by the researchers who have done their studies on swirling jets. In the present study the spread angle of a swirling jet is compared with a non swirling jet. The experimental set up was built in house to carry out the experiment. The challenging part of the experiment set up building was to fabricate the jet issuing nozzle, where the fluid should be ejected while rotating the nozzle. On the other hand the nozzle was fixed at the bottom of the tank so that while rotating no water should be leaked from the bottom of the tank. The dye visualisation techniques was used to gather data and MATLAB was used to analyse the images of dye visualisation. The spread angle of the non swirling jet was observed to vary between 18^0 to 20^0. The measured spread angle value for non swirling jet confirms the accuracy of measurement technique and data analysis technique where the spread angle results of the non swirling jets found by other researchers also lies between the values 18^0 to 20^0. On the other hand from the observation it can be seen that the spread angle value of the non swirling jet is comparatively less time dependant than the swirling jet. It was observed that the spread angle of the swirling jet is greater than that of the non swirling jet for all heights of the jet and varying between 21.5^0 to 24.5^0. Therefore a wider spread angle can be achieved by a swirling jet but too much speed of the nozzle leads to break down of the jet as observed by the many researchers.

6 ACKNOWLEDGEMENTS

The authors are thankful to Mr. K.C. K Deraniyagala and Mr. P. K. Sisira Kumara. For their technical support on the design and fabrication of experimental set up.

REFERENCES

Billant, P., Chomaz, J. M., & Huerre, P. (1998). Experimental study of vortex breakdown in

swirling jets. *Journal of Fluid Mechanics*, 376, pp. 183-219.

Gallaire, F., Rott, S., & Chomaz, J. (2004). Experimental study of a free and forced swirling jet. *Physics of Fluids*, 16 , pp. 2907-2917.

Kopecky, R. M., & Torrance, K. E. (1973). Initiation and structure of axisymmetric eddies in a rotating stream. *Computers Fluids*, pp. 289-300.

Khorrami, M. R. (1991). On the viscous modes of instability of a trailing line vortex. *Journal of Fluid Mechanics*, 225, pp. 197-212.

Leclaire, B., & Jacquin, L. (2011). On the generation of swirling jets: high Reynolds number rotating flow in a pipe with a final contraction. *Journal of Fluid Mechanics*, 692, 78-111.

Lessen, M., Paillet, F., & Singh, P. J. (1974). The stability of a trailing line vortex. part 1. inviscid theory. *Journal of Fluid Mechanics*, 63, pp. 753-763.

Leibovich, S., & Stewartson, K. (1983). A sufficient condition for the instability of columnar vortices. *Journal of Fluid Mechanics*, 126, pp. 335-356.

Liang, H., & Maxworthy, T. (2005). An experimental investigation of swirling jets. *Journal of Fluid Mechanics*, 525, pp. 115-159.

Luginsland, T. (2015). How the nozzle geometry impacts vortex breakdown in compressible swirling-jet flows. *AIAA Journal*, 53 (10), 2936-2950.

Luginsland, T., Gallaire, F., & Kleiser, L. (2016). Impact of rotating and fixed nozzles on vortex breakdown in compressible swirling jet flows. *European Journal of Mechanics - B/Fluids*, 57, 214 -230.

Luginsland, T., & Kleiser, L. (2015). Effects of boundary conditions on vortex breakdown in compressible swirling jet flow simulations. *Computers & Fluids*, 109(C), 7284.

Mayer, E. W., & Powell, K. G. (1992). Viscous and inviscid instabilities of a trailing vortex. *Journal of Fluid Mechanics*, 245, pp. 91-114.

Martinelli, F., Olivani, A., & Coghe, A. (2007). Experimental analysis of the precessing vortex core in a free swirling jet. *Experiments in Fluids*, 42, 814-841.

Meliga, P., Gallaire, F., & Chomaz, J.-M. (2012). A weakly nonlinear mechanism for mode selection in swirling jets. *Journal of Fluid Mechanics*, 699, 216-262.

Melville, R. (1996). The role of compressibility in free vortex breakdown. AIAA, 2075 , pp. 116.

Muller, S., & Kleiser, L. (2008a). Large-eddy simulation of vortex breakdown in compressible swirling jet flow. *Computers & Fluids*, 37 (7), 844 - 856.

Oberleithner, K., Sieber, M., Nayeri, C., Paschereit, C., Petz, C., Hege, H., Noack, B., & Wygnanski, I. (2011). Three-dimensional coherent structures in a swirling jet undergoing vortex breakdown: stability analysis and empirical mode construction. *Journal of Fluid Mechanics*, 679, pp. 383-414.

Qadri, U. A., Mistry, D., & Juniper, M. P. (2013). Structural sensitivity of spiral vortex breakdown. *Journal of Fluid Mechanics*, 720, 558-581.

Syred, N., & Béer, J. M. (1972). The damping of precessing vortex cores by combustion in swirl generators. *Astronautica Acta*, 23 , pp. 783-801.

Swithenbank, J., & Chigier, N. A. (1986). Vortex mixing for supersonic combustion. *In 21st International Symposium on Combustion*, pp. 1154-1162.

Weber, R., Boysan, F., Swithenbank, J., & Roberts, P. A. (1986). Computation of near field aerodynamics of swirling expanding flows. *In 21st International Symposium on Combustion*, pp. 1435-1443.

Journal of Engineering and Technology
of The Open University of Sri Lanka (JET-OUSL), Vol. 8, No.2. pp 22-34

Design of a mobile device charger using a Stand-alone PV System

P. W. D. M. Fernando, R. H. G. Sasikala*

Department of Electrical and Computer Engineering, The Open University of Sri Lanka, Nawala, Nugegoda, Sri Lanka

*Corresponding Author: email: rhsas@ou.ac.lk, Tele: +94112881272

Abstract – *Stand-alone photovoltaic (PV) systems with battery banks are ideal for remote rural areas and applications where other power sources are either impractical or are unavailable. The solar-powered mobile phone charging station is considered as one of the stand-alone PV systems invented as the solution for mobile travellers to charge their mobile devices since portable batteries or DC buses are not commonly available among the general public.*

The major problem with the photovoltaic charging system is the energy conversion efficiency of solar panel and load fluctuation. Therefore, to provide continuous electrical power supply to the load, a storage facility must be used. The efficient charging system is required with lesser charging time to store solar energy within the battery. This study proposed implementing a 12 V DC bus with a stand-alone PV system, including voltage reference Maximum Power Point Tracking (MPPT) system and a battery backup. This would be an alternative to the above-mentioned solar-powered mobile charging station considering the cost, accessibility and mobility.

Therefore, the proposed system used a control circuit to manage the output power of the solar panel. It used the fractional open circuit voltage MPPT algorithm, and as necessary it controls the voltage by checking the load conditions. This system mainly consists of two DC-DC buck converters, 50 W solar panel, microcontroller, 12 V battery, controllable switches and USB ports to connect the mobile device for charging. The controller unit does MPPT process and PWM generation, battery monitoring for overcharging and over discharging process.
The proposed stand-alone PV system is equipped with 12 V DC bus and two 5V USB ports that can be used to charge the mobile phones, pad, iPhone and tablets etc. This system can be used in places such as bus stands and communities inaccessible to the national grid. At the emergencies, people can charge their mobile devices only using the USB cable. The proposed system can be used throughout the day since the system equipped with a battery backup.

***Keywords**: Buck converters, maximum power point tracking, photovoltaic systems, voltage reference*

1 INTRODUCTION

Solar energy is one type of renewable energy, which plays a significant role in the present energy market. Converting solar energy to electrical energy is one form of the application using grid-connected and off-grid electricity systems. The photovoltaic systems which use solar panels are most popular as stand-alone PV systems at present. The solar-powered mobile phone charging station is considered one of the stand-alone PV systems invented as the solution for travellers to charge their mobile devices since portable batteries or DC buses are not commonly available among the general public. The major problem with the photovoltaic charging system is the energy conversion efficiency of

solar panel and load fluctuation. Solar panels convert solar energy directly into the electricity. Ordinarily, solar panels convert 15% - 20% of energy incident on it into electrical energy (Agrawal and Tiwari, 2011). The output of the solar cell does not have the linear V-I characteristic. According to the climate, solar radiation varies from time to time; hence, the solar panel's energy fluctuates. Also, the demand from the load does not always equal to the solar panel capacity. Therefore, to provide continuous electrical power supply to the load, a storage facility is required. The efficient charging system is required with lesser charging time to store solar energy within the battery. Most of the systems used the Maximum Power Point Tracking (MPPT) system to get the maximum output from the solar panel. The maximum power extracted from the PV panels depends mainly on three factors such as irradiation, ambient temperature and the load.

Nowadays, there are vast numbers of houses having rooftop solar systems as net metering. The problem is when installing the rooftop solar systems total panel capacity is selected much greater than the chosen inverter capacity. The oversizing of solar panels increases energy production because usually panel does not produce its rated power and commonly PV systems used the MPPT to extract the maximum power from the panels. Because of this extra sizing of panels, inverters can run at higher efficiency. But rarely at right weather conditions, these panels produce the rated power. This will not be a problem if the sizing of panels considers the power tolerance of the inverter. But most of the systems do not assess the inverter stability and hence always system is always disconnected when sensing the overvoltage. Actually, at that time energy is available but cannot be extracted because the system is already disconnected. Therefore, we can't extract the available power. It is a waste of energy. By introducing a battery charging with a stand-alone PV system, this paper suggests a method to use that available power in the PV system.

This study proposed implementing 12 V DC bus with a stand-alone PV system, including voltage tracking MPPT (Maximum Power Point Tracking) system and a battery backup. This would be an alternative to the above-mentioned solar-powered mobile charging station considering the cost, accessibility and mobility. This system uses a control circuit to manage the output power of the solar panel by checking the load condition.

The proposed stand-alone PV system is mainly included with 12 V DC bus and additional two 5 V USB ports which can be used to charge the mobile phones, pad, iPhone and tablets etc. This system can be used in bus stands and areas where people live without electricity access. At the emergencies, people can charge their phones only using the USB cable. The proposed system can be used in the daytime and at the night-time using the battery backup.

2 LITERATURE SURVEY

Voltage based MPPT for PV system

Ahmad (2009) and Kim (2009) describes the design of a voltage based maximum power point tracker for photovoltaic applications. This method considered as the most straightforward and cost-effective method. But in this method, it disconnected the PV array from the load for the sampling of its open-circuit voltage, which results in power loss.

MPPT system with Perturb and Observe technique

Ulaganathan, et. al, (2014) in their research paper confirm that maximum power has been extracted by P&O method irrespective of atmospheric temperature and solar irradiance

with the Arduino Microcontroller. Also, it tracks the maximum power point quickly without oscillation. In the system, it used boost converter topology to maximize the efficiency of the PV array. PV array are connected with the load by DC/DC converter. The PV array can always work at the maximum power point by adjusting the DC/DC converter's duty cycle. The duty cycle was adjusted according to the Perturb and Observe algorithm.

A Comparative Study of MPPT techniques for PV Systems

This paper has presented a comparison between ten different Maximum Power Point Tracking techniques (Faranda and Leva,2008). Under these methods, it describes the three methods which only track the voltages. These methods have low efficiency compared to the other methods and the P&O and IC algorithms are the most efficient of the analyzed MPPT techniques. Also, it shows the experimental comparisons between different MPPT techniques, implementation cost and complexity.

Stand-alone Photovoltaic-Battery Hybrid Power system

According to the research done by Xiong (2016) on Closed-Loop Design for Standalone Photovoltaic-Battery Hybrid Power System, the system may operate in a MPPT mode or off-MPPT mode to regulate the output voltage, and at the same time, the battery may provide power to the load or store energy from solar power. The operating conditions use the nonlinear analysis method based on discrete-time mapping model and is complex.

Performance of buck and buck-boost convertor with PV system

Atallah, et. al, (2014) design a PV system with direct control the using the buck and buck-boost convertor. This module is connected to a power converter and varies the current from the PV array to the load. It says that Both buck and buck-boost converters have succeeded in tracking the MPP, but buck converter is much more effective specially in suppressing the oscillations produced due to the use of P&O technique.

MPP tracking solar charger controller with buck convertor

The Conference Paper of Design and Implementation of Maximum Power Point Tracking Solar Charge Controller represents the required calculations for selecting the buck convertor (Pathare, et. al, 2017). This demonstrate system is a low cost, low power consumption, microcontroller-based control unit with high power efficiency. This controller system is controlled using the Arduino.

Battery charging using MPPT to improve the durability of the battery

This paper presents a complete methodology for the design and construction of a stand-alone photovoltaic power supply. (Lopez, et. al, 2013). It gives the method sought to prevent the battery from a malfunction in its operation that could compromise its durability. It proposes a control strategy for the battery charging and control strategy to maximize photovoltaic energy production by incorporating an MPPT technique. According to the first region of voltage-current characteristics of the battery, the fully discharged state it is essential the photovoltaic modules' arrangement operates at the maximum power to apply the largest admissible current to the batteries to charge them in the shortest time interval possible.

3 METHODOLOGY

This study proposed implementing 12 V DC bus with a stand-alone PV system, including voltage tracking MPPT (Maximum Power Point Tracking) system and a battery backup. To achieve this, the first detailed study was carried out to identify different MPPT techniques and studied the behaviour of existing stand-alone PV systems. Also studied about the battery charger controller functions. The overall system is designed with relevant sub-sections such as designing and developing a charger controller unit with voltage tracking MPPT, design over charging protection, and over-discharging protection to the battery. Then the system is implemented as a hardware prototype and tested in real-time.

4 DESIGN OF THE SYSTEM

This system mainly consists of two DC-DC buck converters, 50 W solar panel, microcontroller, 12 V battery, controllable switches and 5 V USB ports to connect the phone for charging. MPPT process and PWM generation, battery monitoring for overcharging and over-discharging process are done by the controller unit, which is the heart of the system. It also controls the operating mode by controlling the switches.

4.1 DETAILED DESIGN OF THE PROPOSED SYSTEM

Figure 1 shows the overall system as a block representation. Fractional open circuit voltage MPPT algorithm is used due to its simplicity. Mainly there are three switches to control the 12 V output voltage from the buck converter 1. The controller unit monitors the battery conditions and if over discharging limit occurs, then disconnected the discharging path, and it does not give a chance to overcharging (Atallah, et. al, 2014). Buck converter 2 is used to step down the 12 V to 5 V for mobile phone charging purposes.

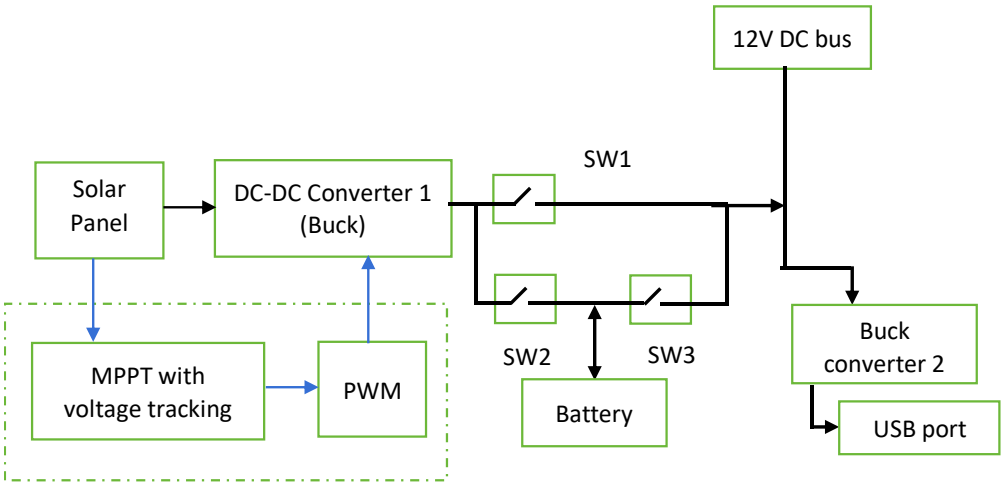

Fig. 1. Block diagram of the system

The heart of the system is the controller unit which is shown in figure 2. The controller unit does MPPT process and PWM generation, battery monitoring for overcharging and over discharging process. It also controls the ways of providing the power to the load by controlling the switches.

Solar energy is directly converted to the electricity, and this energy goes through the DC-DC buck converter to regulate the voltage. For switching purposes at the MPPT, the buck

converter needs PWM pulses. These pulses are generated from the controller circuit with respect to the MPPT process. There are different types of MPPT algorithms and among them, fractional open circuit voltage MPPT algorithm is used for this system due to its simplicity (Jyothi, et. al, 2016)

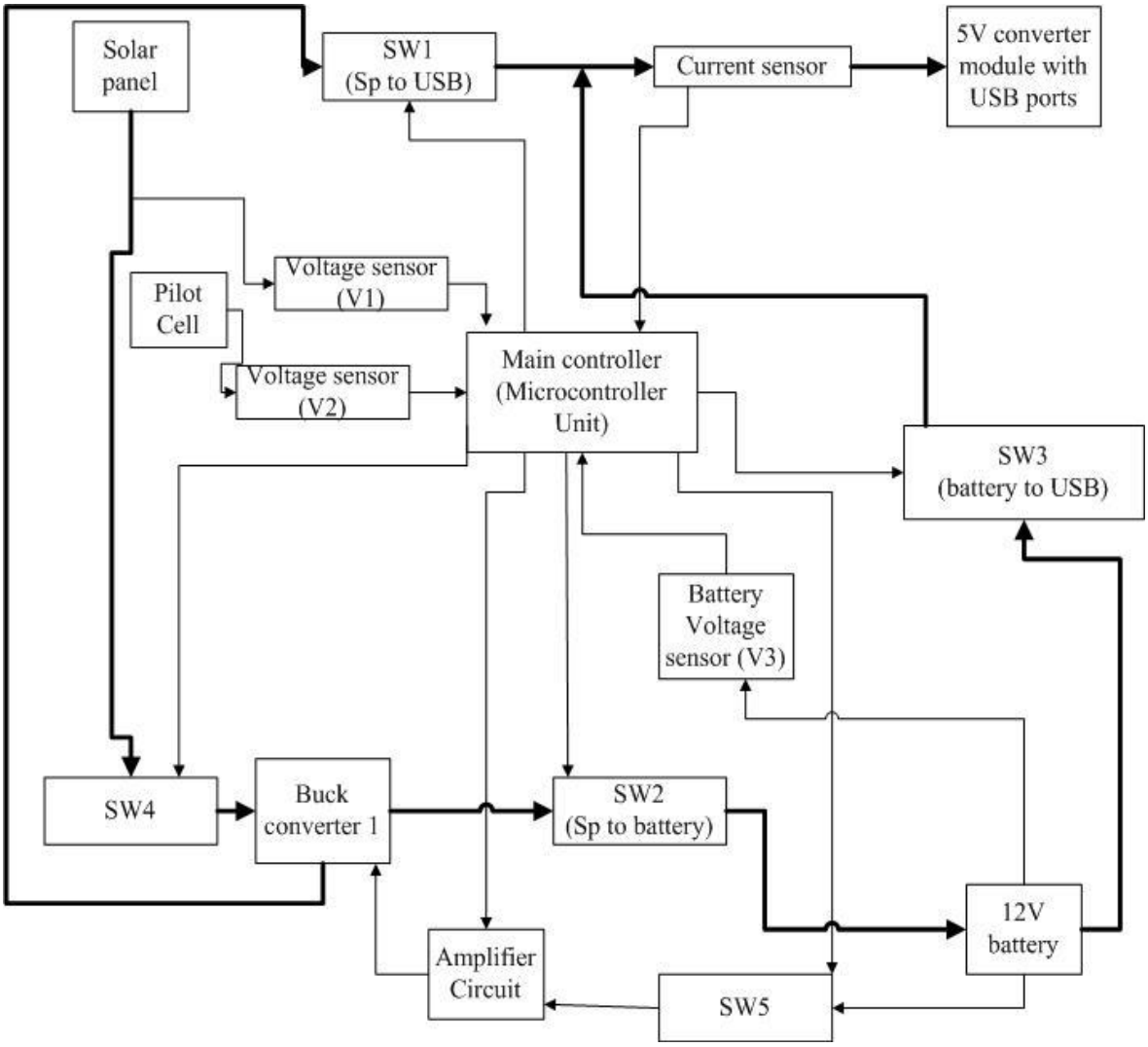

Fig. 2. Main control system

Mainly there are three switches to control the 12V output voltage from the buck converter-1. When the solar panel provides sufficient power, it can supply the load directly without discharging the battery. If the solar panel does not generate any power, then the battery can be discharged. When there is no load connected, the battery can be charged using solar energy. The controller unit monitors the battery conditions and when over discharging limit occurs, discharging path disconnected and it does not overcharge.

4.2 OPERATING MODES OF THE PROPOSED SYSTEM

The proposed system can provide four operating modes. When load connected to the system;

Mode 1: solar PV panel directly give power to the load

Mode 2: Load power provides by both battery and the PV.

Mode 3: Load power provides only by the battery
When there is no load connected to the system,
Mode 4: if the solar panel can give power, then charge the battery.

Mode 1: When the 12V battery is fully charged, PV can provide sufficient power to the load. Then it doesn't need the MPPT process.

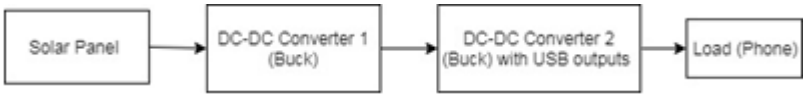

Fig. 3. Operating mode 1

Mode 2: When 12V battery is in the float charge region, and PV produces sufficient power, it doesn't need the MPPT process. It can manage the power requirement without tracking the MPPT.

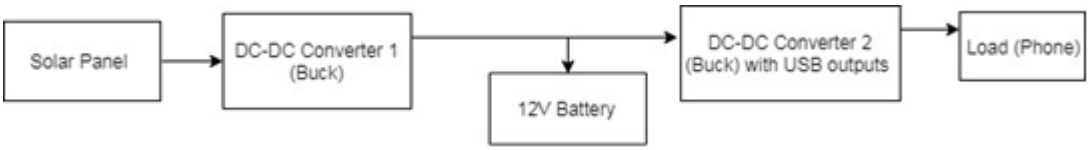

Fig. 4. Operating mode 2

Mode 3: At the night or cloudy weather PV cannot produce the power. Then the 12V battery can provide the required power to the load.

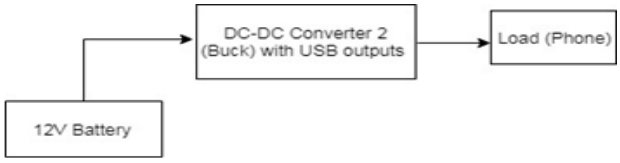

Fig. 5. Operating mode 3

When MPPT process in on mode,

Mode 4: If the 12V battery in bulk charge region. Then by providing maximum current, we can charge the battery within less time. This mode tracks the MPPT and tries to extract the maximum power from the system. Also, the system can provide the required power to the load too.

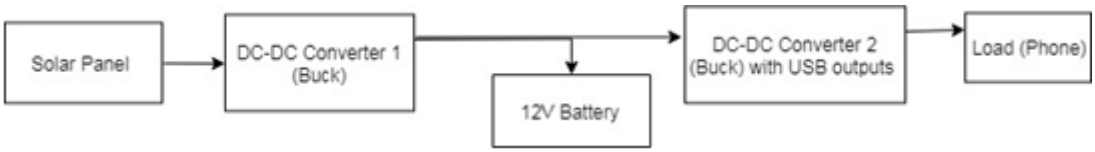

Figure 6. Operating mode 4

The solar panel is disconnected from the system when the panel voltage reaches 14.5 V. The system has IN4007 diode to protect the panel from reverse current. It is assumed that the battery never dead and State of Charge (SOC) values are selected considering the temperature values.

4.3 BATTERY CHARGING, SELECTED BATTERY AND VOLTAGE LEVELS

Proposed system used a 12V Lead-acid battery as the battery backup. Mainly lead-acid battery charging cycle has four regions, and for the proposed system first region is neglected because it is assumed that battery never dead. Battery charging regions are shown in Figure 7.

Bulk charge region: The first region is corresponding to a fully discharged battery. In this region, it can apply maximum charge current with considering the specification of the battery. This current can apply till the battery voltage reach the overcharge voltage. In this region, to apply the largest satisfactory current to the batteries to charge the battery with lesser time, MPPT can be used.

Overcharge region: This is corresponding to partially charged battery, constant charging voltage with a current limit can be used in this region. (According to the battery manufactures manual).

Float charge region: This is corresponding to the battery at almost fully charged. In this, it controls the voltage within the float voltage limit. This voltage is applied to the battery to avoid its auto discharge.

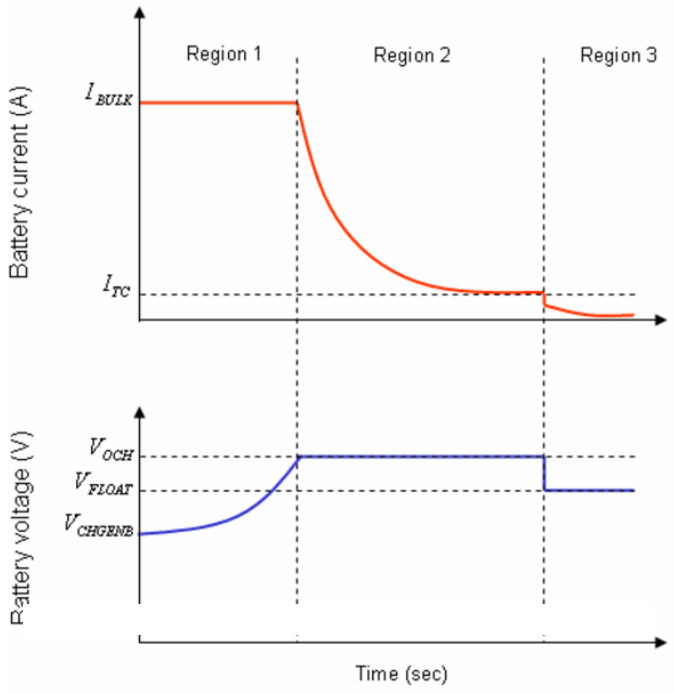

Fig. 7. Battery charging regions (L.M.F. Morais)

The 12V, 7Ah lead-acid battery is used as the storage. Since this prototype system is used to charge the phones and tablets, the battery can give 86Wh (12V x7Ah). Usually, smartphone battery consumes 10-11Wh to full charge. Thus, this battery storage is sufficient to charge approximately 8 phones fully (without considering the loss). To control the battery overcharging and over-discharging process ATmega328P microcontroller board is used(*Arduino Uno Rev3*,Anon.., n.d)

This battery is a lead-acid battery, and let's assume as the cell voltage is 2 V and 12 V battery has the 6 number of cells. When a cell is fully charged the voltage become 2.15 V and when it discharged the voltage become 1.9 V. By considering these factors state of the charge (SOC) for the 12V battery can get as follows.

Full charged battery voltage = 2.15 x 6 = 12.9V

Discharged battery voltage (V_{bt}) = 1.9 x 6 = 11.4V

Voltage difference of cell, between charging and discharging states = 2.15 - 1.9 = 0.25V. Since for 12V battery voltage difference = 0.25 x 6 = 1.5V.

The open circuit battery SOC = % charging

$$\% C = \frac{(Vbt - 11.4)}{1.5} \times 100 \qquad (1)$$

Using equation (1), noted the open-circuit voltage at 30%, 80% and 100% states.

at 30% SOC = 11.85 V

at 80% SOC = 12.6 V

at 100% SOC = 12.9 V

This system battery is disconnected from the charging and discharging paths to get the open-circuit voltage every 1 minute. If the open-circuit voltage value is in-between 11.85 V and 12.6 V, then operate the MPPT process. If the voltage value is above 12.6 V, then normal charging happens. Also, if the voltage is 11.85 V, disconnect the discharging path and if the voltage is 12.9 V then disconnect the charging path.

4.4 MPPT TECHNIQUE USED FOR THE IMPLEMENTATION

Among the various techniques used to track the maximum power, voltage based maximum power point tracker (MPPT) system is used in many applications. This method is considered as the most straightforward and cost-effective method. But in this method, it disconnected the PV panel from the load for the sampling of its open-circuit voltage, which results in power loss. The proposed system fractional open-circuit voltage (FOCV) method with the pilot cell is used as the MPPT technique. Since the proposed system is used only for battery charging purposes, easy and cheap implementation is significant (Siddhant, 2014). The FOCV algorithm measured the Open circuit voltage (V_{oc}) from the pilot cell and current voltage $V_{pv}(t)$ get from the solar module. Then calculates the V_{mpp} by using the equation (2).

$$Vmpp = Koc \times Voc \qquad (2)$$

where, V_{mpp} = voltage at the maximum power-point

V_{oc}=open circuit voltage of the panel

K_{oc} = constant depends on the solar panel characteristic value for the constant k is get as the 0.81. It gets by considering the solar panel specifications at the standard condition. (Irradiation = 1000 watts/m², temperature =250 °C)

After considering and comparing the V_{mpp} and $V_{pv}(t)$ it changes the voltage by increasing or decreasing the duty cycle which give to the DC-DC buck converter with considering the difference between V_{mpp} and $V_{pv}(t)$. Flow chart for the proposed MPPT algorithm is shown in Figure 8.

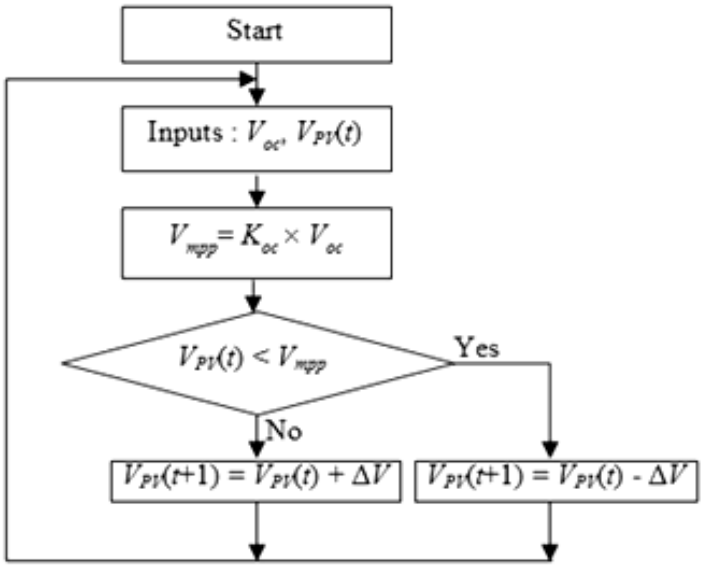

Fig. 8. Flow chart for proposed MPPT algorithm

5. SYSTEM IMPLEMENTATION

Adjustable buck converter module based on LM2596S is used as the main buck converter which has input voltage range 4.5V - 40V and output voltage adjustable from 1.23V - 37V. Fixed 5V buck converter module with two USB port is used for mobile phone charging. For the controlling unit, it used ATmega328P (ArduinoUno) microcontroller.

Pulse Width Modulation (PWM) is used in this system for the MPPT process. Adjustable buck converter module (LM2596S) used for the main buck converter block for step down the PV voltage. At the MPPT process, created PWM signals given to the feedback pin and extracted the system's maximum power. For this purpose, a small circuit which acts as the low pass filter and Op-Amp to convert the PWM signal to analog signal is used.

5.1 FABRICATION OF HARDWARE

Prototype implementation for the stand-alone PV system is shown in figure 9 and testing of the prototype is shown in figure 10.

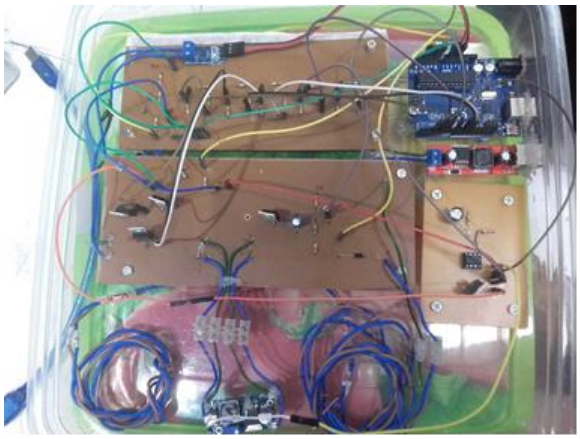

Fig. 9. Prototype implementation

Fig. 10. Testing of the implemented prototype

6 . RESULTS

Duty cycle which must give to the converter is decided by comparing the current solar panel voltage and pilot solar panel voltage to maintain the MPPT algorithm. The buck converter module is used in the implementation and created duty cycle according to the MPPT algorithm is given to the feedback pin of the LM2596 IC in the module.

Changing the PWM from the control circuit, measured the variation of the current in the charging path.

After battery voltage reached 12.6 V, it disconnected the MPPT process and then the battery charged by getting current as required. When the battery voltage become 12.9 V battery charging path is disconnected.

To charge only the 12 V/7 Ah battery, it took nearly 9 hrs without MPPT, and it gets almost 8 hrs to charge the battery with the implemented system (in a sunny day).

Table 1. Measured current with MPPT and without MPPT

V_{oc} of the pilot panel(V)	Current (A) (Without MPPT)	Current (A) (With MPPT)
19.25	0.52	0.63
18.16	0.47	0.59
17.5	0.42	0.44
15.52	0.22	0.24
15.23	0.21	0.24
16.7	0.4	0.43
17.25	0.42	0.45
18.61	0.49	0.6
19.35	0.54	0.64
18.75	0.51	0.63

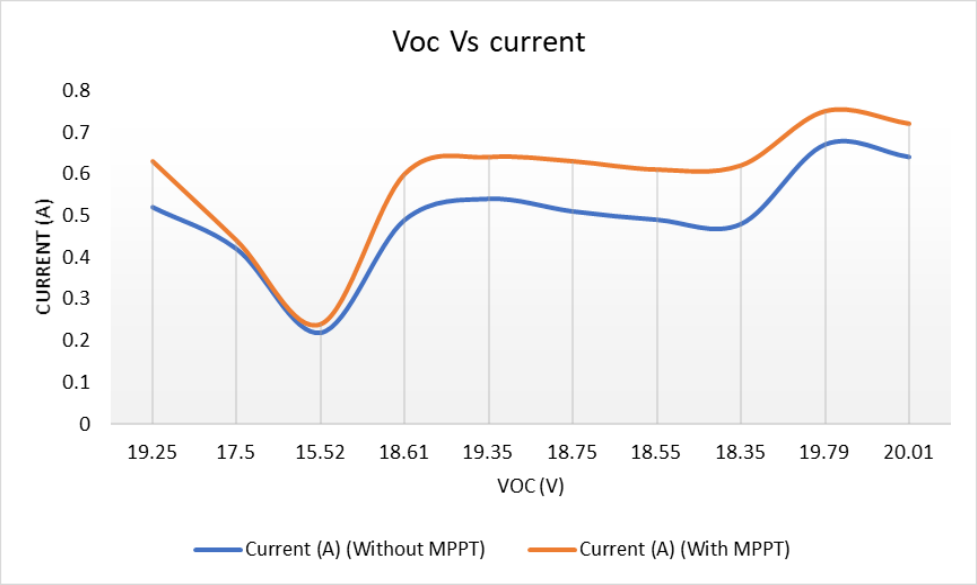

Fig. 11. Current variation at the MPPT process

Charging the mobile phone:

Mobile phones are charged using a buck converter with a fixed 5 V output, and readings were collected using two smartphones with the Li-ion batteries of 2600 mAh,9.88 Wh, and 6.84 Wh.

The 9.88 Wh battery is charged by getting 0.49 A from the solar panel or 12 V battery.

The 6.84 Wh battery is charged by getting 0.41 A from the solar panel or 12 V battery.

When both phones connected at once module pass the current of 1.03 A, to fully charged the mobile phone with 6.84 Wh battery, it takes nearly 5 hrs.

7 DISCUSSION

Selected buck converter module to step down the solar panel voltage to the battery can pass only 3 A maximum current but when current reaches to 1 A module become heated. Converter module which used for phone charging also has 3 A maximum current rating. But when it drags 1.1 A, it becomes heated. Heat sink needs to be used for both modules. Since selected battery (12V,7 Ah) is limited in the capacity, it cannot use for a longer time. So that battery is selected only for the implementation purpose.

Use of buck-boost converter would give optimum results for the system as it gives more benefits even at the low voltage output from the panel. However, at the boost range, it reduces the current output.

In the MPPT process, while it gives the PWM signal to the LM2596 IC in the converter module when the voltage at the feedback pin is lower than the 1.23 V reference value, it increases the output power. Also, when the voltage is above 1.23V reference, then it reduces the output power. It is needed to keep feedback voltage range between 1.18 V and 1.28 V. If it is not in the given range, then there is no current flowing through the charging path.

In this system, FOCV method is used as the MPPT algorithm, and as the cell, a separate pilot solar panel is used for the implementation. If this module is fabricated as a commercial product, it can use only one cell for one setup.

When monitoring the battery, the load side and the charging side always need to be disconnected to get the battery's open-circuit voltage. This will create considerable power loss since this happens every half minute. By applying a proper method to get the battery SOC at the charging, the above problem can be eliminated.

8 CONCLUSION

In stand-alone PV systems, MPPT exports the maximum power from the solar panel, without considering the load conditions. Therefore, the system can be cut off when it does not connect to a sufficient load. When considering the battery's charging, it cannot always charge with the MPPT because it can only give the high current at the bulk charging region of the battery charging curve while in the other areas of the curve it can provide the normal power from the solar panel for charging.

The proposed system uses a control circuit to manage the solar panel's output power by checking the load condition and effectively charging the battery. In results it clearly shows with MPPT charging, current of the battery is significantly increased. Therefore, the stand-alone PV system is used to design a mobile device charger more efficiently.

It shows that using this mobile device charger devices can be fully charged with the acceptable time where electricity from the national grid is inaccessible. Results also show that 12 V DC bus also can be used as an emergency charger for mobile devices.

REFERENCES

Agrawal, S., Tiwari, G.N. (2011) Energy and exergy analysis of hybrid micro-channel photovoltaic thermal module. Solar energy 85 (2), 356-370

Atallah, A. M., Abdelaziz, A. Y., Jumaah, R. S., (2014), Implementation of perturb and observe MPPT of PV system with direct control method using buck and buck boost converters. *Emerging Trends in Electrical, Electronics & Instrumentation Engineering: An international Journal,* Vol. 1.

Ahmad, J., Kim, H. J., (2009). A Voltage Based Maximum Power Point Tracker for Low Power and Low Cost Photovoltaic Applications, *s.l.: International Journal of Electrical, Computer, Energetic, Electronic and Communication Engineering.*

Anon., n.d. *Arduino Uno Rev3.* https://store.arduino.cc/usa/arduino-uno-rev3

Faranda, R., Leva, S., (2008), A Comparative Study of MPPT techniques for PV Systems. Milano, ITALY, s.n.

Jyothi, V.M., Muni,V.,Lalitha, S. V. N. L., (2016), An Optimal Energy Management System for PV/Battery Standalone System. *International Journal of Electrical and Computer Engineering (IJECE),* Vol. 6,P 2088-8708

Lopez, J., Seleme, S. I., Donaso, P.F., Mendes, M. S., Morais, L. M. F., Cortizo, P., (2013). Methodology for the design of a stand-alone photovoltaic power supply. *Ingeniare. Rev. chil. ing. ,* vol.21(3).p 380-393

Pathare, M., Shetty, V., Datta, D., Pai, S., (2017), Designing and Implementation of Maximum Power Point Tracking(MPPT) Solar Charge Controller, *International Conference on Nascent Technologies in Engineering (ICNTE)*

Siddhant, K., (2014). Implementation of fractional open circuit voltage mppt algorithm in a low cost microcontroller, Rourkela: s.n.

Ulaganathan, M.K.D., Saravanan, C., Chitranjan, O.R., (2014), Cost-effective Perturb and Observe MPPT Method using Arduino Microcontroller for a Stand-alone Photo Voltaic System. *International Journal of Engineering Trends and Technology (IJETT)* , Vol 8.

Xiong, X., (2016). Closed-Loop Design for Standalone Photovoltaic-Battery Hybrid Power System. *Journal of Electrical and Electronic Engineering*., Vol. 4(5), 131-138.

Journal of Engineering and Technology
of The Open University of Sri Lanka (JET-OUSL), Vol. 08, No.2, pp 35-48

Does the Extent of Photosynthetic surface and Potential Gross Primary Productivity (GPP) of Mangrove Ecosystems Depend on Climate? : A Case Study from Sri Lanka

K. A. R. S. Perera[1]*, M. D. Amarasinghe[2]

[1] Department of Botany, The Open University of Sri Lanka, Nawala, Nugegoda, Sri Lanka
[2] Department of Botany, University of Kelaniya, Kelaniya, Sri Lanka

*Corresponding Author: email: kaper@ou.ac.lk, Tele: +94112881269

Abstract – *Mangrove forests characterized as an important agent of carbon sequestration due to its rapid rate of primary production and slow rates of sediment organic carbon decomposition. Mangrove productivity has shown a wide variation among sites due to variations in many factors, including climate. Comparison of the Leaf area index (LAI) and Gross Primary Productivity (GPP) of mangrove ecosystems located in different climatic zones in Sri Lanka and its relationship with rainfall and the vegetation structure are the main objectives of the study. Absorption of photosynthetically active radiation (PAR) is governed by the extent of photosynthetic surface which is estimated with LAI of vegetation canopies and then calculated the GPP of respective area. Intensity of PAR above (I0) and below (I) the canopy of the study areas was recorded using LI-191SA line Quantum sensor. Mangrove vegetation structure was characterized with species richness, plant density, basal area and stand height of study areas were quantify with standard methods The GPP was performed in seven mangrove ecosystems representing wet, intermediate, and dry climatic zones in Sri Lanka. Highest average values of LAI and GPP were recorded from the mangroves in the wet and the intermediate zone. and the lowest average values for LAI and GPP were recorded for the dry zone mangroves. Statistically significant positive linear relationship with high coefficient of determination (r2>0.7) were revealed to occur between GPP values of wet and dry periods of mangroves and GPP with vegetation structural complexity. The average LAI of mangrove ecosystems in Sri Lanka was 5.66, with a GPP of 40.92 Mg ha-1 y-1. A positive correlation was revealed between estimated average annual gross primary productivity (GPP) values and annual rain fall of the areas. Results revealed that LAI and GPP of mangroves are potentially driven by annual rainfall pattern among other factors, by climate.*

Keywords: *Mangroves, Leaf area index (LAI), Gross Primary Productivity (GPP), Climate*

1 INTRODUCTION

Gross primary productivity (GPP) is the rate at which an ecosystem's producers capture from a given amount of chemical energy during a given length of time. Net production is the balance between gross photosynthesis and leaf dark respiration and represents the amount of carbon available for growth and tissue maintenance. High primary productivity of mangroves facilitates the high carbon sequestration function of mangrove ecosystems (Perera et al., 2012). Mangrove forests have been recognized as an important agent of carbon sequestration with reported half of the biomass content organic carbon (Lovelock et al., 2015). The rapid rate of primary production and slow rates of sediment carbon decomposition bring about the preservation of huge amounts of organic carbon in mangrove forests (Alongi, 2014). GPP represents the rate at which an ecosystem's

producers capture from a given amount of chemical energy during a given time length.

Photosynthetically active radiation (PAR) absorbed by the plant canopies/ leaves gives a reliable measure of its gross primary production. The light response curves of mangroves are similar to other plants, with a steep linear increase up to 300 -400 μ mol photons m^{-2} s^{-1} after which saturation is reached (Alongi 2009) Extent of photosynthetic surface (leaf area) solar zenith angle, which is a function of time, day length and latitude also plays a part in determining the total quantum of PAR absorbed by plant leaves (Okimoto et al., 2007; Jayakody et al., 2008). Measurement of PAR absorption by the mangrove canopy is used to estimate the LAI and then it can be converted to gross primary productivity in mangrove forests. Amount of light absorbed by the mangrove canopy is related to the total canopy chlorophyll concentration and was then multiplied by a rate of carbon fixation per unit of chlorophyll to give an estimate of GPP. The method described by Bunt et al. (1979) has been used widely in recent years to estimate GPP of mangroves (Jayakody et al., 2008; Kathiresan and Khan, 2010). However recent work suggests that potential GPP calculated using this method (Bunt et al., 1979), significantly underestimates the photosynthetic capacity of mangroves. English et al., (1997) proposed theoretically, that measuring photosynthetic capacity of mangroves is a more robust method in estimating canopy LAI (with the ratio of PAR below and above the canopy), that can be used to estimate GPP.

Although a low extent of mangroves in Sri Lanka, supports 23 true mangrove plants species (Amarasinghe and Perera, 2017) and present study was conducted with the objective of estimating the GPP of Sri Lankan mangrove ecosystems by capturing of solar energy through photosynthesis. Although number of services and traditional uses of Sri Lankan mangroves were reported, quantifiable measures of primary productivity of mangroves are inadequate. Present study focused on estimates the gross primary productivity of Sri Lankan mangroves and its dependency on main climatic factor i.e., rainfall which vary in coastal zone in Sri Lanka. Findings of the study may be helpful to making of decisions in maintain mangrove areas for carbon sequestration process to mitigation the effects of climatic changes.

2. MATERIALS AND METHODS

2.1 Study area

Intensive data collection was carried out in two mangrove areas, Kadolkele and Wedikanda located in Negombo estuary on west coast of Sri Lanka. Other than that total of six (6) study areas i.e, Chilaw lagoon, Rekawa lagoon, Kala Oya estuary, Malwathu Oya estuary, Uppar and Batticaloa lagoons, were selected around the Sri Lanka to represent all the climatic zones found along the coastal line of the country (Fig.1). Data was collected form 2014 – 2016 period. Study locations and their basic climatic characteristics are presented

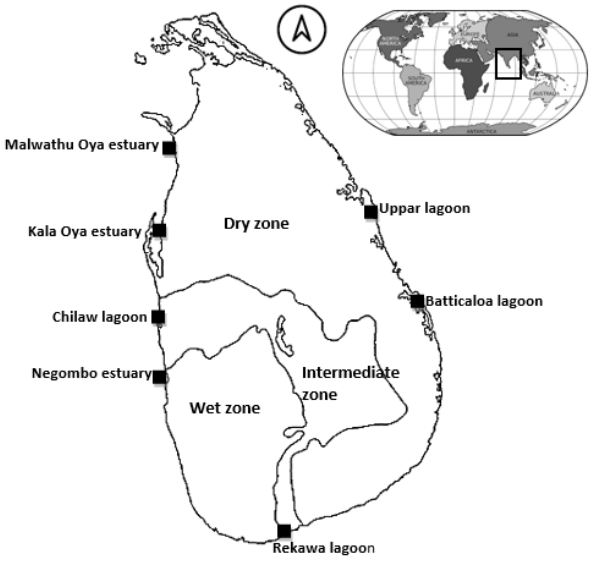

Fig 1. Study areas located along the coastal line of the Sri Lanka

in Table 1.

Table 1: Study locations and their climatic characteristics

Study area	Climatic zone	Location	Annual rainfall (mm) *	Relative humidity (%)	Annual temperature (^{0}C)
Negombo estuary	Wet zone	7^{0}11'50.48" N; 79^0 50'47.50" E	2161	87-93	25.6 – 28.5
Chilaw lagoon	Intermediate zone	7^{0}30'46.40" N; 79^0 49'11.70" E	1507	86-93	25.2 – 29.3
Rekawa lagoon	Intermediate zone	6^{0}02' 51.70" N; 80^0 50' 57.92" E	1082	86-90	25.6- 29.0
Kala Oya estuary	Dry zone	8^{0}17' 11.31" N; 79^0 50' 45.65" E	1200	83-95	25.6 - 29.8
Malwathu Oya estuary	Dry zone	8^{0}49' 02.64" N; 79^0 55' 09.24" E	923	83-88	26.2 - 29.8
Uppar lagoon	Dry zone	8^0 05' 13.25" N; 81^0 26'15.92 E	1786	76-88	25.8 - 30.5
Batticaloa lagoon	Dry zone	7^0 44' 50.70" N; 81^{0}41'17.67" E	1810	76.88	25.8 - 30.5

*Source - Bastiaanssen and Chandrapala (2003)

2.2 Sampling strategy

For gathering data on photosynthetically active radiation (PAR) and mangrove vegetation structure, 10 m wide belt transects were laid perpendicular to the shoreline across the environmental gradient in randomly selected locations in each of study area. Each belt transects then divided in to 10m x 10m (100m2) sampling plots. Total of hundred and thirty-seven (137) sampling plots, including forty (40) permanent sampling plots at Negombo estuary and ninety-seven (97) sampling plots at other six study areas, Chilaw lagoon, Rekawa lagoon, Kala Oya estuary, Malwathu Oya estuary, Uppar and Batticaloa lagoons. were used to collect the data.

2.3 Mangrove vegetation structure

Standard methods were adopted to quantify the vegetation structure of the mangrove ecosystem, as described by Kathiresan and Khan, (2010). Data on mangrove structural properties including species richness, tree diameter at breast height (dbh) and tree height of the stands were gathered from each sampling plot. Complexity index (CI), indicates the diversity and abundance of flora within the forest community and it is calculated using data on the number of species, stand density, basal area and height (Kathiresan and Khan, 2010; Perera and Amarasinghe, 2016; Umayangani, Perera, 2017). For the present study, CI was calculated as, Number of species x stand density x stand basal area x stand height x 10^{-5}.

2.3 Mangrove vegetation structure

Standard methods were adopted to quantify the vegetation structure of the mangrove ecosystem, as described by Kathiresan and Khan, (2010). Data on mangrove structural properties including species richness, tree diameter at breast height (dbh) and tree height of the stands were gathered from each sampling plot. Complexity index (CI), indicates the diversity and abundance of flora within the forest community and it is calculated using data on the number of species, stand density, basal area and height (Kathiresan and Khan, 2010; Perera and Amarasinghe, 2016; Umayangani, Perera, 2017). For the present study, CI was calculated as, Number of species x stand density x stand basal area x stand height x 10^{-5}.

2.4 Leaf area index (LAI)

Leaf area index (LAI), the total area of (one side) leaf surface per unit ground-surface area, has been used to calculate the potential GPP of mangrove ecosystems. Measurement of photosynthetically active radiation (PAR) absorption by the canopy used to estimate the leaf area index. The method described by Jayakody et al., (2008); Kathiresan and Khan (2010) has been used to calculate the leaf area index.

$I = I_0 e^{-k\ LAI\ I}$

$LAI^I = \log e (I/I_0)-k$

$LAI = LAI^I \times \text{Cos} (\theta \times 3.141593/180)$

Where,

I = photon flux density beneath the canopy;

Io = photon flux density incident on the top of the canopy or fully exposed position outside the canopy;

LAI^I = Leaf area index correction;

LAI = Leaf area index;

θ = zenith angle of sun;

k = canopy light extinction coefficient.

Light intensity of above canopy or in open space of the study area (I0) and under canopy (I) was recorded between 10.00 and 14.00 hr. using LI-191SA line Quantum sensor. Approximately 50 readings of I were taken from each study plot (100 m2). Values of zenith angle (angle of the sun from the vertical) at the time that measurements of I were made, obtained from the Metrological Dept. of Sri Lanka and website www.solardat.uoregon.edu.

Photosynthetically active radiation (PAR) absorption data of study sites of Negombo estuary, were collected during a two-year period, once in three months, which encompassed the two monsoon periods and inter monsoon periods, i.e., total study period covered four monsoon periods. The PAR data of other mangrove areas, Chilaw lagoon, Rekawa lagoon, Kala Oya estuary, Malwathu Oya estuary, Uppar lagoon and

Batticaloa lagoon were once in dry period only, during same year.

2.5 Gross primary productivity (GPP)

Gross primary productivity (net rates of maximum light saturated leaf photosynthesis) of mangrove ecosystems in Negombo estuary was estimated by using the LAI. The potential gross primary productivity of the canopy per unit area was calculated with the following formula (Bunt et al., 1979; Clough and Dalhaus., 1997; Kathiresan and Khan, 2010).

GPP = A x d x LAI

Where d is the day length in hours, LAI is the leaf area index and A is the average rate of photosynthesis per unit area (g C m-2 hr-1) for all leaves in the canopy. This value A varied with climatic conditions. While it is desirable to measure the actual rate of photosynthesis at each site and according to the explanation by English et al., (1997), approximate rate of 0.216 g C m-2 hr-1can be used for dry period, and 0.648 g C m-2 hr-1 for wet/raining conditions. Accordingly, potential GPP of estuarine mangroves at Negombo was calculated during wet and dry periods separately by using the data of two consecutive years. Ratio of GPP of wet period to dry period was also calculated.

2.6 Rainfall data

Considering the local daily rainfall data, (obtained from nearest station of the Meteorological Department of Sri Lanka), number of rainy and dry months was separated. Actual dry and wet/raining months were enumerated with the criteria used by the Department of Meteorological, Sri Lanka i.e., daily rainfall recorded to be less than 1 mm in 15 consecutive days of a month is considered a dry month and daily rainfall recorded to be more than 3 mm in 15 consecutive days of a month is considered as wet month. The mean annual GPP was then calculated for each mangrove area at Chilaw, Rekawa, Kala Oya, Malwathu Oya, Uppar, Batticaloa lagoons and estuaries.

2.7 Data analysis

Statistical analyses were carried out by using of SPSS Ver. 20 (SPSS, 2012). Initially, all the data was tested using Shapiro-Wilk normality test and results indicated that there was no violation of normality ($p \leq 0.05$). Mean and standard errors were calculated and presented along with number of samples used for the purpose.

3. RESULTS

3.1 Gross primary productivity (GPP) of Negombo mangrove ecosystems

A statistically significant difference ($p > 0.05$) was not observed between the values of photon flux density beneath the canopy (I), above the canopy (I_0), LAI and GPP recorded from the two study areas (Kadolkele and Wedikanda) in Negombo estuary within the same climatic period, thus data was pooled and averaged the values for Negombo estuary.

GPP and LAI were revealed to be lower in dry period than in wet/rainy period of the year. Higher values of GPP and LAI were recorded at the study plots near the estuarine waterfront and it declined with distance towards the land (Fig 2).

3.2 Relationship between dry and wet seasons Gross Primary Productivity (GPP) at Negombo estuary

GPP data of wet period and corelated with dry period data and a linear curve was observed the most fitted for the data set and therefore, the relationship was derived with linear curve. A statistically significant positive correlation ($p<0.05$) and a high coefficient of determination ($r2=0.82$) with linear relationship was revealed between the GPP of dry and wet seasons in mangroves (Fig. 3).

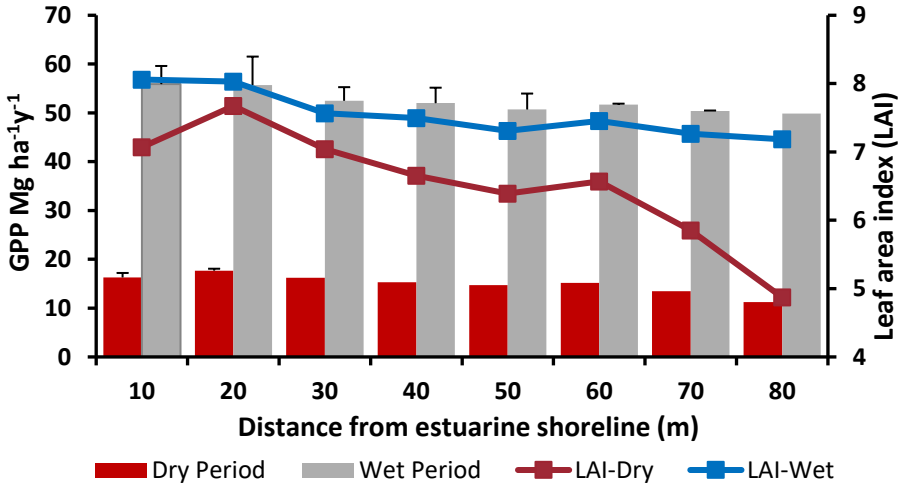

Fig. 2. Variation of GPP and LAI during wet/rainy and dry conditions of different distances from estuarine shoreline at Mangrove areas in Negombo estuary

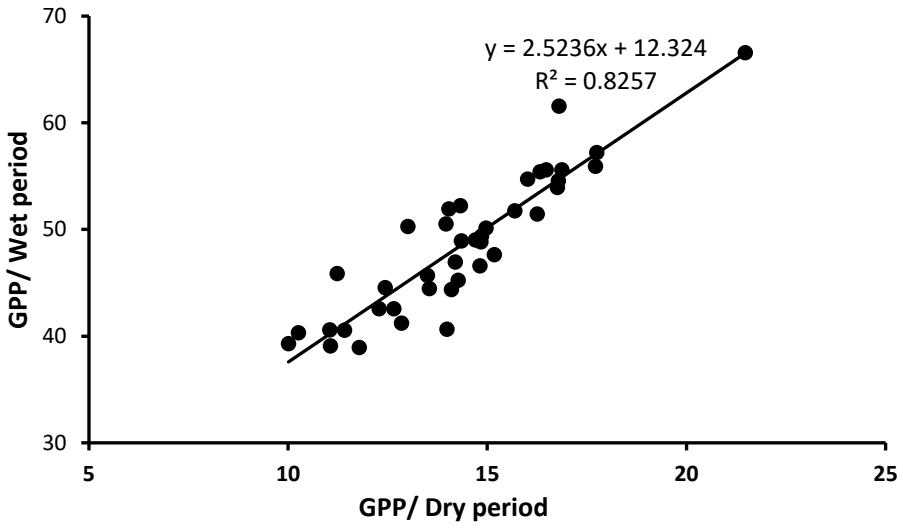

Fig. 3. Relationship between GPP and structure of mangrove vegetation

3.3 Gross primary productivity (GPP) of mangrove ecosystems in Sri Lanka

PAR (photosynthetically active radiation) data was used to calculate the LAI followed by calculation of GPP of mangrove ecosystems in Chilaw lagoon, Rekawa lagoon, Kala Oya

estuary, Malwathu Oya estuary, Uppar lagoon and Batticaloa lagoon. Although, PAR data of Negombo estuary, was collected during a two-year period, the PAR data of other mangrove areas were collected once in dry period only, during same year. Using the relationship between wet and dry GPP of Negombo estuarine mangroves (Fig. 2), GPP of wet season of other study areas were estimated.

Average annual GPP of study areas were estimated and number of rainy months was determined with the local rainfall data (section 2.6) was obtained from the nearest station of the Meteorological Department of Sri Lanka (Table 2).

Table 2. Estimated average values of the annual GPP (Mgha-1y-1) at mangrove ecosystems of Negombo estuary, Chilaw lagoon, Rekawa lagoon, Kala Oya estuary, Malwathu Oya estuary, Uppar lagoon and Batticaloa lagoon.

Study area	Climatic zone	Mean GPP at dry season	Mean GPP at wet/rain season	No.wet months	No. dry months	Estimated Average annual GPP
Negombo estuary	Wet zone	18.25 ± 0.37	61.35 ± 1.11	11	1	57.75 ± 1.04
Rekawa lagoon	Intermediate zone	10.10 ± 0.37	33.96 ± 0.39	11	1	31.97 ± 0.36
Chilaw lagoon		16.84 ± 0.19	56.60 ± 0.65	11	1	53.28 ± 0.61
Kala Oya estuary	Dry zone	12.20 ± 0.35	41.01 ± 1.17	10	2	36.21 ± 1.03
Malwathu Oya estuary		12.18 ± 0.29	42.40 ± 0.99	6	6	27.29 ± 0.64
Uppar lagoon		12.96 ± 0.46	43.57 ± 1.54	9	3	35.92 ± 1.27
Batticaloa lagoon		15.98 ± 0.50	53.42 ± 1.68	9	3	44.06 ± 1.38

Relatively a high GPP values were recorded in intermediate zone mangroves (average 52.71 Mg ha-1 y-1) followed by wet zone (37.77 Mg ha-1 y-1) and the lowest was recorded in mangrove areas at dry zone (average 33.64 Mg ha-1 y-1). Average annual GPP of mangrove ecosystems in Sri Lanka was calculated to be, 41.37 Mg ha-1 y-1 (Table 2).

3.4 Relationship between gross primary productivity (GPP) and annual rainfall

A positive correlation was revealed between estimated average annual GPP values and annual rain fall of the areas. Power curve was observed the most fit for the data set and therefore, the relationship was derived from power curve (Fig. 4).

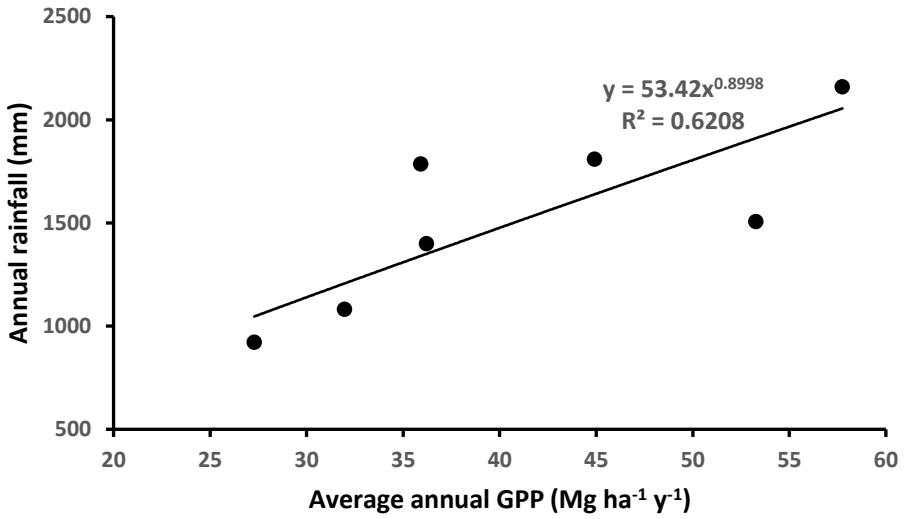

Fig. 4. Relationship between average annual GPP of mangroves and annual rainfall of the area

3.5 Mangrove vegetation structure and gross primary productivity (GPP)

Data on mangrove vegetation structure (CI) gathered from all seven study areas were corelated with the calculated GPP values for respective areas. A linear curve was observed the most fitted for the data set and therefore, the relationship was derived with linear curve. Therefore, a statistically significant positive correlation ($p<0.05$) and a high coefficient of determination ($r2=0.709$) with linear relationship was revealed to occur between gross primary productivity and vegetation structural complexity in mangrove ecosystems (Fig.5).

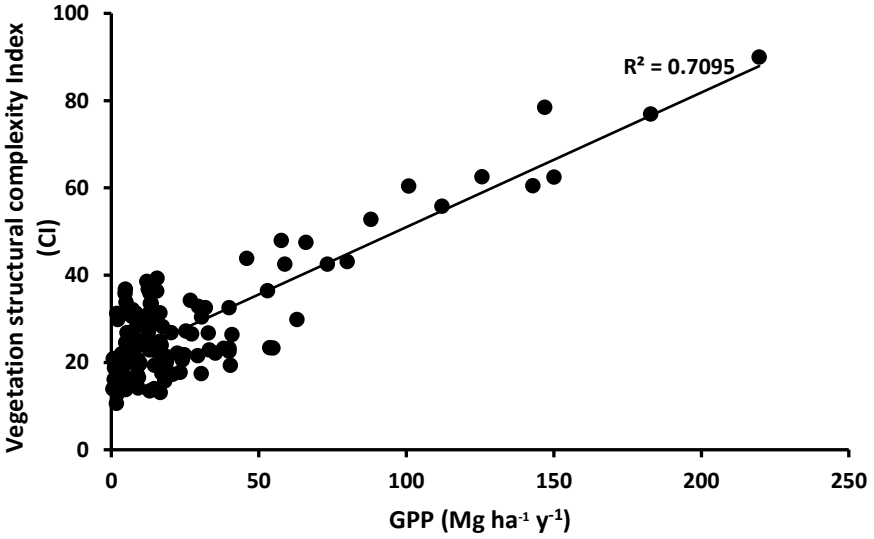

Fig. 5. Relationship between gross primary productivity vegetation complexity index of Wedikanda mangroves

4. DISCUSSION

The higher values of potential GPP observed during and immediately after the raining season, at Kadolkele and Wedikanda mangrove areas at Negombo estuary, may be due to the enhanced nutrient inputs from surface and river runoff and decreased soil salinity (Gammanpila et al, 2009) that in turn may lead to low leaf fall in comparison to dry period, thus resulting a higher LAI. The availability of freshwater indicated an important factor for development and growth of mangroves. Freshwater supply has often been indicated by the ratio of rainfall to evapotranspiration (Barr et al, 2014). Under the humid conditions where the ratio exceeds 1, the mangroves grow abundantly and under the arid climates, where the ratio of rainfall to evapotranspiration falls below 1, the mangroves get stunted (Kathiresan and Khan, 2010). High rainfall in humid conditions leaches out residual salts from mangrove soil and thus encourages growth of mangroves. In general mangrove vegetation is more luxuriant in lower salinities (Chen and Ye, 2014). Experimental evidence indicates that at high salinity, mangroves spend more energy to maintain water balance and ion concentration rather than for primary production and growth (Alongi,2014). High salinities result in physiological responses similar to terrestrial plants that experience drought, as highly saline soils have low osmotic potential that constrain water relations of mangroves (Sparks, 2003; Artiola et al, 2019)

Photosynthetic capacity of mangrove leaves however depends on their location of the canopy as it affects the leaf morphology, anatomy and physiology. Based on the experimental evidence Farnsworth & Ellison, (1996), reported that the photosynthetic rate of sun leaves of Rhizophora mangal, which are smaller in size and occupy the upper parts of the canopy having a thick cuticle and tannin cells, are twice as that of shade leaves which occupy the lower strata of the canopy and thus are larger in size with a thin cuticle.

Leaf fall rates have been observed to be significantly greater during dry period than in the wet season (Pahalawattarachchi, 1995) which in turn reduces LAI and the GPP of the mangrove stand. In addition, reduction of leaf size has been observed to be an initial morphological reaction to environmental stress on plants (Parida and Das, 2005) and therefore relativity a high salinity exists during the months of low rainfall and it may cause stress on mangroves resulting lower GPP than recorded in rainy periods.

Rate of photosynthesis vary widely among the physical environmental factors as well as vegetation structural characteristics. Complexity index (CI) represents the vegetation structure of the mangrove stand, that contributes to functions of the mangrove ecosystem, revealed a strong positive relationship ($p>0.05$) with the GPP calculated for Negombo estuary ($r2 = 0.802$) and similar relationships were reported by Jayakody et al. (2008) and Perera et al. (2010) for mangrove areas in Negombo estuary.

Estimated GPP values in the present study were revealed higher in both wet and dry periods than those reported by Jayakody et al. (2008), the only study on GPP of Sri Lankan mangroves that has been conducted in Negombo estuarine mangroves, during one wet and a dry period. On contrary to GPP values reported by Jayakody et al. (2008), i.e., 12.77 – 23.89 t ha-1y-1 during dry season and 20.81 -37.28 t ha-1y-1 during the wet season. Present study revealed the dry season and wet season GPP are to be 13.00 – 21.47 t ha-1y-1 and 44.45 – 66.56 t ha-1y-1 respectively.

Calderon et al, (2014) explain geomorphology and hydrology determined by local geology, sea-level change, tide, freshwater input, shoreline structure, watershed morphology, groundwater influence, natural disturbance regimes and climate, contribute to development of physico-chemical gradients which in turn govern the structure and function of the intertidal ecosystems. Many of the estuaries and lagoon in Sri Lanka can be categorized as riverine which receive continuous input of nutrient rich freshwaters through rivers and get mixed with saline waters resulting reduced salinity and this water inundates areas close to the shoreline most frequently than in the landward areas. High mangrove structural complexity, which is represented by high number of species, plant densities and heights, high leaf area indexes is observed with the mangrove areas close to the shoreline and it was revealed to decrease along the environmental gradient towards inland, thus GPP also declines along the water-land gradient in the estuary.

The GPP values for dry period of other six (6) mangrove areas in Sri Lanka, i.e., Chilaw lagoon, Rekawa lagoon, Kala Oya estuary, Malwathu Oya estuary, Uppar lagoon and Batticaloa lagoon, comparatively high value was resulted in Chilaw lagoon than in others. High input of fresh water may be a potential reason for this situation where this lagoon is located in intermediate climatic zone, (mean annual rainfall 1507 mm) while other estuaries/lagoons are situated in the dry zone of Sri Lanka which mean annual rainfall recorded lesser than that. Although Rekawa is located in the intermediate zone annual rainfall recorded 1082 mm which is lower than that of recoded annual rainfall in other dry zone mangrove areas.

Comparison of data on GPP of the present study with published estimates, reveal that they are relatively lower than that have been recorded by Clough and Dalhaus (1997), at Matang mangrove forest at Malaysia, where GPP was recorded to be 56 t ha-1y-1. Estimated GPP of 102.9 t ha-1y-1 has been reported from Kandelia candel forests in Okinawa Island, Japan (Suwa et al., 2006) and it is much higher than those values recorded by the present study. Only a very few studies have been dedicated to estimating mangrove GPP and even among them, no consideration has been given to the seasonal variations in climate that leads to changes in physiological traits of mangrove leaves. It was revealed that PAR data is highly variable with the climatic conditions (wet or dry) and therefore seasonal changes in photosynthesis and dark respiration rates of leaves are probably necessary for obtaining reliable estimates of annual canopy photosynthesis and respiration rates.

5. CONCLUSION

Estimation of the Leaf area index (LAI) and Gross Primary Productivity (GPP) of mangrove ecosystems located in different climatic zones in Sri Lanka and its relationship with rainfall and the vegetation structure were the main objectives of the study. Highest average values of LAI and GPP were recorded from the wet and the intermediate zone mangroves. Statistically significant positive linear relationship with high coefficient of determination ($r2>0.7$) were revealed to occur between GPP values of wet and dry periods of mangroves and GPP with vegetation structural complexity. The average LAI of mangrove ecosystems in Sri Lanka therefore was 5.66, with a GPP of 40.92 Mg ha-1 y-1. A positive correlation was recorded between estimated average annual gross primary productivity (GPP) values and annual rain fall of the study areas. Results revealed that LAI and GPP of mangroves is potentially driven by annual rainfall pattern among other factors, by climate.

REFERENCES

Alongi, D. M., Wattayakorn, G., Pfitzner, J., Tirendi, F., Zagorskis, I., Brunskill, G. J., Davidson, A. and Clough, B. F. (2001). Organic carbon accumulation and metabolic pathways in sediments of mangrove forests in southern Thailand, Marine Geology, 179: 85–103.

Alongi, D.M. (2009). The energetic of mangrove forests. Springer Science Business media B.V. 211 pp.

Alongi, D. M. (2014). Carbon Cycling and Storage in Mangrove Forests. Annual Review of Marine Science, 6(1), 195–219. doi:10.1146/annurev-marine-010213-135020

Amarasinghe, M.D. and Perera, K.A.R.S. (2017). Ecological biogeography of mangroves in Sri Lanka, Ceylon Journal of Science 46 (Special Issue) 2017: 119-125.

Artiola, J. F., Walworth, J. L., Musil, S. A., & Crimmins, M. A. (2019). Soil and Land Pollution. Environmental and Pollution Science, 219–235. doi:10.1016/b978-0-12-814719-1.00014-8

Barr, J. G., M. S. De Longe, and J. D. Fuentes (2014), Seasonal evapotranspiration patterns in mangrove forests, Journal of Geophysical Research: Atmospheres, 119: 3886–3899, doi:10.1002/2013JD021083.

Boto, K., Saffigna, P. and Clough, B. (1985). Role of nitrate in nitrogen nutrition of the mangrove Avicennia marina, Marine Ecology, 21: 259-261.

Bunt, J. S., Boto, K.G. and Boto, G. (1979). A survey method for estimating potential levels of mangrove primary production, Marine Biology, 52: 13-128.

Calderon, H., Weeda, R. & Uhlenbrook, S. (2014). Hydrological and Geomorphological Controls on the Water Balance Components of a Mangrove Forest During the Dry Season in the Pacific Coast of Nicaragua. Wetlands 34: 685–697. https://doi.org/10.1007/s13157-014-0534-1

Carter, M.R., Burns, L.A., Carvinder, K.R., Dugger, P.L., Fore, D.B., Hicks, D.B., Revells, H.L., Schmidt, T.W. and Farley, R. (1973). Ecosystem analysis of the big Cypress swamp and estuaries, US Environmental Protection Authority.

Chen, Y., & Ye, Y. (2014). Effects of salinity and nutrient addition on mangrove Excoecaria agallocha. PloS one, 9(4), e93337. https://doi.org/10.1371/journal.pone.0093337

Clough, B.F. and Dalhaus, D.P. (1997). Allometric relationships for estimating biomass in multi stemmed trees. Australian Journal of Botany. 45: 1023-1031.

Clough, B.F. (1998). Mangrove forest productivity and biomass accumulation in Hinchinbrook Channel, Australia Mangroves and Salt Marsh,2:191–198.

Christensen, B. (1978). Biomass and primary production of Rhizophora apiculata BI. In a mangrove forest in southern Thailand, Aquatic Botany,4: 43-52.

Day, J. W., Coronado-Molina, C., Vera-Herrera, F. R., Twilley, R., Rivera-Monroy, V. H., Alvarez-Guillen, H., Day, R. and Conner. W. (1996). A 7-year record of above-ground net primary production in a south eastern Mexican mangrove, Aquatic Botany 55: 39-60.

English, S., Wilkinson, C. and Basker, V. (1997). Survey manual for tropical marine resources (2nd Ed.), Australian Institute of Marine Science, Townsville, 119-195.

Farnsworth, E.J., Ellison, A.M., and Gong, W.K. (1996). Elevated CO2 alters anatomy, physiology, growth and reproduction of red mangrove (Rhizophora mangle L.). Oecologia ,108: 599–609.

Fujimoto, K. (2004). Below-ground carbon sequestration of mangrove forests in the Asia-Pacific region. In: Vannucci, M. (ed.) Mangrove management and conservation. United Nations University Press, Tokyo, 138–146.

Gammanpila, M., Dahanayaka, D.D.G.L., Jayasiri, H.B., 2009. Effects of limnological characteristics on seasonal abundance and distribution of zooplankton of Negombo Lagoon in Sri Lanka. In: Proceeding of International Conference on Knowledge Management for Sustainable Development, December 2009 in Kathmandu, Nepal.

Jayakody, J.M.A.L., Amrasinghe, M.D., Pahalawattarachchi,V. and De Silva, K.H.W.L. (2008). Vegetation structure and potential gross primary productivity of mangroves at Kadolkallle in Meegamuwa (Negombo) estuary, Sri Lanka, Sri Lanka Journal of Aquatic Sciences,13: 95-108.

Kathiresan, K. and Khan,S.A. (2010). International Training Course on Costal biodiversity in Mangroves: Course manual, Annamalie University (CAS in Marine Biology, Parangipettai), India. 744 pp.

Lee, S.Y. (1990). Primary productivity and particulate organic matter flow in an estuarine mangrove-wetland in Hong Kong, Marine Biology,106: 453-463.

Lovelock, C.E., Simpson, L.T., Duckett, L.J and Feller, I.C.(2015). Carbon Budgets for Caribbean Mangrove Forests of Varying Structure and with Phosphorus Enrichment, Forests, 6: 3528-3546. doi:10.3390/f6103528

Okimoto, Y., Nose, A., Katsuta, Y., Tateda, Y., Agarie, S. and Ikeda, K. (2007). Gas exchange analysis for estimating net CO2 fixation capacity of mangrove (Rhizophora stylosa) forest in mouth of river Fukido, Ishigaki island, Japan, Plant Production Science, 10 (3): 303-313.

Ong, J.E., Gong, W.K. and Clough, B.F. (1995). Structure and productivity of a 20-year-old stand of Rhizophora apiculata B1 mangrove forests, Journal of Biogeography, 22: 417-427.

Pahalawattaarchchi, V. (1995). Litter production and decomposition in the mangrove ecosystems in Negombo lagoon, (M.Phil Dissertation), Department of Botany, University of Kelaniya, Sri Lanka.

Perera, K. A. R. S., Amarasinghe, M. D. and Pahalawattaarachchi, V. (2010). Effect of vegetate on structure on potential gross primary productivity for mangrove ecosystem in Negombo estuary, Sri Lanka, Proceeding of 11th Annual Research Symposium, Faculty of Graduate Studies, University of Kelaniya, Sri Lanka, November 2010 at Kalaniya, Sri Lanka.

Perera K. A. R. S., Amarasinghe M.D. and Sumanadasa W.A. (2012). Contribution of plant species to carbon sequestration function of mangrove ecosystems in Sri Lanka. Proceeding of the International Conference: Meeting on Mangrove ecology functioning and Management (MMM3) Vrije Universiteit Brussel (VUB) the Université Libre de Bruxelles and University of Ruhuna, Sri Lanka 137.

Perera, K. A. R. S. and M. D. Amerasinghe (2016). Atmospheric carbon removal capacity of a mangrove ecosystem in a micro-tidal basin estuary in Sri Lanka, Journal of Atmospheric Environment, 134: 121-128.

Ross, M. S., Ruiz, P. L., Telesnicki, G.J. and Meeder, J.F. (2001). Estimating above-ground biomass and production in mangrove communities of Biscayne National Park, Florida (USA), Wetlands Ecology & Management, 9: 27–37.

Saenger, P. and Snedaker, S. C. (1993). Pantropical trends in mangrove above-ground biomass and annual litterfall, Oecologia, 96: 293–299.

Sherman, R.E., Fahey, T.J. and Martinez, P. (2003). Spatial patterns of biomass and aboveground net primary productivity in a mangrove ecosystem in the Dominican Republic, Ecosystems, 6: 384–398.

Sparks, D. L. (2003). The Chemistry of Saline and Sodic Soils. Environmental Soil Chemistry, 285–300. doi:10.1016/b978-012656446-4/50010-4

Sukardjo, S. and Yamada, I. (1992). Biomass and productivity of a Rhizophora mucronata Lamarck, plantation in Tritih, Central Java, Indonesia. Forest Ecology Management 49: 195-209.

Suwa, R., Khan, M. N. and Hagihara, A. (2006). Canopy photosynthesis, canopy respiration and surplus production in a subtropical mangrove Kandeliacandel forest, Okinawa island, Japan, Marine Ecology Progress Series, 320: 131-139.

Twilley, R. R., Chen, R. H. and Hargis, T. (1992). Carbon sinks in mangrove forests and their implications to the carbon budget of tropical coastal ecosystems, Water Air and Soil Pollution, 64: 265–288.

Umayangani, M.A.D. and Perera, K.A.R.S. (2017). Contribution of Vegetation Structure on Carbon Assimilation Capacity of Mangrove Ecosystem: A Case Study from Negombo Estuary, Sri Lanka, International Journal of Marine Science, 7(46): 439-446.

Zhahg, X. Y., Meng, X. J., Fan, J. J., Gao L. P., and Sun, X. M. (2010). Soil total organic carbon, δ13 C values and their responses to the soil core transferring experiment from high to low elevation forest along natural altitudinal transect of old temperate volcanic forest soils, Chinese Academy of Science knowledge Innovation Programme.

Journal of Engineering and Technology
of The Open University of Sri Lanka (JET-OUSL), Vol. 08, No.2, pp 49-61

Industrial Waste Materials as a Filler in Self Compacting Concrete

H.B.U. Nishajanthani*, G.K. Vidanapathirana, H.G.P.B. Ariyarathne and T. Priyadarshana

Department of Civil Engineering, The Open University of Sri Lanka, Nawala, Nugegoda, Sri Lanka

*Corresponding Author: email: udeshikanisha@gmail.com, Tele: +94703777434

Abstract – *Sri Lanka is currently facing a severe problem on solid waste management as it generates tons of waste per day. The currently adopted predominant method is open dumping mainly due to low cost and less processing involved. Therefore, it was intended in this study to examine the feasibility of using waste materials in self-compacting concrete to reduce their negative impacts on the environment. As such, this research aimed to evaluate the impact on the fresh state properties of self-compacting concrete by partially replacing the fine aggregate content with selected waste materials (rice husk ash, glass powder and asphalt dust waste) and to obtain an optimum percentage of the mix without loss in strength from each waste material. An optimum mix proportion was obtained by conducting performance-based tests such as slump flow test, T500 test, V funnel test, U box test and compressive strength test on the conventional self-compacting concrete mixes. Using the mix proportion obtained from the selected trial mix designs, fine aggregate content was replaced with selected industrial waste materials (rice husk ash, asphalt dust waste and glass powder) separately in percentages of 5%, 10%, 15%, 20% and 25%. Fresh state properties were checked separately for each Self-compacting concrete mix which replaced by waste materials. Hardened state properties too were checked for each mix using compressive strength tests conducted for 1 day, 7 day and 28 days. Next, the results were compared with controlled SCC mix and the optimum mix was obtained from each self-compacting concrete mix with waste materials. The results demonstrated that 5% replacement of rice husk ash (RHA), 15% replacement of glass powder (GP) and 15% replacement of asphalt dust waste (ADW) is the optimum percentages which satisfy and improves both fresh and hardened state properties of self-compacting concrete. Results obtained after 5% replacement of rice husk ash, 15% replacement of glass powder and asphalt dust waste have shown reduction in strength after 28 days. According to the cost analysis, the use of industrial waste materials (RHA, GP and ADW) to use as a filler in the production of self-compacting is profitable only marginally. Therefore, the study concludes that rice husk ash (RHA), glass powder (GP) and asphalt dust waste (ADW) are suitable as a filler in Self-compacting concrete as it improves the fresh state properties considerably without loss in strength.*

***Keywords**: Asphalt Dust Waste (ADW), Fillers, Glass Powder (GP), Rice Husk Ash (RHA), Self-Compacting Concrete (SCC)*

1 INTRODUCTION

Environmental deposition of waste materials from industrial production is a significant problem that the world is facing today since deposition sites for those wastes are getting limited increasingly (Thongkamsuk et al., 2017). As a solution to this problem, researchers are focusing on using industrial waste materials as a raw material in concrete (Mohajerani

et al., 2019). Self-compacting concrete (SCC) is a non-segregating, self-levelling and a highly flowable type concrete that is placed utilizing its weight (Han et al., 2017). The concept was first put forward by Okamura in the mid of 1980s (Esquinas *et al.*, 2018). By the mid-1990s, it was spreading around the world (Aggarwal *et al*, 2015). Since fresh SCC can flow under its weight over a long distance without segregation, bleeding and also without externally applied vibration to achieve compaction, it saves time, reduce overall cost and helps to improve the working environment (Elyamany *et al*, 2014).

Numerous applications of self-compacting concrete are available throughout the world. Some applications are the Anchorage block of the longest cable stays bridge; Akashi Kaikyo in Japan, Shin-Kiba Ohasi Bridge, Bandra Worli sea link project, the Burj Khalifa Dubai which is the tallest building in the world, La Maladiere football stadium at Switzerland and many more (Okamura and Ouchi, 2003). But, very limited applications of self- compacting concrete are available in Sri Lanka and one of the recent examples of SCC application is the silting chamber of the upper Kothmale dam (Sooriyaarachchi and Lasintha, 2016). In Sri Lanka, limited applications of SCC are available due to lack of awareness and high cost associated with its production.

To obtain enhanced quality, SCC should possess the following flow characteristics. They are the ability to flow under its own weight without vibration (filling ability), to retain homogeneity (passing ability) and segregation resistance ability (Kumar, 2015). To obtain fresh state properties, generally, SCC mixtures are adjusted by the aggregate content and by a combination of chemical and mineral admixtures (Da Silva and De Brito, 2015). Filler materials are often used to replace some of the aggregates and to modify the viscosity and also it results in sufficient segregation resistance, low yield stress and good filling ability (Angelin, Lintz and Barbosa, 2016). Chemicals used are often powerful superplasticizers and also a large number of powdered materials are too used as viscosity modifying mixtures (Guru Jawahar et al, 2013). There available several benefits of using powdered or filler materials such as to maintain sufficient stability or cohesion of the mixture so it helps in reducing bleeding, segregation and settlement (Elyamany *et al*, 2014). Self-Compacting Concrete differs from ordinary concrete mainly concerning the increase in the quantity of finer materials and reduction of coarse aggregates (Guerra, 2016). For any type of concrete, when we consider its constituents, their particle sizes and specific surface areas, and plot a graph, there is always a gap between fine aggregates and cement (Meddah et al., 2010). In the conventional concrete, this gap is filled via external compaction. As there is no compaction applied for SCC, additions of fillers are used to fill the gap (D. Han *et al*, 2017). Generally, fillers are used to obstruct pores and voids employing finer grains. In this study, Rice husk ash (RHA), Asphalt dust waste (ADW) and Glass powder (GP) which passes through 0.150mm size were used as filler materials for the partial replacement of fine aggregates.

The main byproduct of industrial processing of rice is rice husk. On average 20% of the weight of paddy is husk which sets the global estimate of the rice husk at 116 million tones (Memon et al., 2011). In Sri Lanka, rice husk is used as a fuel in brick kilns. During the burning process, 25% of the weight of this husk is converted into ash (Muntohar, 2002). In this study, rice husk ash directly put out from the industry was used. Miller (2007) has stated about 10.2 million tons of glasses are manufactured and out of them about 2.76 million tons are recycled and 8.2 million tons are discarded. According to Premachandra (2006), average composition of glass waste in Sri Lanka is 2.03. In this study, soda lime glass powder was considered which is the most prevalent type of glass. In recent past, asphalt pavement has become one of the materials commonly used for road constructions

(Ali Zangena, 2018). When producing asphalt concrete, the aggregates used are heated to a temperature of 180 ^{0}C. Next, during the cooling process, the finer particles that attached to the coarse particles get de-attached from the coarser particles. This is considered as asphalt dust waste. With the increase in demand for the asphalt concrete, there is an increase in asphalt dust waste as well as a decrease in availability of site for dumping.

When incorporating rice husk ash, glass powder and asphalt dust waste into self-compacting concrete, all three waste materials were considered as inert fillers. The impact from these three industrial waste materials on the fresh state properties of self-compacting concrete are investigated separately in this paper. Also, it attempts to determine the optimal level of fine aggregate replacement to attain satisfactory level of fresh state properties and compressive strength for self-compacting concrete.

2 METHODOLOGY

2.1 Sample Preparation

For sample preparation, rice husk ash was obtained directly from the brick kilns after fully burnt. Glass powder was prepared by grinding broken glass pieces using a ball mill. Asphalt dust waste was collected directly from a premix yard. All the materials were sieved through 0.150mm sieve.

The ranges of coarse aggregates used for the experiment were 25% from (10-20) mm range which passed through 20mm and retained on 10mm sieve sizes and 75% from (5-10) mm range that passed through 10mm and retained on 5mm sieve sizes were considered separately. M sand that pass-through 4.75mm sieve size were used for this experimental study. Chemical compositions of rice husk ash, asphalt dust waste and glass powder are shown in Table 1.

Table 1. Chemical composition of rice husk ash, glass powder and asphalt dust waste

Chemical Composition (% by mass)	Rice husk ash (RHA)	Glass Powder (GP)	Asphalt Dust Waste (ADW)
Calcium oxide (CaO)	5.24	9.6	2.90
Silica (SiO_2)	82.71	72.21	44.2
Alumina (Al_2O_3)	3.8	0.4	9.21
Iron oxide (Fe_2O_3)	1.152	0.2	4.25
Magnesium oxide (MgO)	0.89	-	0.62
Sulfur trioxide (SO_3)	0.05	-	-

2.2 Experimental Work

The present work aims to study the effect of filler types on fresh and hardened properties of SCC. Fresh and hardened properties such as slump flow, filling ability, passing ability, compressive strength *etc*. were considered.

2.2.1 Mix Design

Trial mix designs were carried out using design of experiments (DOE) method and a control mix design for high strength concrete of grade 60 was selected. A high strength concrete was selected as there available lots of on going projects relating to high rise buildings. As per the literature survey conducted, optimum results for the self compacting concrete with high strengths were shown by the mix proportions with the water-cement

ratios in the range of 0.33 and 0.35. Therefore, water – cement ratio in the range of 0.33 – 0.35 was selected and several trial mix designs for conventianal self-compacting concrete of grade 60 was carried out. From the trial mix design for conventianal self- compacting concrete, mix design which provided the optimum test results for fresh and hardened state properties was selected and chosen as the controlled mix design. Then 5%, 10%, 15%, 20%, 25% from each waste materials (RHA, GP and ADW) which was taken as a percentage from cement content in order to circumvent possible errors due to the low specific gravities of the waste materials was replaced from the fine aggregate content of the controlled mix. Next, test results were obtained for fresh and hardened state properties. Table 2 shows the controlled mix design selected after conducting the trial mix designs.

Table 2. Mix design for controlled SCC mix

Cement (kg)	W/C ratio	Water (kg)	Total CA (kg)	CA (5-10) mm (kg)	CA (10-20) mm (kg)	FA (kg)	Super Plasticizer (Glenium sky 8233) (kg)
550	0.34	189.01	814.87	611.15	203.72	857.61	5.5

The detailed actual mix design ratio as preliminary data to produce self-compacting concrete by utilizing waste materials (rice husk ash, glass powder and asphalt dust waste) are shown in table 3.

Table 3. Mix design for self compacting concrete with fine aggregate replacement

Cement (kg)	Water cement ratio	Water (kg)	Waste material %	Waste material (kg)	CA (5-10) mm (kg)	CA (10-20) mm (kg)	FA (kg)	Super plasticizer (Glenium sky 8233) kg
550	0.34	189.1	0.05	27.5	611.15	203.72	830.86	5.5
550	0.34	189.2	0.1	55	611.15	203.72	802.96	5.5
550	0.34	189.29	0.15	82.5	611.15	203.72	775.12	5.5
550	0.34	189.38	0.2	110	611.15	203.72	747.28	5.5
550	0.34	189.48	0.25	137.5	611.15	203.72	719.44	5.5

2.2.2 Tests for Physical Properties of Aggregates

Sieve analysis tests were carried out for coarse aggregates and fine aggregates (M- sand) as per BS 882:1992 and for Rice husk ash, glass powder and asphalt dust waste too, to determine the particle size distribution of the materials. Specific gravity and water absorption for M-sand, rice husk ash, asphalt dust waste and glass powder were examined according to BS 1377-part 2:1990.

2.2.3 Determine Fresh State and Hardened State Properties of Self-Compacting Concrete

To determine fresh state properties, Slump flow test, t500 test, V funnel test and U box tests were carried out as per BS EN 206-9:2010. Compressive strength test was carried out to determine the hardened properties of self-compacting concrete. The test was conducted by applying a compressive strength until the specimen was failed according to BS EN 12390. A size of150mmX 150mmX 150mm moulds were used for the test of compressive strength of concrete. For each concrete mix, 9 cubes were cast to check compressive strengths after 1 day, 7 days and 28 days. For each testing day, 3 cubes were crushed and 1-day strength

was determined immediately after demoulding without curing and others were cured.

3 RESULTS AND DISCUSSION

3.1 Physical Properties of Aggregates

Fig. 1 shows the sieve analysis test results obtained for M- sand. The lower and upper limits are specified as per the BS 882:1992. Results show the particle size distribution of M sand lies within the BS grading requirement.

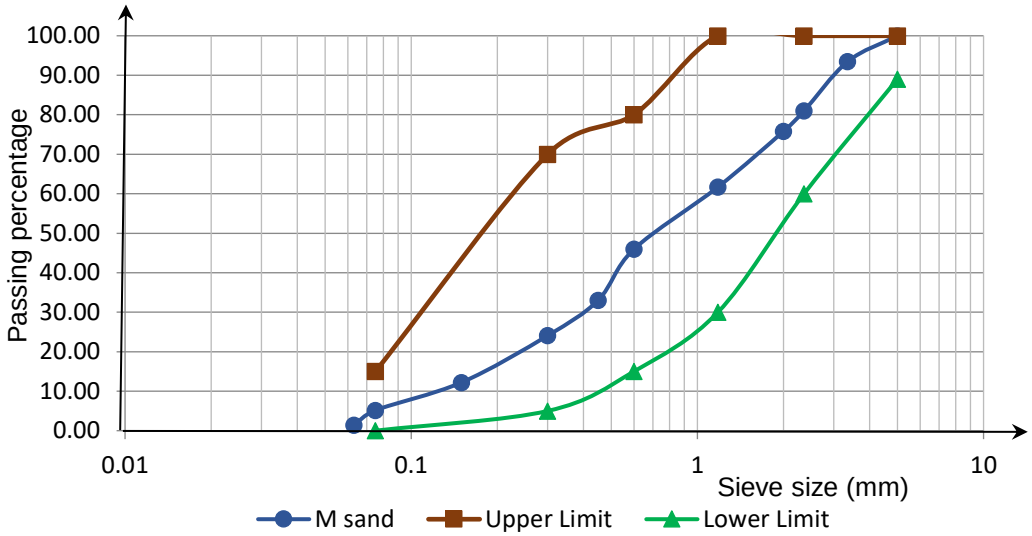

Fig. 1. Particle size distribution for M sand

The particle size distribution (PSD) curves of M sand, RHA, GP and ADW are shown in Fig. 2. Accordingly, particles of M sand, RHA, GP and ADW are well graded in their distributions.

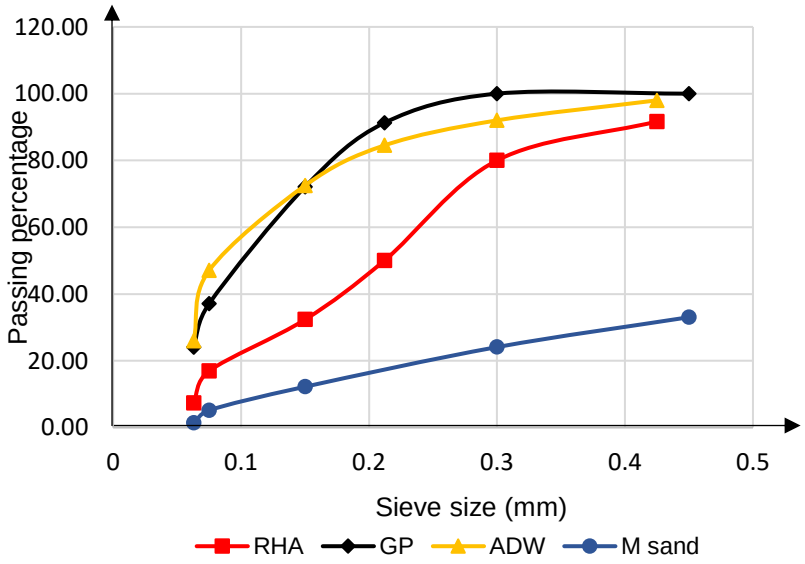

Fig. 2. Particle size distribution for M sand and waste materials

Specific gravity and water absorption for M-sand, rice husk ash, asphalt dust waste and glass powder were examined according to BS 1377-part 2:1990. Results obtained are shown in table 4 and table 5 respectively.

Table 4 – Specific gravity for constituent materials

Materials	Average specific gravity
M-Sand	2.68
Rice husk ash (R.H.A)	1.94
Asphalt dust waste (A.D.W)	2.69
Glass powder (G.P)	2.17

Results obtained for specific gravity of RHA show slight variation when compared with the results reported by Dolage *et al.,* 2011. This might be due to obtaining rice husk ash directly from the kiln and without grinding for our experiment. Results for glass powder are compatible with the results reported by Vanjare and Mahure, 2012.

Table 5. Water absorption for constituent materials

Materials	Water absorption (%)
M-Sand	0.90
Rice husk ash (R.H.A)	1.98
Asphalt dust waste (A.D.W)	1.90
Glass powder (G.P)	1.16

A larger amount of water has absorbed by rice husk ash. This may be due to the amorphous form of silica which presents highly in rice husk ash. RHA in amorphous form shows pozzolanic properties (Habeeb and Mahmud, 2010). The next highest water absorption was observed in asphalt dust waste. This might be due to its higher surface area. Accordingly, most of the results obtained for the physical properties of M-sand and waste materials (*i.e.*, rice husk ash, asphalt dust waste and glass powder) show similarities.

3.2 Fresh State Properties of Self-Compacting Concrete

A self- compacting concrete at fresh state must be stable to achieve homogeneity of the mechanical strength of the structure. Slump flow, V funnel and U box tests are carried out to understand the workability of self- compacting concrete. Criteria required for the fresh state properties of SCC according to BS EN 206-9:2010 are as shown in table 6.

Table 6. Criteria for self-compacting concrete according to BS EN 206-9: 2010

Test method	Properties	Range of values
Slump Flow	Filling ability	660-750 mm
T50	Viscosity	2-7 s
V-Funnel	Viscosity	6-15 s
U-box	passing ability	0-30 mm

Results obtained for fresh state properties obtained for the control mix obtained from trial mixes, RHA-SCC mixes, GP-SCC mixes and ADW- SCC mixes are shown in table 7. Fresh

state property results obtained for the selected conventional trial mix satisfied all the requirements of EN 206-9: 2010.

Table 7. Fresh state properties obtained for control mix, RHA-SCC, GP-SCC and ADW-SCC mixes

	Mix Design	Slump Flow (mm)		Average Flow (mm)	S.F. T500 (s)	V Funnel (s)	U- Box (mm)		
		D1	D2				H1	H2	H1 – H2
Control Mix	TM-5	740	750	745	4.81	10.57	282	282	0
RHA-SCC MIX	RHA 5%	720	730	725	5.93	13.01	282	282	0
	RHA 10%	715	705	710	7.26	14.25	285	269	16
	RHA 15%	685	685	685	7.65	9.64	278	278	0
	RHA 20%	590	600	600	8.43	9.17	294	275	19
	RHA 25%	490	490	490	0	6.54	302	279	23
GP – SCC MIX	GP 5%	745	755	750	6.18	13.58	280	270	10
	GP 10%	715	725	720	5.56	14.65	285	273	12
	GP 15%	720	715	717.5	6.44	14.78	285	285	0
	GP 20%	720	710	715	6.72	15.04	280	280	0
	GP 25%	695	695	695	7.21	14.28	288	280	8
ADW – SCC MIX	ADW 5%	735	735	735	4.05	11.28	284	284	0
	ADW 10%	710	700	705	6.58	13.64	288	276	12
	ADW 15%	705	695	700	6.32	12.36	295	275	20
	ADW 20%	695	695	695	6.00	13.95	295	274	21
	ADW 25%	690	700	695	6.07	14.98	288	271	17

As shown in Fig. 3, the results of slump flow test were obtained between 660 and 750 mm for the mixtures containing rice husk ash up to 15%, glass powder and asphalt dust waste up to 25%. Slump flow of 5% replacement of glass powder has reached to upper limit because of low viscosity. However, replacement of rice husk ash after 15% have decreased from 685mm to 4900mm due to increase in viscosity and thixotropy. Higher water absorption of rice husk ash might be the reason to low slump flow. In similar studies done by Samantaray *et al*. (2016) and Chopra *et al.* (2015), results of the fresh state properties shown up by 15% replacement of RHA tally with the results of this study. According to Safawi *et al.* (2005), there available four parts of the slump flow; between 400 and 500mm,

500 and 600mm, 600 and 700 mm and 700 and 800mm. Generally, highly viscous mixtures have slump flows less than and around 500mm. The viscosity of the mixture would be expected to be optimum at slump flows at 600mm and it would flow easily by virtue of its own weight. Slump flows between 700mm and 800mm would be prone to segregation easily.

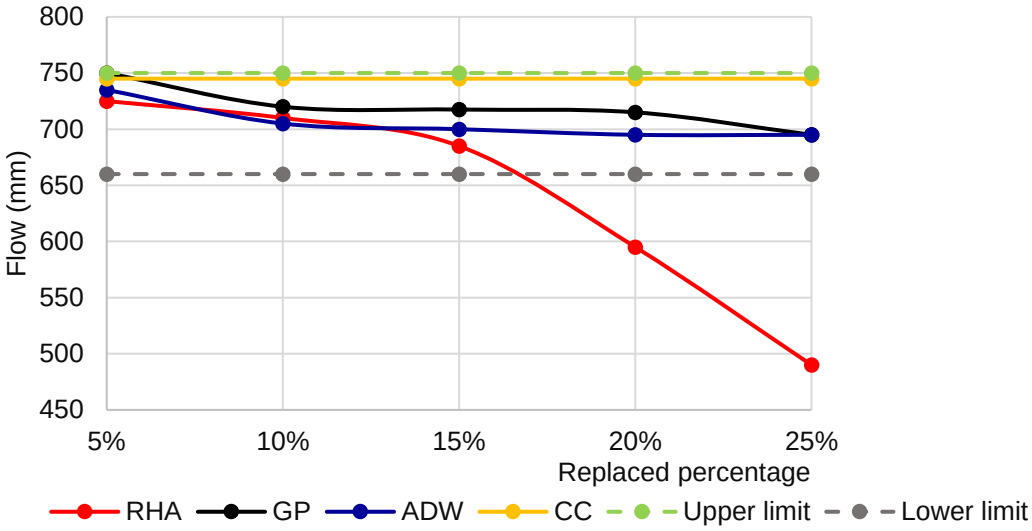

Fig. 3. Slump flow test results

Results obtained for V funnel are shown in fig. 4.

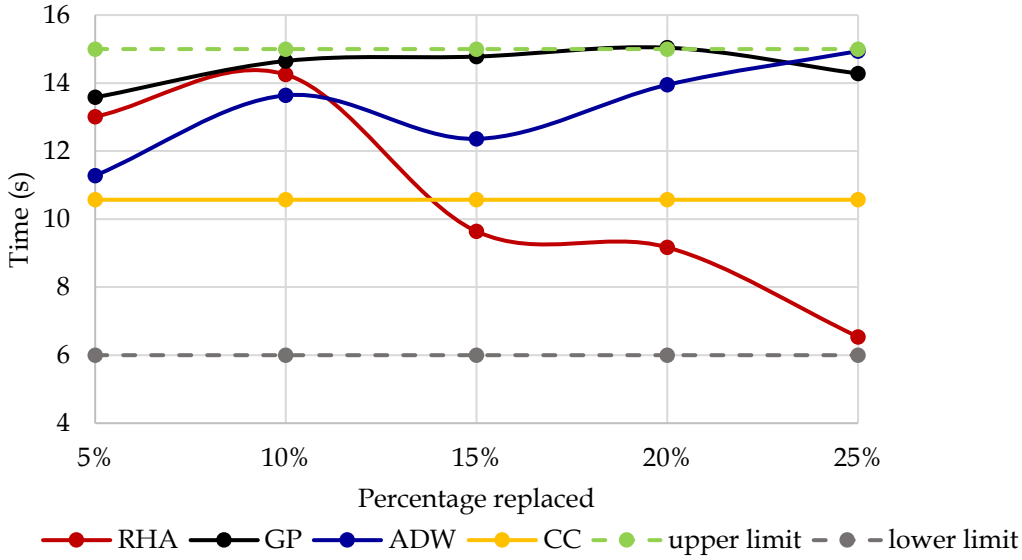

Fig. 4. V funnel test results

15%, 20% and 25% replacement of RHA has shown lower results than that for the results obtained for the conventional concrete mix. Which in turn means good flowability. Except 20% replacement of glass powder, all the other results obtained for each mix were within the limit specified by BS EN 206-9: 2010 which means mixes with good viscosities and segregation resistances. The viscosity of self-compacting concrete with glass powder was

very high and therefore V funnel flow time was closer to 15s which is the upper limit. Reasons for decrease in flow resistance might be due to the increase in packing density of the fresh mix resulting due to various parameters like the reactivity of fillers, the volume of fine particles required to fill the total volume of voids in the mix, water cement ratios and etc.

Fig. 5 indicates the results related to U box and it indicates the filling and passing ability of SCC. U box test is more sensitive to blocking.

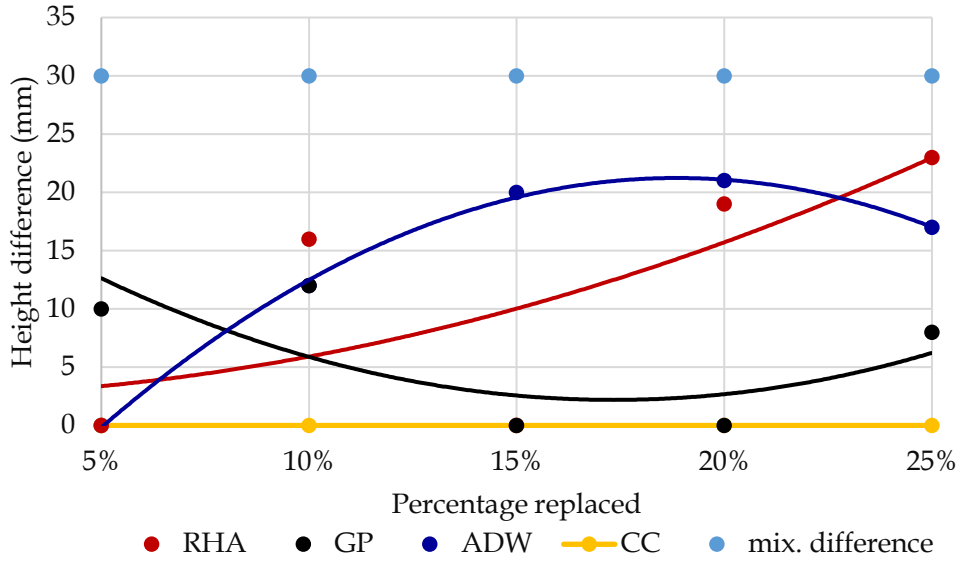

Fig. 5. U box test results

Results obtained for U box test of each mixes were in target range. According to Nguyen et al, (2006), if the standard procedure is followed to carry out the testing and the U box gate is quickly lifted, the flow is controlled by inertia effects, depending on the lifting speed of the gate and thus, depending on the operator. Once the gate is slowly lifted, the kinetic energy is spread over the gate lifting duration. Then the flow moves slowly towards the other side. These can be considered as the reasons for the variations of the results obtained for each percentage.

According to the results obtained for the fresh state properties, 5% and 10% replacement of rice husk ash, 5%, 10%, 15% and 20% replacement of glass powder and 5%, 10% and 15% of asphalt dust waste has shown best performance according to the BS EN 12350-8: 2009.

3.3 Hardened State Properties of Self-Compacting Concrete

Compressive strength of crushed concrete cubes was determined by dividing failure load by surface area of the cube (*i.e.*, 0.0225m^2). Fig. 6 illustrates the results obtained for 28 days compressive strength test results.

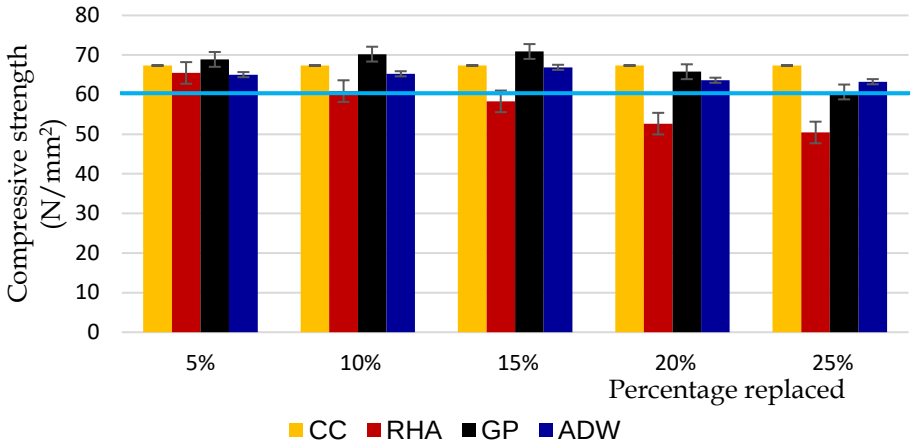

Fig. 6. 28 days compressive strength results

Addition of RHA has a noticeable effect on the compressive strength of the hardened SCC. This may be due to the lightweight of the rice husk ash and higher water absorption. As can be seen from the results obtained for the compressive strengths, 5% and 10% replacement of RHA generates the highest compressive strengths. Furthermore, the compressive strengths decrease as the amount of RHA replacements increase. Compressive strength results obtained are similar to the results reported by Chopra *et al.* (2015). But maximum strength recorded by Chopra *et al.* (2015) is 15%. This might be due to obtaining RHA directly from the kilns without further grinding in our studies.

When considering the addition of glass powder, 5%, 10%, 15% and 20% replacement of glass powder has shown the best result for compressive strengths. The results aren't tally with the results reported by Vanjare et al. 2012 but are similar to the results recorded by Islam et al.2016. As per the results obtained for the 28-day compressive strengths for ADW-SCC mixes, the maximum compressive strength has recorded for the 15% replacement of ADW. The obtained results are compatible with the results recorded by Ismail *et al*, (2017).

The positive effects of different filler contents in SCC on fresh concrete properties have also shown positive results for hardened concrete properties too. Accordingly, it can be seen that the strength of self compacting concrete with fillers have increased up to a certain percentage of addition of fillers because of the good packing arrangement. So, the strengthening effect of fillers on concrete paste derives from the improvement of the pore structure. According to the 28-day test results, 5% replacement of rice husk ash, 15% replacement of glass powder and 15% replacement of asphalt dust waste has shown good results.

3.4 Cost Analysis

Self-compacting concrete should workable as well as profitable when using industrial waste materials without loss in strength. To decide the profitability of the concrete a cost analysis was carried out as per the market price in July 2018. Only, the cost for 1m^3 of constituent materials for self-compacting concrete was analyzed and cost for

transportation was not considered. The mixes selected for calculation and analysis were those which showed optimum results for fresh and hardened state properties. Table 9 shows Cost comparison of controlled self-compacting concrete with RHA-SCC, GP- SCC and ADW-SCC.

Table 8. Cost comparison of controlled self-compacting concrete with M sand only, RHA-SCC, GP- SCC and ADW-SCC

Mixture	The unit price for 1m³		Saving percentage (%)
	LKR	USD	
SCC with M sand only	15568.65	97.50	-
SCC-Rice husk ash	15482.31	96.96	0.55
SCC-Asphalt dust waste	15420.62	96.57	0.95
SCC-Glass powder	15503.12	97.08	0.42

According to table 8, the introduction of industrial waste materials as filler to the self-compacting concrete has resulted in only a marginal profit to the conventional self-compacting concrete. This is due to replacement of fine aggregate contents from fewer amounts of industrial waste materials. The reason for the comparatively lower saving percentage for SCC- glass powder mix is due to additional grinding cost. When comparing the results obtained for fresh and hardened state properties together with the cost analysis, 5% replacement of rice husk ash, 15% replacement of glass powder and 15% replacement of asphalt dust waste has shown optimum results.

4 CONCLUSION

Fresh and hardened state properties of the rice husk ash, glass powder and asphalt dust waste integrated SCC mixes were evaluated and compared with those of the conventional SCC. The results on the properties of fresh self compacting concrete such as slump flow, V funnel time and blocking ratio revealed that rice husk ash, glass powder and asphalt dust waste have a significant effect on the flow, segregation resistance and bleeding resistance. The homogeneity of the pastes containing finest fillers might be a possible cause for obtaining better results for fresh state properties. The increase in rice husk ash, glass powder and asphalt dust waste content from 5% to 15% improved bleeding and segregation resistance of SCC. When compare both results obtained for fresh and hardened properties, 5% replacement of rice husk ash, 15% replacement of glass powder and asphalt dust waste have improved both fresh and hardened state properties of the self compacting concrete. Based on the results, it seems that concrete strength can be increased via improved particle packing. Several of the by products generated from industries widely abundant can therefore be recycled into self-compacting concrete to bring about improvements in strength, durability and rheology while saving material cost upto a certain amount and while preventing environmental pollution caused by open dumpings.

ACKNOWLEDGEMENT

The authors would like to express their gratitude to Siam City Cement (Lanka) Limited for providing required cement for this research.

REFERENCES

Aggarawal, P., Siddique, R., Aggarawal, Y., Gupta, M.S., 2015, Study on Fresh and Mechanical Properties of Coconut Fiber Reinforced Self Compacting Concrete Enhanced with Steel Fibers, Int. J. Eng. Res. V4, 15–24, https://doi.org/10.17577/ijertv4is060939.

Ali Zangena, S., 2018, Performance of asphalt mixture with nanoparticles, Nanotechnology in Eco-efficient Construction: Materials, Processes and Applications. Elsevier Ltd. https://doi.org/10.1016/B978-0-08-102641-0.00008-6.

British Standards Institution (1992) BS 882:1992 Specification for aggregates from natural sources for concrete, 1st ed. Brussels: BSi. Bs 8821992 1–14.

Chopra, D., Siddique, R., Kunal, 2015. Strength, permeability and microstructure of self-compacting concrete containing rice husk ash, Biosyst. Eng. 130, 72–80, https://doi.org/10.1016/j.biosystemseng.2014.12.005.

Da Silva, P.R., De Brito, J., 2015. Fresh-state properties of self-compacting mortar and concrete with combined use of limestone filler and fly ash, Mater. Res. 18, 1097–1108, https://doi.org/10.1590/1516-1439.028715.

DoIage, D.A.R., Mylvaganam, K., Mayoorathan, P., Inparatnam, S., 2011, Use of Rice Husk Ash Blended Cement to Produce Cement Sand Blocks: Optimal Level of Cement Replacement for Compressive Strength, Eng. J. Inst. Eng. Sri Lanka 44, 11. https://doi.org/10.4038/engineer.v44i2.7019.

Elyamany, H.E., Elmoaty, A.E.M., Mohamed, B., 2014, Effect of filler types on physical, mechanical and microstructure of self-compacting concrete and Flow-able concrete. Alexandria Eng. J. 53, 295–307, https://doi.org/10.1016/j.aej.2014.03.010.

Esquinas, A.R., Ledesma, E.F., Otero, R., Jiménez, J.R., Fernández, J.M., 2018, Mechanical behaviour of self-compacting concrete made with non-conforming fly ash from coal-fired power plants. Constr. Build. Mater. 182, 385–398, https://doi.org/10.1016/j.conbuildmat.2018.06.094.

European Standards institution (2010) EN 206- 9, 2010, Additional rules for self-compacting concrete, 1st ed. Brussels: BSi.

Jawahar, G.J., Sashidhar, C., Reddy, R.I. V., Peter, A.J., 2013, Optimization of superplasticiser and viscosity modifying agent in self-compacting mortar, Asian J. Civ. Eng. 14, 71–86.

Habeeb, G.A., Mahmud, H. Bin, 2010, Study on properties of rice husk ash and its use as cement replacement material, Mater. Res. 13, 185–190, https://doi.org/10.1590/S1516-14392010000200011.

Han, B., Zhang, L., Ou, J., 2017. Smart and multifunctional concrete toward sustainable infrastructures, Smart Multifunct. Concr. Towar. Sustain. Infrastructures 1–400, https://doi.org/10.1007/978-981-10-4349-9.

Han, D., Kim, J.H., Lee, J.H., Kang, S.T., 2017, Critical Grain Size of Fine Aggregates in the View of the Rheology of Mortar, Int. J. Concr. Struct. Mater. 11, 627–635, https://doi.org/10.1007/s40069-017-0217-4.

Islam, G.M.S., Rahman, M.H. & Kazi, N., 2016, Waste glass powder as partial replacement of cement for sustainable concrete practise, Science Direct, Vol 6, pp. 37 -44, https://doi.org/10.1016/j.ijsbe.2016.10.005.

Ismail, I., Shahidan, S. & Bahari, N.A.A.S., 2017, Asphalt dust waste material as a paste volume in developing sustainable self-compacting concrete (SCC), American Institute of Physics, 1901(1), pp. 1 -5. https://doi.org/10.1063/1.5010562.

Kumar D, R., 2015, Self-Compacted Concrete Mix Design and its Comparison with Conventional Concrete (M-40), J. Civ. Environ. Eng. 05, https://doi.org/10.4172/2165-784x.1000176.

Meddah, M.S., Zitouni, S., Belâabes, S., 2010, Effect of content and particle size distribution of coarse aggregate on the compressive strength of concrete. Constr. Build. Mater. 24, 505–512. https://doi.org/10.1016/j.conbuildmat.2009.10.009.

Memon, S.A., Shaikh, M.A., Akbar, H., 2011, Utilization of Rice Husk Ash as viscosity modifying agent in Self Compacting Concrete, Constr. Build. Mater. 25, 1044–1048. https://doi.org/10.1016/j.conbuildmat.2010.06.074.

Miller, C., 2007, Glass Containers, Ind. Eng. Chem. 53, 23A-24A. https://doi.org/10.1021/i650623a715.

Mohajerani, A., Suter, D., Jeffrey-Bailey, T., Song, T., Arulrajah, A., Horpibulsuk, S., Law, D., 2019, Recycling waste materials in geopolymer concrete, Clean Technol. Environ. Policy 21, 493–515, https://doi.org/10.1007/s10098-018-01660-2.

Muntohar, A.S., 2002, Utilization of Uncontrolled Burnt Rice Husk Ash in Soil Improvement, Civ. Eng. Dimens. 4, pp.100-105.

Okamura, H., Ouchi, M., 2003, Self-compacting concrete, Journal of Advanced Concrete Technology, Vol. 1, pp. 5 – 15, https://doi.org/https://doi.org/10.3151/jact.1.5.

Premachandra, H.S., 2006, Household Waste Composting & MSW Recycling in Sri Lanka, in: Asia 3R Conference. p. 43.

Safawi, M.I., Iwaki, I., Miura, T., 2005. A study on the applicability of vibration in fresh high fluidity concrete. Cem. Concr. Res. 35, 1834–1845. https://doi.org/10.1016/j.cemconres.2004.10.031

Samantaray, S.S., Panda, K.C., Mishra, M., 2016, Rice husk ash as fine aggregate sustainable material for strength enhancement of conventional and self-compacting concrete, Key Eng. Mater. 692, 94–103, https://doi.org/10.4028/www.scientific.net/KEM.692.94.

Sobolev, K., Flores, I., Torres-Martinez, L.M., Valdez, P.L., Zarazua, E., Cuellar, E.L., 2009, Engineering of SiO2 Nanoparticles for Optimal Performance in Nano Cement-Based Materials, Nanotechnol. Constr. 3 139–148, https://doi.org/10.1007/978-3-642-00980-8_18.

Sooriyaarachchi, H.P. and Lasintha, E.D.L., 2016, Influence of Fine Aggregate Types on the Performance of Self - Compacting Concrete, Engineer: Journal of the Institution of Engineers, Sri Lanka, 49(1), pp.9–20, DOI: http://doi.org/10.4038/engineer.v49i1.6914.

Thongkamsuk, P., Sudasna, K., Tondee, T., 2017, Waste generated in high-rise buildings construction: A current situation in Thailand. Energy Procedia 138, 411–416, https://doi.org/10.1016/j.egypro.2017.10.186.

Journal of Engineering and Technology
of The Open University of Sri Lanka (JET-OUSL), Vol. 08, No.2, pp 62-75

Effect of Irrigation and Nitrogen Fertilization on Growth and Yield of Capsicum (*Capsicum Annum*) under Temperature Induced Water Stress

R. P. D. N. Kumara*, C. S. De Silva, H. K. L. K. Gunasekara

Department of Agricultural and Plantation Engineering, The Open University of Sri Lanka, Nawala, Nugegoda, Sri Lanka.

*Corresponding Author: email: dineshnuwan0110@gmail.com,Tele: +94717561134

Abstract – *Climate change represents abnormal climatic conditions that can effect agricultural production through their impact on temperature changes and water availability. In addition to that the climate change will intensify the existing hunger and food insecurity problems since it can greatly increase the risk of crop failure and the loss of livestock. Nutrients play a vital role in the production of certain crops and its application is one of the quickest and easiest way in increasing yield. Nitrogen fertilization has been reported to mitigate the adverse effects of temperature stress and water stress. Therefore, this study has done to identify the interaction effects of temperature, irrigation and nitrogen fertilization on growth and yield of Capsicum annum. Three factors have used: temperature with two levels (Temperature stress/ T1 and Ambient temperature/T2), Irrigation with three levels (Field capacity/ I1, 150% of field capacity/ I2 and 200% of field capacity/ I3) and nitrogen fertilizer (recommended level/ N1, 150% of recommended level of nitrogen and 200% of recommended level of nitrogen). Three replicates have used for every treatment and trials was replicated thrice. All the treatments were arranged in Completely Randomized Design (CRD) and Analysis of variance (ANOVA) tests were conducted on the measured variables using the PROC MIXED procedure of SAS Software for Windows (University Version).*
The Duncan Multiple Range Test was used to determine the differences in treatment means at $P<0.05$. According to the analyzed data, all the factors and their interaction effects were significantly ($P<0.05$) different and influenced on growth and yield parameters of Capsicum annum. The study findings clearly revealed that under ambient temperature condition, application of currently recommended level of nitrogen by Department of Agriculture Sri Lanka was enough to obtain higher yield. However, under temperature stress condition, plants treated with 150% of the DOA recommended nitrogen fertilizer have shown significantly higher yield. Plants with the application of 200% of Nitrogen have shown poor results on growth and yield either at the temperature stress or ambient temperature conditions.

Keywords: *Temperature, Irrigation, Nitrogen, Growth, Yield*

1 INTRODUCTION

Global warming and climatic changes are huge threats to the world. Climatic changes are occurred in rapidly and its adverse nature negatively influenced on agriculture sector. Agriculture in developing countries, has received considerable attention recently with regard to climate change because of the high dependence of agriculture on the climate. The climate change represents abnormal climatic situations that can effect agricultural production through their impact on temperature changes and water availability (Syaukat, 2011). World's population is increasing at an alarming rate and is expected to reach about

nine to ten billion by the end of year 2050 (Waraich *et al.,* 2012). Therefore, it resulted in additional demand for food production. According to the Second National Communication (2011), in Sri Lanka temperature is expected to rise from 1.1– 2.4 °C by 2100, depending on the rate of emission. The analysis of long-term air temperature data shows that significant warming has taken place in all climatic zones in Sri Lanka, while most locations exceed the global average rate of warming (De costa 2008). Mean surface temperatures show an increasing trend by 2.6 °C /100 years and 1.7 °C /100 years on average in annual average maximum and minimum temperature respectively in Sri Lanka. This means that the warming trend for maximum temperature is twice that for minimum temperature (Zubair *et al.,* 2010). In general, high temperature may lead to significant losses in crop productivity in many species due to limited vegetative and reproductive growth. Temperature stress also resulted in scorching and sunburns on leaves, leaf senescence and abscission, inhibition of shoot and root growth and reduction of yield. In high temperature, plants adapted to decrease leaf area, number of leaves and induced the closure of stomata to decrease transpiration losses. Then it resulted to decrease photosynthesis rate due to reduction of area of the leave, number of leaves and CO_2 fixation.

Due the temperature increment water stress or scarcity is also induced. De Silva *et al.,* (2007) predicted using HadCM3 general circulation model that, by 2050, rainfall will decrease by 9% to 17% in the main *maha* cultivation season resulting lack of water to irrigate farmer fields. Therefore, significant reduction in growth and yield of agricultural crops may be resulted.

Thus, it is very important to mitigate such temperature and water stress condition to obtain higher yield with quality. Nitrogen is very important for temperature tolerance in plants (Waraich, 2012). High temperature resulted high light intensity and it affected on mineral nutrition uptake and negatively affected on plant. Nitrogen plays a major role in utilization of absorbed light energy and photosynthetic carbon metabolism (Kato *et al.,* 2003). Furthermore, plants which were grown under high light intensity with a high N supply had greater tolerance to photo-oxidative damage (Kato *et al.,* 2003). The regulatory function of N in water stress tolerance of plant depends upon the intensity of water stress and N level. The proper N level supports regular plant growth and helps plants to defence stress (Chang *et al.,* 2016). It has been proposed that crops supplied with relatively higher N had better growth and yield performance than that supplied with low N under drought stress (Haefele *et al.,* 2008; Tran *et al.,* 2014 and Wang *et al.,* 2016). According to the earlier statements, higher N reduces the adverse effects of temperature stress and water stress on crop growth and yield.

Therefore, this study was conducted to investigate the interaction effects of temperature, irrigation and nitrogen level on growth and yield parameters of Capsicum in order to find out the best level of nitrogen and irrigation level under temperature stress conditions as well as under ambient temperature condition.

2. METHODOLOGY

Experiment was designed with three factors namely temperature, irrigation and nitrogen levels. Two temperature levels were used as higher temperature (36-37 ^{0}C) and ambient temperature (32-33 ^{0}C). Three irrigation treatments used as Field capacity, 150% from field capacity and 200% from field capacity and volume basis method has used to find above volume. Three N level were used as 100%, 150% and 200% of the recommended nitrogen level by Department of Agriculture Sri Lanka. Urea was used to provide nitrogen. Twelve treatments arranged in Complete Randomized Block Design (CRD) with three replicates.

Pots were arranged randomly at the poly tunnel as well as in a plant house. Experiment was repeated thrice to replicate the poly tunnel effects.

Factor 1: Temperature – Two Levels

Temperature stress – T1 (36-37 ^{0}C)

Ambient temperature – T2 (32-33 ^{0}C)

These temperatures were selected based on IPCC result on global climate (IPCC, 2007) and the HadCM3 predictions of Sri Lankan air temperature in 2050 for A2 scenario of IPCC (De Silva *et al.,* 2007 and De Silva, 2006).

Factor 2: Irrigation Capacity–Three Levels

Field capacity soil moisture – I1

150% of field capacity soil moisture – I2

200% of field capacity soil moisture – I3

Factor 3: Nitrogen (%) – Three levels

100% from recommended level – N1

150% from recommended level – N2

200% from recommended level –N3

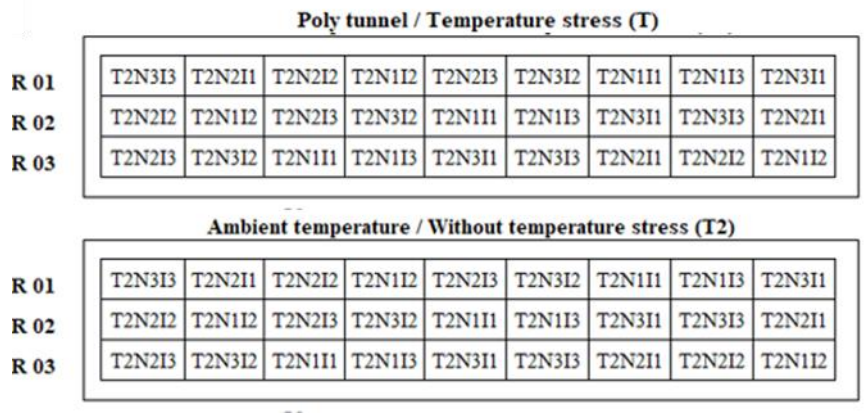

Fig. 1. Field Layout of the Experiment

2.2 LOCATION

2.2.1 Temperature stress in poly Tunnel

The study carried out at the Open University of Sri Lanka. One set of plants kept in temperature stress condition at the poly tunnel and temperature range maintained at 36^{0}C - 37^{0}C through an automated regulatory system. Poly tunnel is consisted with top-vent roof. When the temperature inside the poly tunnel increases above the maximum temperature set in thermostat the ventilation fans start to operate automatically until the

temperature is reduced to the maximum set temperature in the thermostat.

2.2.2 *Ambient Temperature in Plant House*

The other set of plant kept in ambient temperature condition (32^0C - 33^0C) at plant house. Type of net house frame is rigid wall and roof of the plant house was made with polyvinyl chloride (PVC) sheet of 120 micron gauge to have more than 90% transmittance of light. UV-stabilized polyethylene shade net which covered sun by 50% was used to cover the side parts of the plant house and fiberglass hoops to support the fabric and secure it with clothespins. Free movement of air and other climatic conditions are same as outside.

2.2.3 *Temperature and relative humidity variation inside the plant house and poly tunnel*

There were no significant differences in RH observed in the inside and outside environment although elevated day time air temperatures in the poly tunnel resulted in higher partial pressure of water (*Gunawardena et al.,* 2011). This condition was maintained with the opening of the top of the poly tunnel which helped to maintain the same water vapour concentration compared to the outside. According to the observed data for RH, there was no significant differences in RH at the inside and outside of the plant house. In addition to that light intensity in the poly tunnel and plant house was not significantly different. Therefore, apart from the temperature other conditions were approximately similar for poly tunnel and the plant house.

The variation of temperature inside the poly tunnel and the ambient temperature of plant house over a period of 24 hours was observed as shown below (Fig.2). The temperature within the poly tunnel was lower than the maximum temperature set for that particular poly tunnel during a day represents the diurnal variation. However, the temperature maintained inside the poly tunnels was always higher than the ambient temperature at plant house; therefore, temperature stress was forced on the plants during daytime while there was photosynthetic activity.

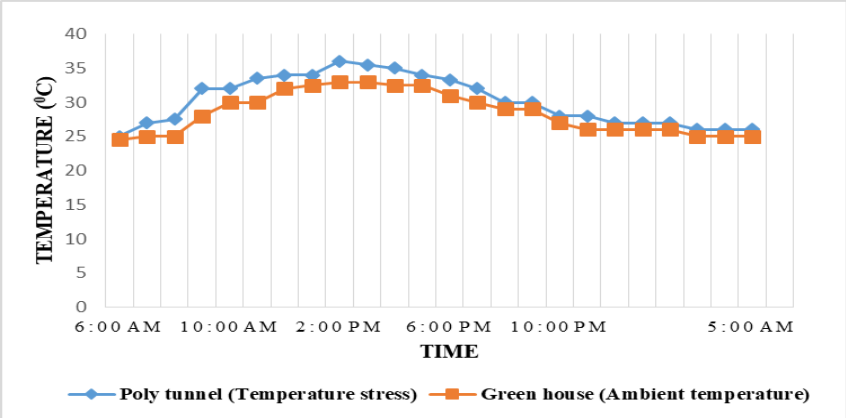

Fig. 2. Variation of temperature with time (day) inside of the poly tunnel and the plant house

2.3 EXPERIMENTAL DESIGN

The experiment was arranged with three factor factorial experiment with twelve treatments in pots. The pots (each 25cm high and 28.5 cm in bottom diameter) were filled with Reddish Brown Earth Soil collected from Anuradhapura. Before experiment started, soil was prepared by removing stones and crop residues air dried, crushed, and well mixed thoroughly to avoid water logging conditions. CA-8 variety of Capsicum (*Capsicum annum*) was used for the experiment and nursery was maintained for one month. Thereafter, one month old plants were planted in pots, fertilization was done according to the recommendation of Department of Agriculture (DOA), Sri Lanka. Application of nitrogen fertilizer at appropriate intervals was done as recommended by DOA. Field capacity of the soil measured using pressure plate apparatus by applying 1/3 bar pressure. As a control, additional ten pots were kept inside the poly tunnel and the plant house without adding fertilizer and plants to determine the weight losses in soil due to evaporation. Pots irrigated to field capacity. Before watering at each time, the pots were weighted and confirmed the constant weight in all pots. According to the weight losses in additional pots, amounts of water required for each pot to fulfill the field capacity, 150% from field capacity and 200% from field capacity were calculated and applied the calculated amount of water to treatments. Therefore, irrigation was done once per two days according to the treatments (Field capacity (I1) 150% from field capacity (I2), 200% field capacity (I3)) by compensating the loss in weight.

Growth parameters were measured once per two weeks till the end of the growing season and yield parameters were taken at harvest. Analysis of variance (ANOVA) tests were conducted on the measured variables using the PROC MIXED procedure of SAS software for Windows (University Version). Treatment effects due to N fertilizer, temperature stress, irrigation amount and their interactions on growth and yield parameters were tested. The Duncan Multiple Range Test was used to determine the differences in treatment means at $P < 0.05$. A probability level of 0.05 was considered to identify significantly different treatment means in this study.

3.0 RESULTS AND DISCUSSION

3.1 Growth parameters of *Capsicum annum*

3.1.1 Plant height (cm)

According to the analysed data, all the factors and their interaction effect have significantly ($P<0.05$) influenced on plant height. Under ambient temperature condition, significantly highest plant heights were shown in treatments with 100% DOA recommended Nitrogen fertilizer and field capacity level of irrigation (T2N1I1), 150% nitrogen fertilizer with field capacity (T2N2I1) and 150% of the field capacity (T2N2I2) level irrigation. Therefore, under ambient temperature conditions, increment of nitrogen fertilizer application or the irrigation above the field capacity level is not necessary as there is no significant difference ($p>0.05$) among these treatments. Under temperature stress condition, significantly highest plant heights were shown in treatments with 150% of the DOA recommended levels of

nitrogen fertilizer with field capacity (T1N2I1) and 150% of the field capacity (T1N2I2) level irrigation. Therefore, under temperature stress condition, application of nitrogen fertilizer higher than the recommended level is beneficial. Efficient nitrogen nutrition has the capability to assuage water stress and temperature stress in crops by sustaining metabolic activities (Saud *et al.*, 2017). However, too much of nitrogen fertilizer application cannot be recommended because treatments with 200% nitrogen of recommendation have resulted lower performances either at temperature stress condition or ambient temperature condition. It could be the excessive use of nitrate fertilizer to plants induce toxicity.

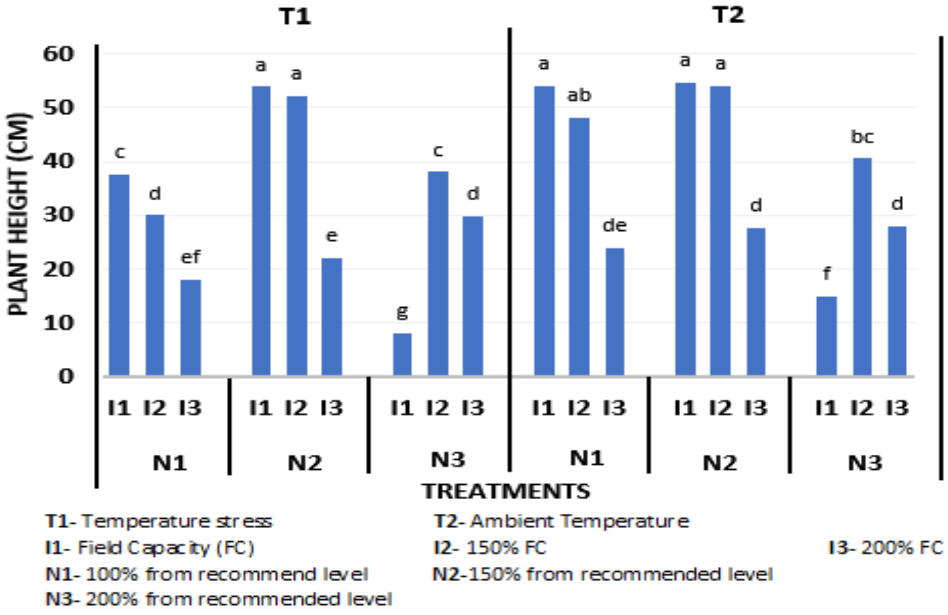

Fig.3. Effect of different treatments on plant height (cm) of *Capsicum annum* at 75days after planting

Note: Values followed by same letter are not significantly different at p =0.05 level

3.1.2 Number of leaves

Results of number of leaves also followed the same pattern as the results of plant height. Treatment of 200% nitrogen (DOA recommendation) with irrigated to field capacity has resulted the lowest number of leaves at both temperature stress and ambient temperature conditions (T1N3I1, T2N3I1). Treatments of 150% nitrogen of DOA recommendation with irrigation at field capacity and 150% of field capacity levels either at the temperature stress or ambient temperature condition (T1N2I1, T1N2I2, T2N2I1, T2N2I2) have resulted higher number of leaves. However, these treatments have not significantly differed (P>0.05) from the treatment with recommended level of nitrogen and irrigated to field capacity (T2N1I1). Therefore, under ambient temperature condition recommended level of nitrogen has enough to obtain higher number of leaves and it is contrast to the results under temperature stress condition. Because, under temperature stress condition, recommended level of nitrogen is not sufficient to obtain higher number of leaves.

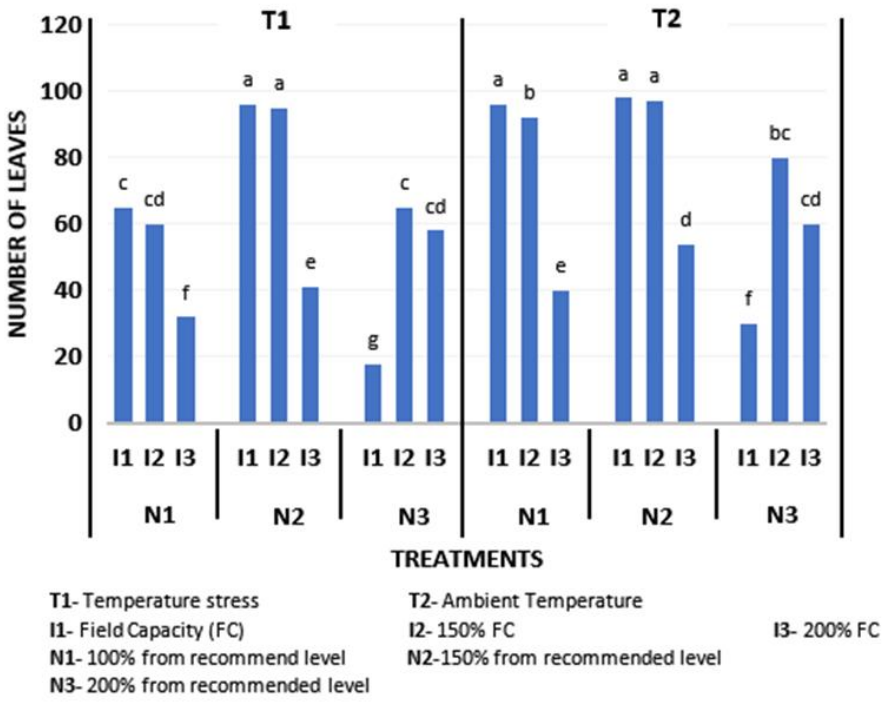

Fig.4. Effect of different treatments on number of leaves of *Capsicum annum* at 75days after planting (*Values followed by same letter are not significantly different at p =0.05 level)***

3.1.3 Leaf area (cm²)

Leaf area is one of the very important parameters because it has influence on photosynthesis. According to the analysed data all the parameters and their interaction effects (Temperature* Nitrogen* Irrigation) have significantly ($P<0.05$) influenced on leaf area. Leaf area of treatments with 150% nitrogen of DOA recommendation and irrigated to field capacity has shown the highest leaf area under the temperature stress condition (T1N2I1) and it was not significantly different ($P>0.05$) from the treatment with that in 150% nitrogen of DOA recommendation and irrigated to 150% of field capacity under temperature stress condition (T1N2I2). Under ambient temperature condition, treatments treated with 150% nitrogen (DOA recommendation) and irrigated to field capacity and 150% of field capacity (T2N2I1, T2N2I2) have shown higher leaf area. However, those treatments are not significantly different from the treatment applied with recommended level of nitrogen and irrigated to field capacity under ambient temperature condition (T2N1I1). According to this finding, it is not needed to increase the amount of nitrogen beyond the recommended level under ambient temperature condition. Barrs (1968) reported that favourable weather condition and management practices are important to increase leaf area.

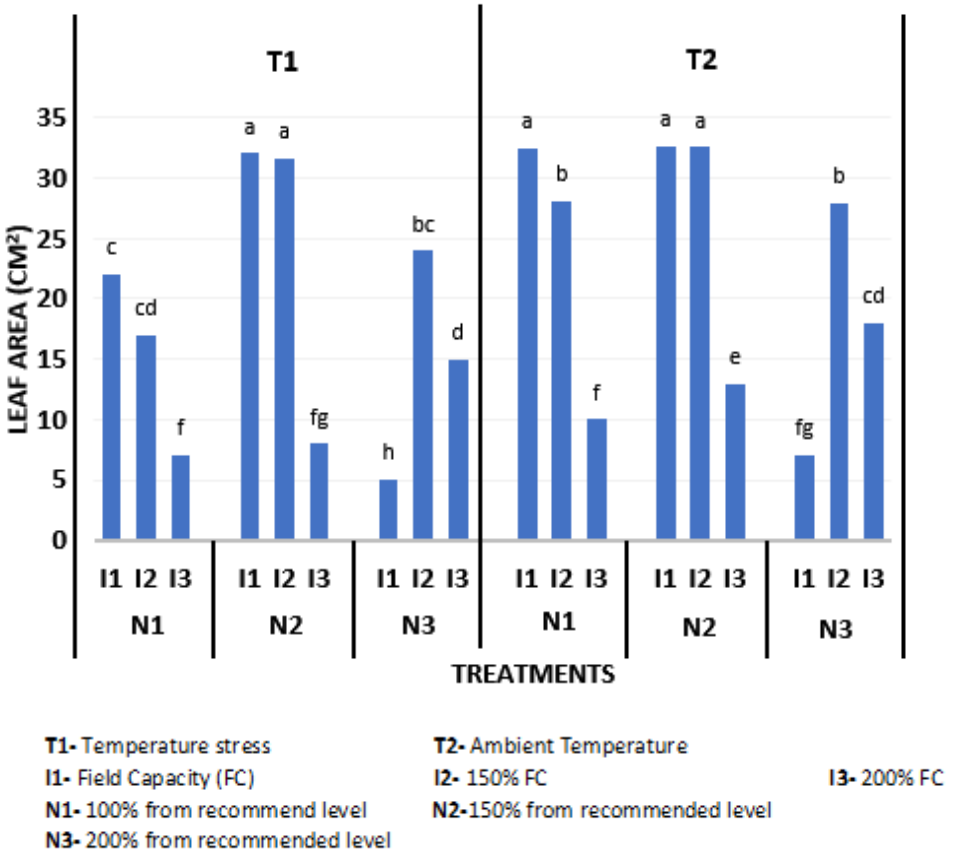

Fig.5. Effect of different treatments on leaf area (cm²) of *Capsicum annum* at reproductive stage

(*Values followed by same letter are not significantly different at p =0.05 level)*

3.1.4 Number of branches

According to analysed data effect of temperature, irrigation and nitrogen has significantly ($p<0.05$) influenced on number of branches. Treatments with 200% nitrogen of recommendation and irrigated to field capacity have resulted lowest number of branches at temperature stress (T1N3I1) and ambient temperature condition (T2N3I1), respectively. Vos *et al.,* (2005) reported that effective level of nitrogen application promoted branching. Treatments with recommended level of nitrogen application under every irrigation at temperature stress condition (T1N1I1, T1N1I2, T1N1I3) have shown lower number of branches. However, treatment with application of DOA recommended level of nitrogen and irrigated to field capacity under ambient temperature condition (T2N1I1) has shown positive influence on number of branches. Therefore, 150%of the DOA recommendation of nitrogen application has given the ability with stand the temperature stress as well as the highest number of branches.

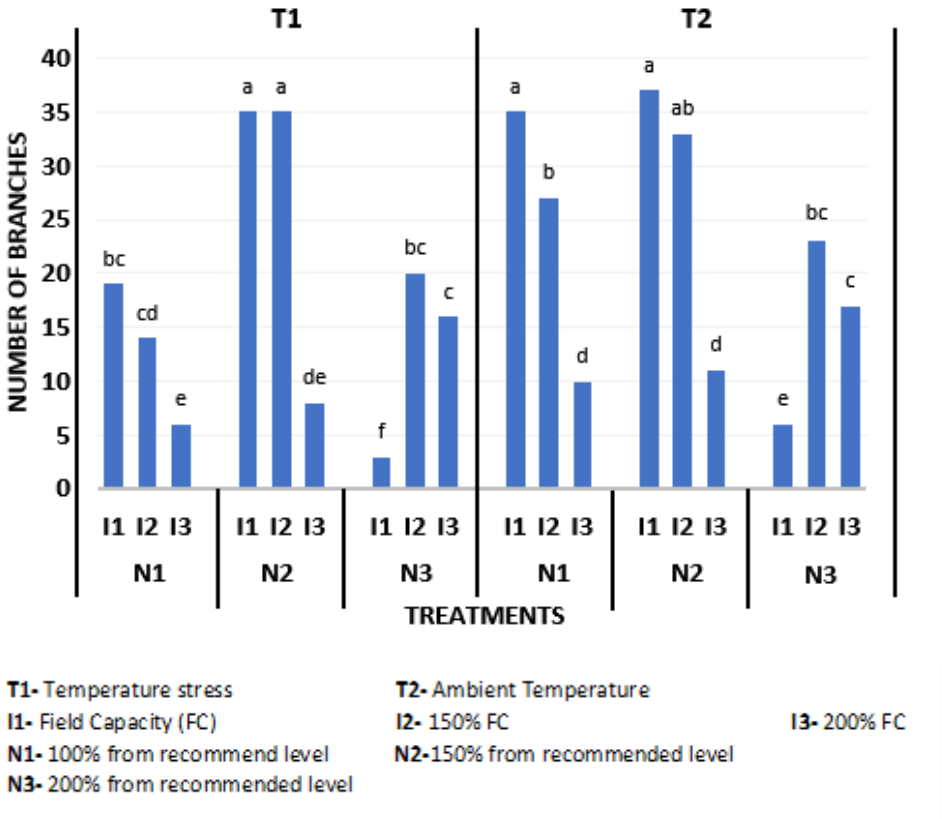

Fig. 6. Effect of different treatments on number of branches of *Capsicum annum* at 75 days after planting

(*Values followed by same letter are not significantly different at p =0.05 level)*

3.2 Yield parameters of *Capsicum annum*

3.2.1 Number of flowers

Number of flowers also significantly influenced ($p<0.05$) by all the factors and their interaction effects. Under temperature stress conditions, application of recommended level of nitrogen fertilizer has not produced higher number of flowers in all three irrigation treatments (T1N1I1, T1N1I2, T1N1I3). However, at the ambient temperature condition treatment with application of DOA recommended level of nitrogen and irrigated to field capacity (T2N1I1) has produced higher number of flowers. Under temperature stress condition, treatments which applied with 150% nitrogen of recommendation with irrigated to field capacity and 150% of field capacity have resulted higher number of flower production. This may be due to the fact that when nitrogen fertilizer applied above the recommended dosage (150%) it enhanced the plants in temperature stress to produce higher number of flowers. Treatments with 200% nitrogen of DOA recommendation have resulted lower number of flowers either at the temperature stress condition or ambient temperature condition under all three irrigation treatments (T1N3I1, T1N3I2, T1N3I3, T2N3I1, T2N3I2, T2N3I3). This may be due to the toxic effect of higher nitrogen dosage to the plants.

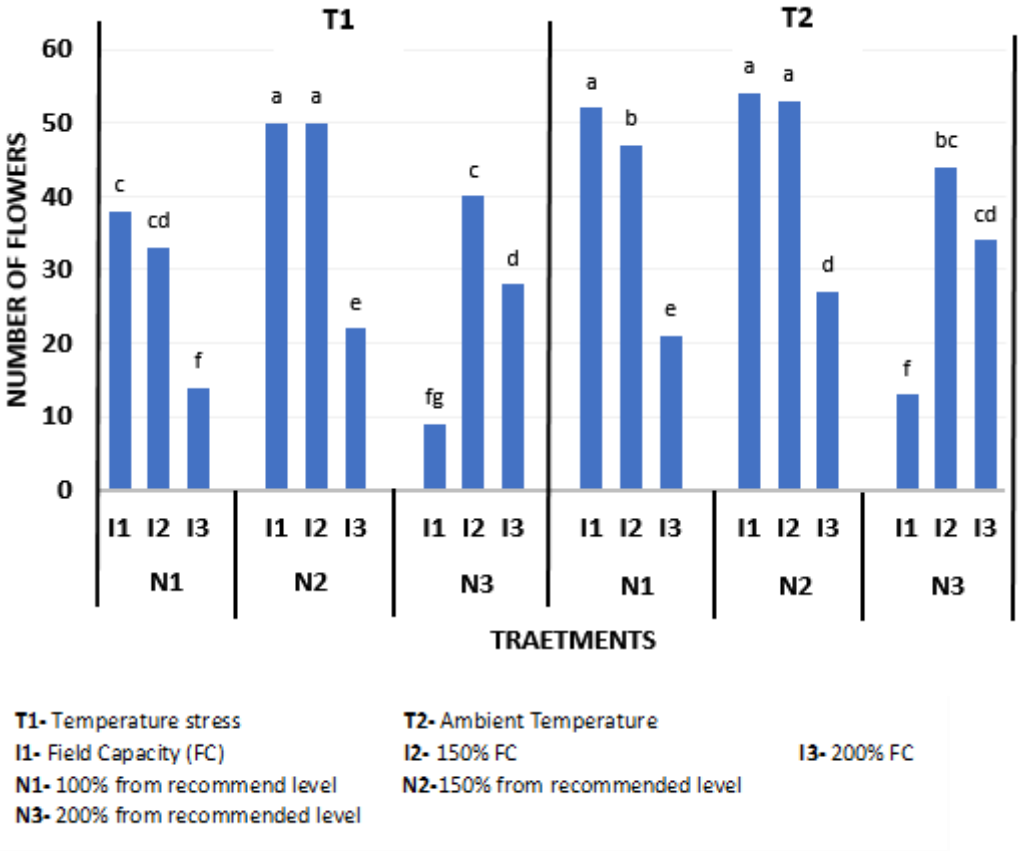

Fig. 7. Effect of different treatments on number of flowers of *Capsicum annum*

(Values followed by same letter are not significantly different at p =0.05 level)

3.2.2 Number of pods

All the treatment and their interaction effect have significant ($p<0.05$) influenced on number pods. Number of pods variation has directly proportional to the number of flowers. According to the analysed data treatments which incorporated with 200% nitrogen of recommendation have resulted lower number of pods similar to number of flowers either at the temperature stress condition or ambient temperature condition under all three irrigation treatments (T1N3I1, T1N3I2, T1N3I3, T2N3I1, T2N3I2, T2N3I3). Temperature stress conditions throughout the growing season significantly reduced yield and fruit size of capsicum (Molla Md *et al.*, 2003). Under temperature stress condition application of recommended level of nitrogen was not sufficient to obtain higher number pods in all three irrigation treatments (T1N1I1, T1N1I2, T1N1I3). Significantly highest number of pods were shown in treatment with 150% of Nitrogen fertilizer in field capacity and 150% of field capacity moisture level irrigations. Therefore, better to increase the amount of nitrogen application, when plants are under temperature stress. However, higher doses above 150% of recommended level of nitrogen application may become toxic to capsicum plants. According to the findings, application 150% nitrogen of DOA recommendation and irrigation at field capacity and 150% of field capacity soil moisture levels have shown better results on number of pod production under temperature stress condition (T1N2I1, T2N2I2). However, under ambient temperature condition, DOA recommended dosage of nitrogen fertilizer is sufficient to produce significant yield in Capsicum plants.

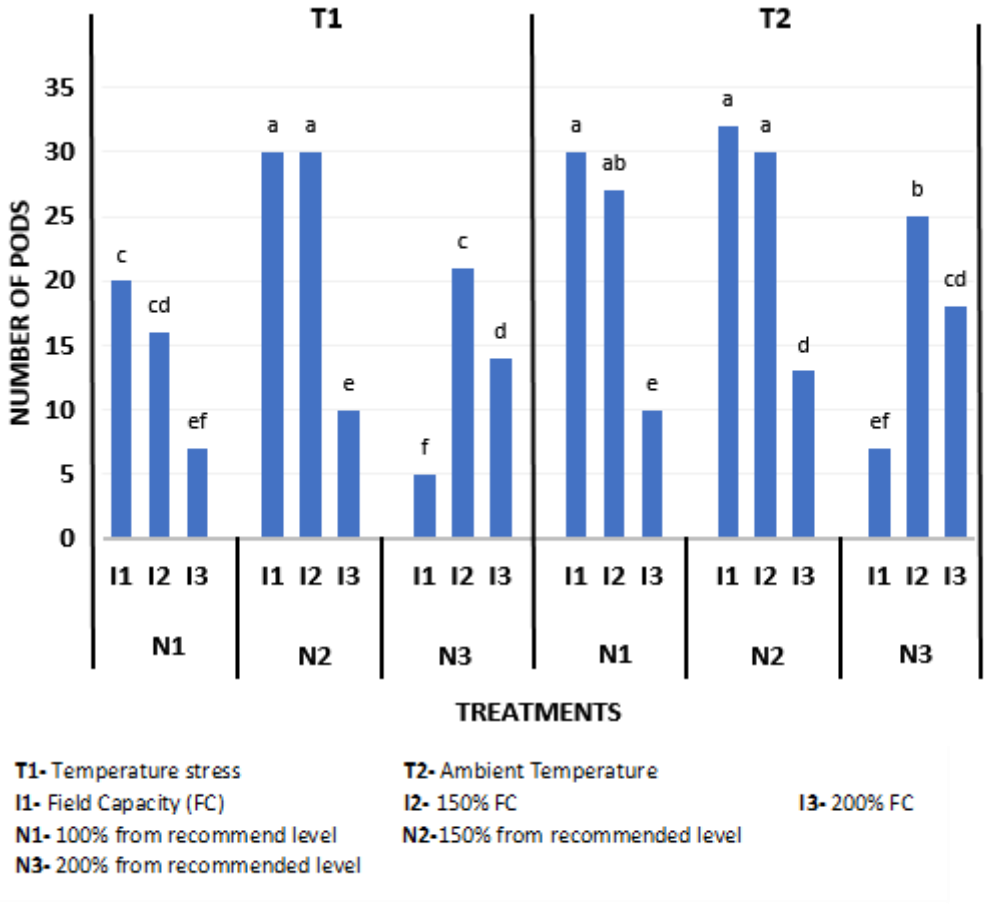

Fig. 8. Effect of different treatments on number of pods of *Capsicum annum* at the harvesting stage

(*Values followed by same letter are not significantly different at p =0.05 level)*

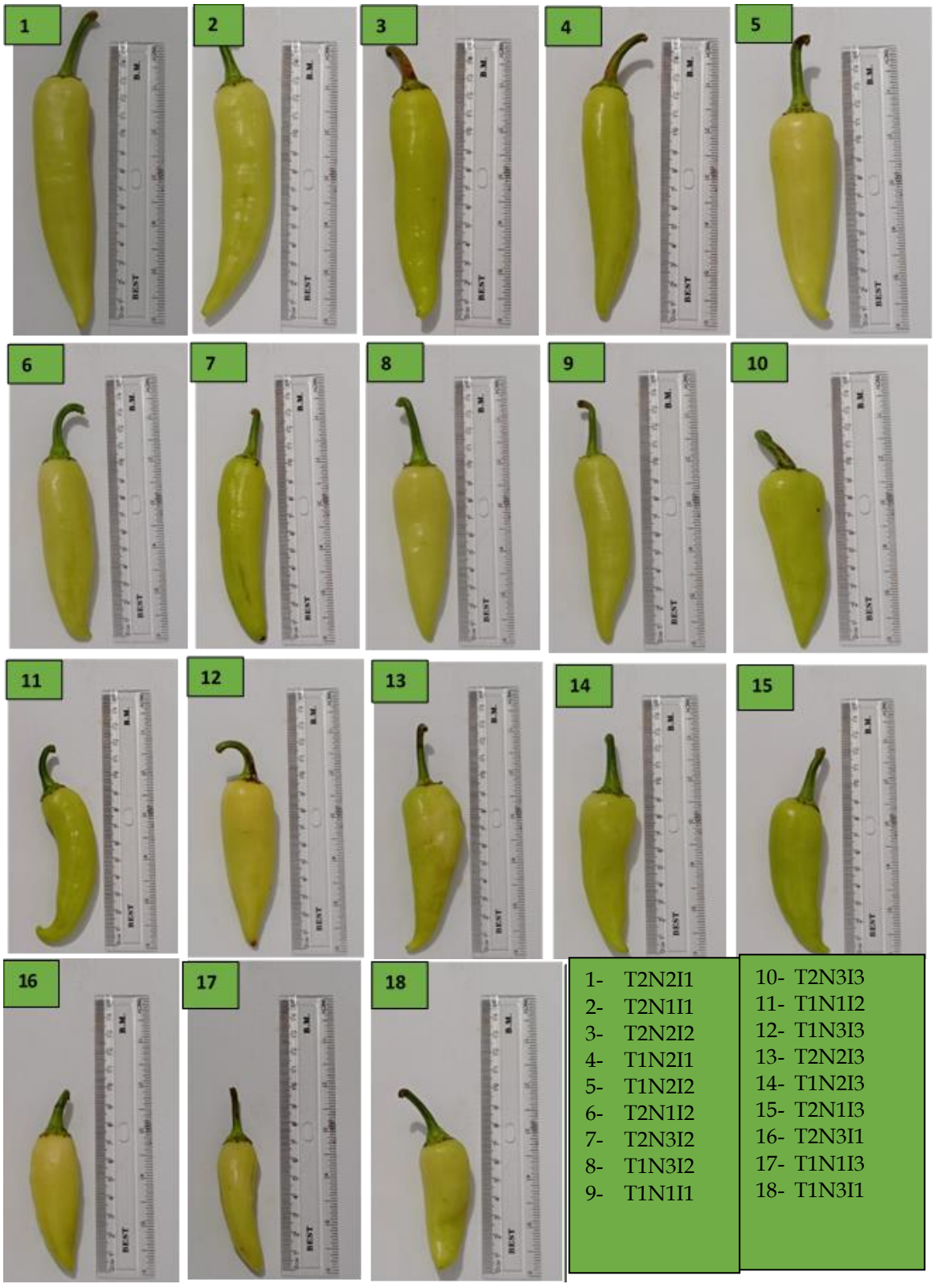

Fig. 9. Effects of different treatments on length of pods (cm) at harvest

4.0 CONCLUSION AND RECOMMENDATION

According to this study interaction effect of temperature, irrigation and nitrogen has significant contribution on growth and yield parameters of *Capsicum annum*. Application of higher level of nitrogen fertilizer is vital to improve growth and yield parameters of Capsicum under temperature stress condition. However, application of too much of nitrogen resulted negative impact on measured parameters of Capsicum either at the temperature stress or ambient temperature. According to the results of the study, application of recommended level of nitrogen fertilizer in all three irrigation treatments under temperature stress condition was not enough to obtain higher yield. Therefore, application of 150% nitrogen of DOA recommendation with irrigation at field capacity level of soil moisture will increase the yield of Capsicum under temperature stress conditions. However, under ambient temperature condition, it is better to follow the currently recommended level of nitrogen fertilizer application by the Department of Agriculture in Sri Lanka.

REFERENCES

Barrs, H.D. (1968). Determination of water deficits in plant tissue, In: Kozlowski, T.T (Ed) water deficits and plant growth. New York, Academic Press, 1968, V.1, P:235-368

Chang, Z., Liu, Y., Dong, H., Teng, K., han, L., hang, X., (2016). Effects of cytokinin and nitrogen on drought tolerance of creeping bentgrass, 11 (4).

Cruz, P. C., (2008). Nitrogen use efficiency in selected rice (*Oryza sativa* L.) genotypes under different water regimes and nitrogen levels. Field Crops Res. 107 137–146. 10.1016/j.fcr.2008.01.007

De Costa, W. A. J. M., (2008). Climate change in Sri Lanka: myth or reality? Evidence from long-term meteorological data. Journal of the National Science Foundation of Sri Lanka, 36. 63-88

De Silva, C.S., Weatherhead, E.K., Knox, J.W. and Rodrihuez-, J.A. (2007). Predicting the impacts of climate change-A case study of paddy irrigation water requirements in Sri Lanka. *Journal of Agricultural Water Management* 93(2007)19-29. Elsevier Publishers, Amsterdam, Netherlands.

De Silva, C.S. (2006). Impact of climate change on potential soil moisture deficits and its use as a climate indicator to forecast irrigation need in Sri Lanka. Water Resources Research in Sri Lanka, Postgraduate Institute of Agriculture, University of Peradeniya., PP: 79-90.

Gunawardena, M.D.M., De Silva C.S.,Godawatta V.N.A., (2011). Impact of temperature and water stress on growth and yield of selected crops. International Conference on Impact of Climate Change on Agriculture, University of Ruhuna, Mapalana Kamburupitiya. Dec 20th 2011, pp 150-157

Haefele, S. M., Jabbar, S. M. A., Siopongco, J. D. L. C., Tirol-Padre, A., Amarante, S. T., Sta Kato, M.C., Hikosaka, K., Hirotsu, N., Makin, A., Hirose, T. (2003). The excess light energy that is neither utilized in photosynthesis nor dissipated by photo protective mechanisms determines the rate of photoinactivation in photosystem II. Plant Cell Physiol. 44:318-325.

Ministry of Environment. Second National Communication on Climate Change under the United Nations Framework Convention on Climate Change (UNFCCC). Democratic Socialist Republic of Sri Lanka, (2011).

Molla M.D., Madramootoo, C.A., Dodds, G.T (2003). Effects of water stress at different growth stages on greenhouse tomato yield and quality, McGill University, 21111 Lakeshore road, Montreal, QC, H9X 3V9, Canada [online]. Available at https://cat.inist.fr/?aModele=afficheN&cpsidt=15421402

Saud, shah., Fahad, S., Yajun, C., Ishan., M.Z., Hammad, H.M, Nasim, W., Arif, A.J.M., Alharby, H (2017). Effects of nitrogen supply on water stress and recovery mechanisms in Kentucky Bluegrass plants, Front. Plant Sci., https://doi.org/10.3389/fpls.2017.00983

Syaukat, Y., (2011). The impact of climate change on food production and security and its adaptation programs in Indonesia, J.ISSAAS, Vol.17, No1:40-51.

Tran, Thiem & Kano-Nakata, Mana & Takeda, Moe & Menge, Daniel & Mitsuya, Shiro & Inukai, Yoshiaki & Yamauchi, Akira. (2014). Nitrogen application enhanced the expression of developmental plasticity of root systems triggered by mild drought stress in rice. Plant and Soil. 378. 139-152. 10.1007/s11104-013-2013-5.

Vos, J., Biemond, H., (2005). Effects of nitrogen on the development and growth of potato plant, Universitairhoofddocentbij de vakgroepAgronomie, p: 17-33

Wang, Z., Wang, Z., Zhang, W., Beebout, S. S., Zhang, H., Liu, L., (2016). Grain yield, water and nitrogen use efficiencies of rice as influenced by irrigation regimes and their interaction with nitrogen rates. Field Crops Res. 193 54–69. 10.1016/j.fcr.2016.03.006

Waraich, E.A., Ahmad, R., Halim, A., Aziz, T. (2012). Allevation of temperatue stress by nutrient management in crop plants. Journal of soil science and plant nutrition, 12 (2), 221-224.

Zubairu, Y., Oladiram, J. A., Osunde, O. A., &Ismaila, U. (2017). Effect of nitrogen fertilizer and fruit positions on fruit and seed yields of Okro (*Abelmoschusesculentus L. Moench*). Journal of Plant Studies, 6(1), 39-45. https://doi.org/10.5539/jps.v6n1p39

Journal of Engineering and Technology of The Open University of Sri Lanka

Volume 08 No. 02 September 2020 ISSN 2279-2627

Desinged by CETMe-OUSL
Prnited by Press OUSL